Technische Universität München
&
Max Planck Institut für Physik

Standard Model Fermion Hierarchies with Multiple Higgs Doublets

Dissertation

by

Ana Solaguren-Beascoa Negre

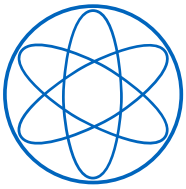

Physik Department T30d

Technische Universität München

Physik Department T30d

Max Planck Institut für Physik

Standard Model Fermion Hierarchies with Multiple Higgs Doublets

Ana Solaguren-Beascoa Negre

Vollständiger Abdruck der von der Fakultät für Physik der Technischen Universität München zur Erlangung des akademischen Grades eines

Doktors der Naturwissenschaften

genehmigten Dissertation.

Vorsitzender:		Univ.–Prof. Dr. Lothar Oberauer
Prüfer der Dissertation:	1.	Univ.–Prof. Dr. Alejandro Ibarra
	2.	Univ.–Prof. Dr. Andrzej Buras

Die Dissertation wurde am 25.04.2016 bei der Technischen Universität München eingereicht und durch die Fakultät für Physik am 24.05.2016 angenommen.

Abstract

The origin of the hierarchies in the Standard Model fermion masses and mixing angles is one of the most puzzling questions in particle physics. In addition, experiments have shown that neutrinos are massive particles, in contrast with the Standard Model predictions. All of these issues indicate the existence of new physics. In this thesis we study extensions of the Standard Model with new Higgs doublets to solve these questions. The lighter fermion masses are generated with small quantum effects, reproducing the hierarchies between the different fermion mass generations. Moreover we can generate neutrino masses in the context of the see-saw mechanism, by extending the model with at least one right-handed neutrino. The mixing angles are calculated using zero-th order in perturbation theory. The Cabibbo–Kobayashi–Maskawa matrix can be generated with a hierarchical structure, whereas the Pontecorvo–Maki–Nakagawa–Sakata matrix follows an anarchical structure, in agreement with experiments. In order to avoid stringent flavour observable constraints, we work in the decoupling limit, taking a sufficiently large scale for new physics.

Zusammenfassung

Der Ursprung der hierarchischen Fermionenmassen und Mischungswinkel im Standard Modell ist eine der größten ungelösten Fragen der Teilchenphysik. Außerdem haben Experimente gezeigt, dass Neutrinos massive Teilchen sind, was im Widerspruch zur Vorsage des Standard Modells steht. Diese Beobachtungen deuten auf die Existenz neuer Physik hin. Um diese Probleme zu lösen werden in vorliegender Arbeit Erweiterungen des Standard Modells mit neuen Higgs Doublets untersucht. Dabei werden die Massen der leichten Fermionen über kleine Quanteneffekte generiert. So können die Massenhierarchien der verschiedenen Fermionengenerationen reproduziert werden. Des Weiteren können die Neutrinomassen im Kontext des See-Saw Mechanismus generiert werden, indem das Modell um mindestens ein rechtshändiges Neutrino erweitert wird. Die Mischungswinkel werden in nullter Ordnung Störungstheorie berechnet. In Übereinstimmung mit Experimenten weist die Cabibbo-Kobayashi-Maskawa Matrix dann eine hierarchische Struktur auf, wohingegen die Pontecorvo–Maki–Nakagawa–Sakata eine anarchische Struktur besitzt. Um die starken Schranken von Flavourobservablen zu umgehen, arbeiten wir im in dem Grenzfall, in dem durch die Wahl einer ausreichend großen Energieskala die neue Physik entkoppelt ist.

Contents

Introduction

We are currently living in a new era of discoveries in particle physics. Perhaps, the biggest achievement of the last few years has been the discovery of the Higgs boson by the ATLAS and CMS experiments, proving the self-consistency of the Standard Model of Particle Physics (SM) as a successful theoretical framework for elementary particles. Nevertheless, there are still many unanswered questions which the SM cannot accommodate, as for example neutrino masses. It is known from neutrino oscillation experiments that neutrinos have mass. But the SM predicts them as massless particles. Furthermore, experiments have shown that the scale of neutrino masses is much lower than all the other SM fermions and the hierarchies between their masses seems to be milder than for all other fermion types. But the nature of neutrino masses remains still completely unknown. There are several models which introduce new physics to explain neutrino masses. For example the so-called *see-saw mechanism* includes new right-handed neutrinos, which couple to SM neutrinos through a Dirac mass term, as all other fermions. As right-handed neutrinos are not charged under the SM gauge group, they can have large Majorana masses. In this way, left-handed neutrinos obtain small masses, compatible with experiments.

Besides the need of new physics to understand experimental results that the SM alone cannot explain, extensions of the SM are also studied to describe the parameters within SM. The origin of the hierarchies in the SM flavour sector is one of the main open issues in particle physics. In the SM, quarks and charged leptons couple to the Higgs boson through Yukawa interactions. After electroweak symmetry breaking, these couplings set the value of the fermion masses. From experiments we know that the SM fermion masses follow a completely hierarchical pattern. At low energies, the corresponding Yukawa interactions are of the order $\mathcal{O}(10^{-6})$ up to $\mathcal{O}(1)$. There have been several attempts to explain these strong hierarchies by extending the SM with new particles or symmetries. A further issue that needs to be addressed is the mixing pattern of fermions. As the Yukawa matrices are not diagonal in the SM flavour basis, flavour changing charged currents appear in the weak sector when working in the mass basis. The fact that neutrinos are massive means that this does not only happen in the quark sector, but also in the lepton sector. Yet, the mixing pattern in the quark sector shows a strong hierarchical structure, whereas the lepton mixing matrix has a completely anarchical arrangement. All of these problems are discussed in detail in Chapter 1.

The hierarchies in the mass and mixing sector for quarks and leptons somehow suggests that there must be an underlining mechanism which generates such a flavour structure. In this thesis we introduce a framework to generate the masses and mixing angles of the SM fermion sector in

one of the simplest extension of the SM, the Two Higgs Doublet Model (2HDM). This model adds one extra Higgs doublet with the same quantum numbers of the SM Higgs to the SM. The theoretical background of the 2HDM is presented in Chapter 2. Here we discuss the different terms of the 2HDM Lagrangian and its phenomenological consequences, such as new sources of Flavour Changing Neutral Currents (FCNCs) or CP violation.

In Chapter 3 we introduce a model to explain the quark masses and mixing angles in the context of a general 2HDM with rank-1 Yukawa couplings at tree level. Within this framework we are able to reproduce the strong hierarchies between the second and third generation of quarks together with a completely hierarchical structure for the corresponding mixing sector. In order to avoid current experimental limits on new scalar particles, we chose to work in the decoupling limit, where the masses of the new Higgs bosons are much larger than the electroweak scale. The lepton sector for this model is discussed in Chapter 4, where we extend the 2HDM with right-handed neutrinos in order to generate the neutrino masses in the context of the see-saw mechanism. As for the quark sector, we are able to generate the masses for the second and third generation of leptons with their corresponding hierarchies. Additionally, the mixing sector for leptons can be generated with the correct anarchical structure. In this part we also take the decoupling limit to avoid flavour constraints.

The main problem of these scenarios is that the first generation of fermions remains massless. Adding a new direction in flavour space for each fermion type can cure this problem. For this reason, in Chapter 5, fermion masses are presented in the context of a general Three Higgs Doublet Model (3HDM) with rank-1 Yukawa matrices. A basis independent analysis is performed to present the results. As for the 2HDM, the decoupling limit is taken in order to avoid the strong constraints from FCNCs. In this framework we are able to generate the mass of each one of the SM fermions with the correct hierarchy, using the see-saw mechanism for the neutrino sector.

A phenomenological analysis of a model which contains physics beyond the SM can constrain the parameter space of the model and give us information on which are the most interesting observables to study with new experimental data. In the case of the 2HDM and 3HDM, the Yukawa interactions with the new Higgs can generate new sources of FCNCs and CP violation. In the SM, there are no FCNCs at tree level and are suppressed at higher orders. For this reason FCNCs are a good candidate to study models which might generate them at tree level and deviate their value from the SM predictions. A similar situation happens with new sources of CP violation, as the SM contains just one CP violating phase in the quark sector. In Chapter 6 we make a first study of the impact of a the 2HDM explained above on different flavour observables which are strongly constrained from experiments. This analysis allows us to set limits on the new Higgs masses and determine which are the most interesting observables to study for these kind of models.

Some parts of this work have been also discussed in the following articles:

[1] **Radiative Generation of Quark Masses and Mixing Angles in the Two Higgs Doublet Model**,
A. Ibarra and A. Solaguren-Beascoa,
Phys. Lett. B **736**, 16 (2014))

[2] **Lepton parameters in the see-saw model extended by one extra Higgs doublet**,
A. Ibarra and A. Solaguren-Beascoa,
JHEP **1411**, 089 (2014)

[3] **Standard Model Fermion Masses and Mixing Angles generated in 3HDM**,
A. Ibarra and A. Solaguren-Beascoa,
Proceedings of the XIV International Conference on Topics in Astroparticle and Underground Physics (TAUP2015), 7-11 September 2015, Torino, Italy.

[4] **Flavour Observables in a Radiative 2HDM**,
J. Girrbach-Noe, A. Ibarra and A. Solaguren-Beascoa
In preparation

[5] **Generating Standard Model Fermion Parameters in a 3HDM**,
A. Ibarra and A. Solaguren-Beascoa
In preparation

Part I

Particle Physics in the LHC Era

CHAPTER 1

The Flavour Puzzle

The SM is a theory which successfully predicts the interaction between elementary particles. Nevertheless, it is still an incomplete model as there are several questions which it cannot address. The SM does not provide an explanation for the flavour structure in the fermion sector. The Yukawa couplings with the SM Higgs boson generate the masses for all quarks and charged leptons after spontaneous symmetry breaking. The enormous differences between fermion masses is not well understood. The structure of the mixing sector is also an open problem which remains unexplained in the SM. A further issue is the origin of neutrino masses. The SM does not predict the existence of right-handed neutrinos. The absence of the latter forbids left-handed neutrinos to acquire mass via Yukawa interactions, as all other fermions do. A renormalizable Majorana mass term for left-handed neutrinos is not invariant under the SM gauge group, hence cannot be included as part of the SM Lagrangian. Therefore neutrinos are massless particles in the SM. This statement is in disagreement with experimental data. All of these problems are known as the *flavour puzzle*.

In this chapter the physics regarding these open questions are presented. The chapter is divided in three different sections. First, a brief theoretical introduction to flavour structures in the SM is presented. In the second section the evidence for mixing in the lepton sector is discussed. This leads us to the third section where different theoretical scenarios for neutrino masses are presented. In particular we focus on the see-saw mechanism, as this is the framework used during this thesis to generate neutrino masses.

1.1 Flavour in the Standard Model

The SM is a relativistic quantum field theory with gauge group $G_{SM} = SU(3)_C \times SU(2)_L \times U(1)_Y$. The minimum SM fermion content to explain observations is summarised in Table 1.1. Each row corresponds to three different generations of fermions. It contains a total of 6 flavour species for quarks and 6 for leptons. Right-handed neutrinos are the only right-handed fermion partner which is not included as part of the SM, as there is no experimental evidence of their existence. If right-handed neutrinos were part of the particle content of the SM, they would not be charged

under the SM gauge group. In other words, they would not have SM gauge interactions and therefore, do not need to be included in the theory. Of course, a SM gauge singlet can always be added as a theoretical extension.

	$SU(3)_C$	$SU(2)_L$	$U(1)_Y$
$L_L = \begin{pmatrix}\nu_{eL}\\ e_L\end{pmatrix}, \begin{pmatrix}\nu_{\mu L}\\ \mu_L\end{pmatrix}, \begin{pmatrix}\nu_{\tau L}\\ \tau_L\end{pmatrix}$	1	2	$-\frac{1}{2}$
$Q_L = \begin{pmatrix}u_L\\ d_L\end{pmatrix}, \begin{pmatrix}c_L\\ s_L\end{pmatrix}, \begin{pmatrix}t_L\\ b_L\end{pmatrix}$	3	2	$\frac{1}{6}$
e_R, μ_R, τ_R	1	1	-1
u_R, c_R, t_R	3	1	$\frac{2}{3}$
d_R, s_R, b_R	3	1	$-\frac{1}{3}$

Table 1.1: SM fermion content.

The current status of the fermion parameters within the SM is discussed in the next part. First the SM fermion masses are presented. Second, the mixing in the quark sector is discussed.

Standard Model Fermion Masses

If SM fermions would be massless, the SM would have the following global flavour symmetry

$$G_f = U(3)_{Q_L} \times U(3)_{L_L} \times U(3)_{u_R} \times U(3)_{d_R} \times U(3)_{e_R}. \tag{1.1}$$

This symmetry group is broken as soon as the Yukawa couplings are introduced in the Lagrangian. The masses of the SM fermions arise from the Yukawa interactions with the SM Higgs boson after electroweak symmetry breaking. These couplings are described by the following Lagrangian

$$-\mathcal{L}^{\text{Yuk}} = (Y_u)_{ij}\bar{Q}_{Li}\tilde{\Phi}u_{Rj} + (Y_d)_{ij}\bar{Q}_{Li}\Phi d_{Rj} + (Y_e)_{ij}\bar{L}_{Li}\Phi e_{Rj} + \text{h.c.} \tag{1.2}$$

where $Y_{u,d,e}$ are the Yukawa couplings for each fermion type and ij indicates the matrix element. The corresponding masses are proportional to the Yukawa singular values

$$\text{diag}\,(m_{\tilde{x}_1}, m_{\tilde{x}_2}, m_{\tilde{x}_3}) = \frac{v}{\sqrt{2}} V^{\dagger}_{\tilde{x}_L} Y_{\tilde{x}} V_{\tilde{x}_R} \tag{1.3}$$

where $v \simeq 246$ GeV corresponds to the SM Higgs vacuum expectation value (vev), which sets the scale of electroweak symmetry breaking. Here $V_{\tilde{x}_{L,R}}$ (with $\tilde{x} = u,\ d,\ e$) are the matrices which generate the singular value decomposition of $Y_{\tilde{x}}$. Thus, they determine the rotation from the

weak eigenstates $\left|\tilde{x}^{\mathrm{f}}_{L,R}\right\rangle$ to the mass eigenstates $\left|\tilde{x}^{\mathrm{m}}_{L,R}\right\rangle$ for SM fermions

$$\left|\tilde{x}^{\mathrm{f}}_{L,R}\right\rangle = V_{\tilde{x}_{L,R}} \left|\tilde{x}^{\mathrm{m}}_{L,R}\right\rangle . \tag{1.4}$$

Note that in eq. (1.2), neutrinos have no Yukawa coupling which generates their masses due to the non-existence of their right-handed partner. This is the reason why neutrinos are massless particles in the SM.

Table 1.2 contains the different SM fermion masses and the corresponding approximate Yukawa coupling value. Clearly, there is a strong hierarchy between the different fermion masses. For example, the top quark mass is about 6 orders of magnitude larger than the electron mass or 5 orders of magnitude larger than the up quark mass. This strong mass hierarchy is not well understood in the context of the SM. This scenario somehow suggests that there must be an underlining mechanism to generate this mass pattern. There have been several ideas discussed

	Mass [MeV]	Yukawa coupling
m_e	0.511	3×10^{-6}
m_μ	105.6	6×10^{-4}
m_τ	1776.86 ± 0.12	10^{-2}
m_u	$2.3^{+0.7}_{-0.5}$	10^{-5}
m_d	$4.8^{+0.5}_{-0.3}$	2×10^{-5}
m_s	95 ± 5	5×10^{-4}
m_c	1275 ± 25	7×10^{-3}
m_b	4180 ± 30	2×10^{-2}
m_t	$(173.21 \pm 0.51) \times 10^3$	1

Table 1.2: SM fermion masses extracted from [6] and the corresponding approximate Yukawa coupling value. The u, d, s, c and b mass are given in the $\overline{MS}$ scheme.

in the literature which try to explain the hierarchies between SM fermion masses. A popular approach is to assume that the heaviest fermion masses are generated at tree level whereas the lighter generations acquire their masses via quantum effects. In this way the hierarchy between the different generations can be naturally explained. Some examples can be found in [7, 8] in the context of supersymmetry, or by extending the gauge sector, for example in [9–11].

Let us finally mention that after quark and charged lepton masses are included as part of the SM Lagrangian, the model is still invariant under the following accidental symmetry

$$U(1)_B \times U(1)_{L_e} \times U(1)_{L_\mu} \times U(1)_{L_\tau}. \tag{1.5}$$

Here $U(1)_B$ corresponds to baryon number conservation and $U(1)_{L_e}$, $U(1)_{L_\mu}$ and $U(1)_{L_\tau}$ corre-

spond to the conservation of the individual lepton family numbers, L_e, L_μ and L_τ, respectively.

The Quark Mixing Sector

The mixing sector in the SM arises because the mass eigenstates are not aligned in flavour space. For quarks and charged leptons in the SM, the rotation from the flavour basis to the mass basis described in eq. (1.4). The quark Yukawa couplings in the flavour basis are non-diagonal and complex. Nevertheless, when one rotates the model to the mass basis, the Yukawa matrices become diagonal matrices with real elements in the diagonal. This rotation also affects the weak sector and introduces flavour changing couplings (charged vertices containing different flavour species) and a CP violating phase. This information is contained in the Cabibbo–Kobayashi–Maskawa (CKM) matrix. After rotating from the flavour basis to the mass basis, the weak charged current transforms as

$$\frac{-g}{2\sqrt{2}}\begin{pmatrix}\bar{u} & \bar{c} & \bar{t}\end{pmatrix}_f (1-\gamma_5)\gamma^\mu W_\mu^\dagger \begin{pmatrix}d\\ s\\ b\end{pmatrix}_f + \text{h.c.} \longrightarrow \frac{-g}{2\sqrt{2}}\begin{pmatrix}\bar{u} & \bar{c} & \bar{t}\end{pmatrix}_m (1-\gamma_5)\gamma^\mu W_\mu^\dagger V_{CKM} \begin{pmatrix}d\\ s\\ b\end{pmatrix}_m + \text{h.c.} \tag{1.6}$$

where the f and m subscripts indicate the flavour or the mass basis, respectively and V_{CKM} corresponds to the CKM matrix, defined as

$$V_{CKM} = V_{u_L}^\dagger V_{d_L}. \tag{1.7}$$

The CKM matrix contains the misalignment between the left-handed up and down sector mass eigenstates. As the up and down quark types have different flavour to mass basis rotation matrices, the product of the left-handed rotation matrices generates a non-diagonal and complex CKM matrix. This is experimentally testable through processes which contain the coupling of the W boson with quark pairs. An example of such process is the $B^0 - \bar{B}^0$ mixing, represented in Fig 1.1. The CKM matrix elements enter in the vertices of the Feynman diagram and generate flavour changing charged currents. Note that as $V_{u_L}V_{u_L}^\dagger = V_{d_L}V_{d_L}^\dagger = \text{diag}(1,1,1)$, there are no FCNCs at tree level in the SM.

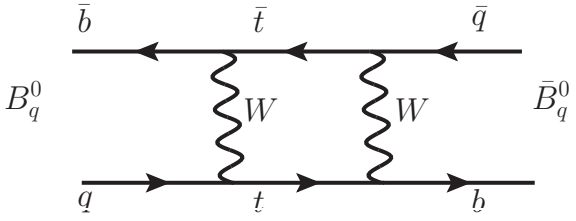

Figure 1.1: Feynman diagram for $B^0 - \bar{B}^0$ mixing. Here $q = d$ or s. The vertices of the diagram contain the entries of the CKM matrix which allow charged current flavour violating interactions.

The CKM matrix with 3 quark generations is a 3×3 unitary matrix, which can be parametrised by three mixing angles and one CP violating phase as follows

$$V_{CKM} = \begin{pmatrix} c_{12}c_{13} & s_{12}c_{13} & s_{13}e^{-i\delta} \\ -s_{12}c_{23} - c_{12}s_{23}s_{13}e^{i\delta} & c_{12}c_{23} - s_{12}s_{23}s_{13}e^{i\delta} & s_{23}c_{13} \\ s_{12}s_{23} - c_{12}c_{23}s_{13}e^{i\delta} & -c_{12}s_{23} - s_{12}c_{23}s_{13}e^{i\delta} & c_{23}c_{13} \end{pmatrix} \tag{1.8}$$

where $c_{ij} = \cos\theta_{ij}$, $s_{ij} = \sin\theta_{ij}$, θ_{ij} are real mixing angles and δ is the CP violating phase. The global fit presented in [12] for the CKM matrix at 1σ *C.L.* is

$$|V_{CKM}| = \begin{pmatrix} |V_{ud}| & |V_{us}| & |V_{ub}| \\ |V_{cd}| & |V_{cs}| & |V_{cb}| \\ |V_{td}| & |V_{ts}| & |V_{tb}| \end{pmatrix} = \begin{pmatrix} 0.974242^{+0.000079}_{-0.000158} & 0.22548^{+0.00068}_{-0.00034} & 0.00355^{+0.00017}_{-0.00015} \\ 0.22534^{+0.00068}_{-0.00034} & 0.97341^{+0.00011}_{-0.00018} & 0.04117^{+0.00090}_{-0.00114} \\ 0.00855^{+0.00021}_{-0.00027} & 0.04043^{+0.00088}_{-0.00112} & 0.999146^{+0.000046}_{-0.000038} \end{pmatrix}. \tag{1.9}$$

This fit has been done with the CKMfitter [13], using several flavour observables to constraint different parts the parameter space. The strong hierarchies in the quark mixing sector are immediately visible in V_{CKM}. The matrix contains terms of order $\mathcal{O}(10^{-3})$ up to terms of order $\mathcal{O}(1)$. As for the mass sector, such an unnatural hierarchy suggests that there might be a mechanism beyond the tree level Yukawa couplings to explain quark mixing angles.

The CP violating part of the CKM matrix can be parametrised with the Jarlskog invariant J, defined as follows in the mass basis [14]

$$J \sum_{m,n} \epsilon_{ikm}\epsilon_{jln} = \mathrm{Im}\left(V_{ij}V_{kl}V_{il}^{*}V_{kj}^{*}\right) \tag{1.10}$$

where V_{ab} corresponds to the (a, b) entry of the CKM matrix. Another way of parametrising the Jarlskog invariant in terms of the parameters in eq. (1.8) is

$$J = c_{12}c_{23}c_{13}^{2}s_{12}s_{23}s_{13}\sin\delta \tag{1.11}$$

The current experimental value for the Jarlskog invariant is [6]

$$J = (3.06^{+0.21}_{-0.20}) \times 10^{-5}. \tag{1.12}$$

In the lepton sector, as neutrinos are massless particles, one can always rotate to the basis with no flavour changing charged currents for leptons by redefining the neutrino eigenstates as follows

$$|\nu_L^{\mathrm{m}}\rangle \to V_{e_L} |\nu_L^{\mathrm{m}}\rangle \tag{1.13}$$

where V_{e_L} is the matrix which rotates the left-handed charged leptons from the flavour basis to the mass basis. This rotation can always be done, as there is no neutrino mass term in the SM Lagrangian. Therefore in the charged weak interactions for leptons are flavour conserving

$$\frac{-g}{2\sqrt{2}}\begin{pmatrix}\bar{e} & \bar{\mu} & \bar{\tau}\end{pmatrix}_f (1-\gamma_5)\gamma^{\mu}W_{\mu}\begin{pmatrix}\nu_e \\ \nu_{\mu} \\ \nu_{\tau}\end{pmatrix}_f + \text{h.c.} \longrightarrow \frac{-g}{2\sqrt{2}}\begin{pmatrix}\bar{e} & \bar{\mu} & \bar{\tau}\end{pmatrix}_m (1-\gamma_5)\gamma^{\mu}W_{\mu}V_{e_L}^{\dagger}V_{e_L}\begin{pmatrix}\nu_e \\ \nu_{\mu} \\ \nu_{\tau}\end{pmatrix}_m + \text{h.c.} \tag{1.14}$$

as $V_{e_L}^\dagger V_{e_L} = \mathbb{1}$. As will now discuss be, this is an invalid scenario from observations.

1.2 Flavour with Massive Neutrinos

As just explained, in the SM neutrinos are massless particles implying there is no mixing in the lepton sector. This is in contradiction with the experimental data. If neutrinos are massive particles, charged leptons and neutrino flavour eigenstates cannot be simultaneously rotated to the mass basis while leaving the Lagrangian invariant, just as happens in the SM quark sector. With massive neutrinos, the product of the left-handed rotation matrices for charged leptons and neutrinos determines the Pontecorvo–Maki–Nakagawa–Sakata (PMNS) matrix. The latter determines the strength of flavour changing charged currents through the W boson. One can work in the basis where all the mixing comes from the neutrino sector. In this case the rotation from the left-handed neutrino flavour eigenstates $\left|\nu_L^{\mathrm{f}}\right\rangle$ to the mass eigenstates $|\nu_L^{\mathrm{m}}\rangle$ is described as follows

$$\left|\nu_L^{\mathrm{f}}\right\rangle = U_{PMNS}^* \left|\nu_L^{\mathrm{m}}\right\rangle . \tag{1.15}$$

Here U_{PMNS} corresponds to the PMNS matrix, which can be parametrised as [15]

$$U_{PMNS} = \begin{pmatrix} 1 & 0 & 0 \\ 0 & c_{23} & s_{23} \\ 0 & -s_{23} & c_{23} \end{pmatrix} \begin{pmatrix} c_{13} & 0 & s_{13}e^{-i\delta} \\ 0 & 1 & 0 \\ -s_{13}e^{i\delta} & 0 & c_{13} \end{pmatrix} \begin{pmatrix} c_{12} & s_{12} & 0 \\ -s_{12} & c_{12} & 0 \\ 0 & 0 & 1 \end{pmatrix} \begin{pmatrix} e^{i\alpha_1} & 0 & 0 \\ 0 & e^{i\alpha_2} & 0 \\ 0 & 0 & 1 \end{pmatrix} \tag{1.16}$$

where $s_{ij} = \sin\theta_{ij}$, $c_{ij} = \cos\theta_{ij}$, δ is the Dirac CP phase (analogue to the CKM CP phase) and $\alpha_{1,2}$ are the two Majorana phases. In order to have a better understanding of the phenomenology of lepton mixing, neutrino oscillation is now presented.

1.2.1 Neutrino Phenomenology

It is known from quantum mechanics that an eigenstate $|a\rangle$ of a Hamiltonian H_a evolves from time $t = t_1$ to time $t = t_2$ as

$$|a(t_2)\rangle = e^{-iH_a\Delta t} |a(t_1)\rangle \tag{1.17}$$

with $\Delta t = t_2 - t_1$. This can be used to calculate the probability of a neutrino created in flavour eigenstate a to be detected as a flavour eigenstate b after a time Δt. Using the approximation for ultrarelativistic neutrinos [1]

$$E_i - E_j \simeq \frac{m_i^2 - m_j^2}{2E} \tag{1.18}$$

[1] The approximation of ultrarelativistic neutrinos is valid, as the masses of neutrinos are known to be $\mathcal{O}$(eV) and the energy at which neutrinos can be detected is at least of 100 keV [16].

and taking $L \simeq \Delta t$, being L the distance between creation and detection, the probability for $|\nu_a\rangle \to |\nu_b\rangle$ happening is [17]

$$P(\nu_a \to \nu_b; E, L) = |\langle \nu_b | \nu_a(t) \rangle|^2 \tag{1.19}$$
$$= \delta_{ab} - 4\sum_{i<j}^{n} \mathrm{Re}\left[U_{ai}U_{aj}^* U_{bi} U_{bj}^*\right] \sin^2 \frac{(m_i^2 - m_j^2)L}{4E} + 2\sum_{i<j}^{n} \mathrm{Im}\left[U_{ai}U_{aj}^* U_{bi} U_{bj}^*\right] \sin \frac{(m_i^2 - m_j^2)L}{2E}$$

where U_{xy} corresponds to the xy entry of U_{PMNS}. From this equation one can see that there are two main necessary conditions for neutrinos to oscillate from one flavour eigenstate to another. First, neutrino mass eigenstates must have different eigenvalues and second, leptons must mix. Thus, U_{PMNS} cannot be a diagonal matrix. Note that Majorana phases do not play any role in neutrino oscillations. This means that measuring neutrino oscillations cannot determine whether neutrinos are Dirac or Majorana particles. What makes neutrino oscillations particularly interesting is that in contrast to the other fermions in the SM, due to the small difference between their masses, their coherence length is large enough for oscillations to be measured at experiments. For example, long-baseline accelerator experiments ($L \sim 10^5$ m) with neutrino energies of $E \sim 10$ GeV are most sensitive to mass differences of $\Delta m^2 = m_i^2 - m_j^2 \sim 10^{-3}$ eV^2 which is comparable to the actual neutrino mass differences as will now be seen. Furthermore, for a well determined L/E, if the mass differences are distant from each other, the oscillation probability can be well approximated by a two-family case.

This description has been done assuming that neutrinos are travelling in vacuum. If neutrinos travel through matter, neutrino oscillation might be modified due to their interaction with charged leptons and nuclei. This is known as the Mikheyev–Smirnov–Wolfenstein (MSW) effect [18, 19].

Experimental Evidence for Neutrino Oscillations

Let us start discussing solar neutrino oscillation. Electron neutrinos are produced inside the Sun via the proton-proton (pp) chain and the CNO cycle. Experiments which study solar neutrino fluxes on Earth, such as GALLEX [20], BOREXINO [21], SNO [22] or SuperKamiokande [23], have measured a considerable lack of captured electron-neutrinos coming from the Sun with respect to the theoretical predictions of the Standard Solar Model (SSM) [24]. The explanation of such a disappearance is that electron neutrinos oscillate into muon and tau neutrinos. Actually, solar neutrino oscillations can also be studied with reactor experiments with the proper L/E. For example, the KamLAND experiment produces neutrinos by inverse β-decay, with energies of $\mathcal{O}$(MeV) and $L \sim \mathcal{O}(100\,\mathrm{km})$, which is indeed in the appropriate L/E range to study solar neutrino oscillations. The two-flavour fit (taking into account the mixing just between two neutrino flavour states) for several solar experimental results together with the KamLAND data for solar neutrino oscillation correspond to $\Delta m^2_{21} = (7.46^{+0.2}_{-0.19}) \times 10^{-5}$ eV^2 and $\tan^2\theta_{12} = 0.427^{+0.027}_{-0.024}$ [25]. The global analysis done in [26, 27] shows that the MSW effect in the region of large mixing angle is indeed the solution to explain solar neutrino oscillations.

In second place, atmospheric neutrinos are produced due to the interaction of cosmic rays with nuclei in the atmosphere, creating hadrons such as pions and kaons. These then decay into

electrons or muons, and neutrinos. These neutrinos are produced at ~ 15 km from detection if they are vertically down-going or $\sim$13000 km if they are vertically up-going. Experiments which study atmospheric neutrino oscillations, such as Soudan2 [28], MACRO [29] or Super-Kamiokande, search in an energy range of $\sim 0.1 - 10$ GeV, hence are mostly sensitive to mass differences of $10^{-4} < \Delta m^2_{atm} < 0.1$ [17]. Neutrinos created at long-baseline accelerators ($L \sim 100 - 1000$ km and $E \sim 10$ GeV) can also study similar mass ranges [6, 17]. These experiments have reported a deficit of muon neutrinos events. The MINOS results in 2013 for a two-flavour hypothesis are $\Delta m^2_{32} = (2.41^{+0.09}_{-0.10}) \times 10^{-3}$ and $\sin^2 2\theta_{23} = 0.95^{+0.035}_{-0.036} \pm 0.01$ [30].

Finally, reactor neutrino experiments have $L \sim 1$ km and produce antineutrinos at $E \sim$ MeV. This L/E is sensitive to $\Delta m^2 \sim \Delta m^2_{atm}$, but due to the low neutrino energies only positrons can be produced via $\bar{\nu}_e + p \to e^+ + n$. This means that reactor experiments can measure θ_{13} directly, which corresponds to the third mixing angle. Some of these experiments are for example Chooz [31], Double Chooz [32], RENO [33] and Daya Bay [34]. In 2012 the Daya Bay collaboration reported a evidence of a non-zero θ_{13} mixing angle with an updated value of $\sin^2 2\theta_{13} = 0.084 \pm 0.005$ [35].

Even if θ_{13} is small, it leads to subdominant oscillation effects due to interference in the oscillation probability of the other types of processes. This interference has to be taken into account to determine neutrino parameters. The most recent global fit analysis for the six neutrino parameters, taking into account solar, atmospheric, reactor, and accelerator data at 1σ confidence level [36, 37] is summarised in Table 1.3.

	Normal hierarchy (NH)	Inverted hierarchy (IH)
$\sin^2\theta_{12}$	$0.304^{+0.013}_{-0.012}$	$0.304^{+0.013}_{-0.012}$
$\sin^2\theta_{23}$	$0.452^{+0.052}_{-0.028}$	$0.579^{+0.025}_{-0.037}$
$\sin^2\theta_{13}$	$0.0218^{+0.0010}_{-0.0010}$	$0.0219^{+0.0011}_{-0.0010}$
δ	306^{+39}_{-70}	254^{+63}_{-62}
Δm^2_{21}	$(7.5^{+0.19}_{-0.17}) \times 10^{-5}\text{eV}^2$	$(7.5^{+0.19}_{-0.17}) \times 10^{-5}\text{eV}^2$
Δm^2_{3l}	$(2.457^{+0.0.047}_{-0.047}) \times 10^{-3}\text{eV}^2$	$(-2.449^{+0.048}_{-0.047}) \times 10^{-3}\text{eV}^2$

Table 1.3: Global fit parameters from neutrino oscillation data [36, 37]. $l = 1$ for NH, $l = 2$ for IH.

From this global fit, the 3σ range for the elements of the PMNS matrix are [36, 37]

$$|U_{PMNS}| = \begin{pmatrix} |U_{e1}| & |U_{e2}| & |U_{e3}| \\ |U_{\mu 1}| & |U_{\mu 2}| & |U_{\mu 3}| \\ |U_{\tau 1}| & |U_{\tau 2}| & |U_{\tau 3}| \end{pmatrix} = \begin{pmatrix} 0.801 \to 0.845 & 0.516 \to 0.580 & 0.137 \to 0.158 \\ 0.225 \to 0.517 & 0.441 \to 0.699 & 0.614 \to 0.793 \\ 0.246 \to 0.529 & 0.464 \to 0.713 & 0.590 \to 0.776 \end{pmatrix} \tag{1.20}$$

which show a completely anarchical structure in contrast with the strong hierarchies of CKM matrix.

From neutrino oscillation data only the squared difference between neutrino masses is known. This scheme of masses leaves two possible scenarios:

- $m_1 < m_2 \ll m_3$ known as the normal hierarchy
- $m_3 \ll m_1 < m_2$ known as the inverted hierarchy.

The neutrino hierarchy can be determined thanks to the MSW effect, as the resonant condition for the neutrino oscillation in matter depends on the sign of the mass difference squared Δm^2 [19,38]. Other methods to experimentally determine neutrino mass hierarchy is by the direct neutrino mass measurement, if the mass hierarchy is normal [39].

As for neutrino oscillation data only the squared neutrino mass differences of can be determined, the actual neutrino mass scale remains unknown. For this reason several experiments try to constrain this mass. The most stringent current limits from the Troitsk experiment with ^{3}H β decay is $m_\nu^{2(eff)} = \sum_i |U_{ei}|^2 m_{\nu_i}^2 < (2.05 \text{ eV})^2$ [40]. The total neutrino mass defined as $m_{tot} = \sum m_\nu$, has an upper bound of 0.23 eV from the Planck collaboration results in 2015 [41]. This implies that the mass scale for neutrinos is very small in comparison to all other SM fermions.

1.2.2 Neutrino Mass Models

Neutral fermions can be either Dirac or Majorana particles. Dirac fermions are a four component spinor, $\psi_\text{D} \equiv \psi_L + \psi_R$ and their mass term connects two different Weyl spinors. This is the case of SM quarks and charged leptons. On the other hand, Majorana fermions are two component spinors, $\psi_\text{M} \equiv \psi_L + \psi_L^C$, where $\psi_L^C = C\bar{\nu}_L^T$ and C is the charge conjugation operator. The Majorana mass term connects a Weyl spinor to its own CP conjugate.

In this section, these two different possible scenarios to describe the nature of neutrino masses are discussed. The see-saw mechanism is also presented as a framework to generate neutrino masses.

Dirac or Majorana?

As explained at the beginning of this chapter, SM fermions acquire their masses through the Yukawa interactions with the SM Higgs after electroweak symmetry breaking. Accordingly, fermion masses are proportional to the different Yukawa singular values, which take values between $\mathcal{O}(10^{-6})$ and $\mathcal{O}(1)$.

The SM predicts neutrinos as massless particles. As new particles which are singlets under the SM gauge group can always be added to the theory, one can easily add a Dirac mass term to neutrinos by introducing right-handed neutrinos ($SU(2)_L \times U(1)_Y$ singlets). In such case, the corresponding Yukawa interactions for neutrinos are

$$-\mathcal{L}_\nu^\text{mass} = (Y_\nu)_{ij} \bar{L}_{Li} \tilde{\Phi} \nu_{Rj} + \text{h.c.}. \tag{1.21}$$

This means that the neutrino Dirac mass matrix is

$$M_{\mathrm{D}} = Y_\nu \frac{v}{\sqrt{2}}. \tag{1.22}$$

Even if this mass term is a simple SM extension, it seems quite an unattractive scenario. To reach ∼eV neutrino masses the Yukawa couplings should be of the order $\sim \mathcal{O}(10^{-11})$. The need for such small Yukawa couplings suggests that the generation of neutrino masses arises from a different mechanism than all other SM fermions.

An alternative scenario to generate neutrino masses is to assume that left-handed neutrinos are Majorana particles. In this case, the mass term for left-handed neutrinos would be

$$-\mathcal{L}_\nu^{\mathrm{mass}} = M_{\mathrm{M}_{ij}} \bar{\nu}^C_{L_{L_i}} \nu_{L_{L_j}} + \mathrm{h.c.}. \tag{1.23}$$

This mass term violates lepton number by two units, breaking the $U(1)_{L_e} \times U(1)_{L_\mu} \times U(1)_{L_\tau}$ accidental symmetry presented in eq. (1.5). Such a mass term is not allowed in the SM for the other fermions due to electric charge conservation. But neutrinos are neutral particles.

If we want to generate a left-handed neutrino Majorana mass after spontaneous symmetry breaking, higher dimensional terms have to be introduced. As left-handed leptons and the Higgs field are $SU(2)_L$ doublets, a mass term such as $L_L L_L \phi$ is not invariant under the $SU(2)_L \times U(1)_Y$ gauge group, thus is forbidden in the SM. But, if one introduces higher order terms, for example $(\bar{L}_L \tilde{\phi})(\tilde{\phi}^T L_L^C)$, a Majorana mass term for left-handed neutrinos can be generated, as such a term is invariant under the SM gauge group. Nevertheless, this is a dimension 5 operator, which means it is not renormalizable and has to be suppressed by some mass scale. Generating left-handed neutrino masses with higher order operators is an attractive scenario, as the large mass suppression might be able to generate small neutrino masses.

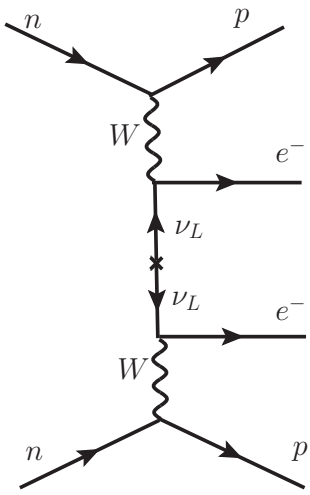

Figure 1.2: Feynman diagram for the neutrinoless double β decay due to a Majorana mass term for left-handed neutrinos.

Experimentally, a way to determine whether the nature of neutrinos masses is Dirac or

Majorana is through the search for the neutrinoless double β decay. This process consists of the decay of two neutrons into two electrons and two protons (see Fig. 1.2), hence violates lepton number by two units and can only take place if neutrino are Majorana particles. The current limits set by the GERDA collaboration for the half-life in neutrinoless double β decay are $T_{1/2}^{0\nu} > 2.1 \times 10^{25}$ years [42].

The see-saw mechanism

As previously discussed, there are two main scenarios to explain neutrino masses. Dirac neutrino masses can be generated by including right-handed neutrino singlets to the SM. Majorana masses can be accomplished by adding a non-renormalisable operator which is suppressed by some energy scale. The see-saw mechanism is a scenario which involves both a Dirac mass term, generated after spontaneous symmetry breaking, and a Majorana mass term for right-handed neutrinos. It provides a natural way to explain the smallness of neutrino masses in comparison with other SM fermions. This is known as the Type-I see-saw mechanism. The most general see-saw neutrino mass Lagrangian is

$$-\mathcal{L}_\nu^{\text{mass}} = (Y_\nu)_{ij}\bar{L}_{Li}\tilde{\Phi}\nu_{Rj} + M_{\text{M}_{ij}}\bar{\nu}_{R_i}^C\nu_{R_j} + \text{h.c.}. \tag{1.24}$$

In this case a Majorana mass term for right-handed neutrinos is not forbidden by any symmetry, as they are singlets under the SM gauge group. The mass matrix $\mathcal{M}_\nu$ in the neutrino flavour basis takes the form

$$\mathcal{M}_\nu = \begin{pmatrix} 0 & M_{\text{D}} \\ M_{\text{D}}^T & M_{\text{M}} \end{pmatrix}. \tag{1.25}$$

The key point of this scenario is that the Majorana mass scale can be much larger than the electroweak scale as it is not generated by electroweak symmetry breaking. If the mass matrix is diagonalised, one gets two different submatrices, M_1 and M_2

$$\mathcal{M}_\nu^{\text{diag}} = U^T\mathcal{M}_\nu U = \begin{pmatrix} M_1 & 0 \\ 0 & M_2 \end{pmatrix}. \tag{1.26}$$

Here M_1 is a 3×3 matrix which corresponds to the left-handed mass eigenstates and M_2 is an $n \times n$ matrix which contains the mass eigenvalues of the n right-handed neutrinos. Taking into account that $M_{\text{M}} \gg M_{\text{D}}$ these mass matrices can be approximated as

$$M_1 \simeq -M_{\text{D}}M_{\text{M}}^{-1}M_{\text{D}}^T, \qquad \text{and} \qquad M_2 \simeq M_{\text{M}}. \tag{1.27}$$

This means that the singular values of M_1 are suppressed by the large Majorana mass. In effective field theory, at energies much lower than M_{M}, right handed neutrinos are decoupled and left-handed neutrino masses can be described by a dimension-5 operator

$$-\mathcal{L}_\nu^{\text{eff}} = \frac{\kappa_{ij}}{2}(\bar{L}_{L_i}\tilde{\Phi})(\tilde{\Phi}^T L_{L_j}) + \text{h.c.} \tag{1.28}$$

where the coefficient κ_{ij} is defined as

$$\kappa_{ij} = Y_\nu M_{\rm M}^{-1} Y_\nu^T. \tag{1.29}$$

This is indeed the dimension-5 operator that was previously presented for Majorana masses. Here it naturally arises due to the large value of the Majorana mass term for right-handed neutrinos.

There are several advantages and disadvantages of the see-saw mechanism. In this scenario small left-handed neutrino masses are naturally reproduced due to the large suppression $\sim v^2/M_{\rm M}$ without the need of including very small Yukawa couplings in the neutrino sector. As a consequence, it also generates mixing in the lepton sector and new sources of CP violation. These kind of models are phenomenologically rich, as Lepton Flavour Violation (LFV) arises from the mixing terms. Also leptogenesis in the early Universe can be generated due to new sources of CP violation and Lepton Number Violation (LNV).

Even if the see-saw scenario is a attractive framework to explain the smallness of neutrino masses, it tends to generate a hierarchy between neutrino masses which is too large neutrino mass hierarchies [43]. As will later be discussed, this drawback is indeed cured when introducing an extra Higgs doublet to the model. Additionally, if one assumes Yukawa couplings comparable to the other SM Yukawa couplings, the new right-handed singlets need to be very heavy, too heavy to be produced at collider experiments. It is therefore a theoretical scenario which is experimentally difficult to test. Nevertheless, due to the high scale for new physics, the see-saw model predicts small contributions to LFV processes, in agreement with experimental bounds.

In this chapter we have presented the SM flavour sector and explained the evidence for and consequences of massive neutrinos. The main four open questions have been discussed are

- The strong mass hierarchies between SM fermions.
- The smallness and mildness of neutrino masses with respect to the quarks and leptons.
- The strong hierarchies in the quark mixing sector.
- The anarchical structure of the lepton mixing matrix.

In the next chapters we present different scenarios where we try to understand this pattern, commonly referred to as the flavour puzzle.

CHAPTER **2**

The Two Higgs Doublet Model

Even if the SM successfully describes the properties and interactions of almost all elementary particles, many extension in the scalar sector have been studied in order to explain the questions that the SM cannot solve. One of the simplest scenario is the SM extended by one additional Higgs doublet with the same quantum numbers as the SM Higgs boson. This model is known as the 2HDM. The new Higgs doublet can couple to the SM particles offering a rich phenomenology in different sectors: new sources of CP violation, effects on FCNCs and LFV, or even different dark matter scenarios.

In this chapter the theory of a general 2HDM is presented. First the theory of the most general 2HDM is described. This leads us to discuss the phenomenological implications on flavour observables in these scenarios. We then present different theoretical frameworks to reduce the impact of general 2HDM on flavour observables in order to fulfil the strong experimental constraints. Later, the CP violating part of a general 2HDM is explained. Finally we give a brief overview of the current direct searches of Higgs particles beyond the SM at the LHC.

2.1 The Model

The 2HDM is an extension of the SM with one extra Higgs doublet with the same quantum numbers as the SM Higgs. The most general scalar potential for two scalar doublets Φ_1 and Φ_2 with hypercharge $Y = \frac{1}{2}$ can be written as follows [44]

$$\begin{aligned} V = {} & m_{11}^2 \Phi_1^\dagger \Phi_1 + m_{22}^2 \Phi_2^\dagger \Phi_2 - \left(m_{12}^2 \Phi_1^\dagger \Phi_2 + \text{h.c.} \right) + \\ & + \frac{1}{2}\lambda_1 \left(\Phi_1^\dagger \Phi_1 \right)^2 + \frac{1}{2}\lambda_2 \left(\Phi_2^\dagger \Phi_2 \right)^2 + \lambda_3 \left(\Phi_1^\dagger \Phi_1 \right) \left(\Phi_2^\dagger \Phi_2 \right) + \lambda_4 \left(\Phi_1^\dagger \Phi_2 \right) \left(\Phi_2^\dagger \Phi_1 \right) + \\ & + \left[\frac{1}{2}\lambda_5 \left(\Phi_1^\dagger \Phi_2 \right)^2 + \lambda_6 \left(\Phi_1^\dagger \Phi_1 \right) \left(\Phi_1^\dagger \Phi_2 \right) + \lambda_7 \left(\Phi_2^\dagger \Phi_2 \right) \left(\Phi_1^\dagger \Phi_2 \right) + \text{h.c.} \right]. \end{aligned} \tag{2.1}$$

The two complex $SU(2)$ doublets contain a total of eight fields

$$\Phi_a = \begin{pmatrix} \phi_a^+ \\ \phi_a^0 \end{pmatrix} = \begin{pmatrix} \phi_a^+ \\ (v_a + \rho_a + i\eta_a)/\sqrt{2} \end{pmatrix} \tag{2.2}$$

where $a = 1, 2$, $v_1/\sqrt{2}$ and $v_2/\sqrt{2}$ correspond to the values of the vev of each field after spontaneous electroweak symmetry breaking

$$\langle \Phi_a \rangle = \begin{pmatrix} 0 \\ \frac{v_a}{\sqrt{2}} \end{pmatrix}. \tag{2.3}$$

Note that this is not the most general vacuum for the 2HDM, as in the most general case, $\langle \Phi_2 \rangle$ is

$$\langle \Phi_2 \rangle = \begin{pmatrix} u \\ \frac{v_2}{\sqrt{2}} e^{i\xi} \end{pmatrix} \tag{2.4}$$

where u and ξ are real numbers. Nevertheless, if $u \neq 0$, the photon becomes a massive particle [45]. The value of ξ determines if there is spontaneous symmetry breaking of CP (see [44] for a review). We set these two parameters to 0.

There are several conditions that the scalar potential should fulfil. First, there should not be any directions in field space in which the Higgs potential $V \to -\infty$. The necessary and sufficient conditions to fulfil this requirement are [46, 47]

$$\begin{aligned} &\lambda_1 > 0 && \lambda_2 > 0 \\ &\lambda_3 > -\sqrt{\lambda_1 \lambda_2} && \lambda_3 + \lambda_4 - |\lambda_5| > -\sqrt{\lambda_1 \lambda_2} \end{aligned} \tag{2.5}$$

Second, the conditions for minimizing the Higgs potential are [48]

$$m_{11}^2 = m_{12}^2 \tan\beta - \frac{1}{2} v^2 \left[\lambda_1 \cos^2_\beta + \lambda_{345} \sin^2\beta + 3\lambda_6 \sin\beta \cos\beta + \lambda_7 \sin^2\beta \tan\beta \right] \tag{2.6}$$

$$m_{22}^2 = m_{12}^2 \tan^{-1}\beta - \frac{1}{2} v^2 \left[\lambda_1 \sin^2_\beta + \lambda_{345} \cos^2\beta + 3\lambda_6 \cos^2\beta \tan^{-1}\beta + \lambda_7 \sin^2\beta \cos\beta \right] \tag{2.7}$$

where $\lambda_{345} = \lambda_3 + \lambda_4 + \lambda_5$, $\tan\beta = \frac{v_2}{v_1}$ and $v^2 = v_1^2 + v_2^2$. Note that not all the Higgs fields are physical. Three out of the eight scalar fields are Goldstone bosons that give mass to the $W^\pm$ and Z bosons, just as in the SM. The remaining five fields correspond to physical Higgs bosons.

The Higgs Basis

In the most general 2HDM the scalar fields Φ_1 and Φ_2 are indistinguishable. This means that one can always redefine the Higgs fields as an orthonormal linear combination of the fields in eq. (2.2) without changing any phenomenological prediction of the model. In other words, the

doublets can always be rotated to a new Higgs basis through the following transformation

$$\begin{pmatrix} \bar{\Phi}_1 \\ \bar{\Phi}_2 \end{pmatrix} = \begin{pmatrix} \cos\chi & \sin\chi \\ -\sin\chi & \cos\chi \end{pmatrix} \begin{pmatrix} \Phi_1 \\ \Phi_2 \end{pmatrix}. \tag{2.8}$$

Therefore, one can always rotate to the basis where just one of the Higgs , in this case $\bar{\Phi}_1$, has a vev $v = \sqrt{v_1^2 + v_2^2}$ and $\left\langle \bar{\Phi}_2 \right\rangle = 0$. This is done by choosing $\chi = \beta$, with β defined above. This basis is known as the Higgs basis [49]. In this basis, the charged Goldstone bosons and the physical charged Higgs states can be written in terms of the initial fields $\phi_1^\pm$ and $\phi_2^\pm$ as

$$\begin{aligned} G^\pm &= \phi_1^\pm \cos\beta + \phi_2^\pm \sin\beta \\ H^\pm &= -\phi_1^\pm \sin\beta + \phi_2^\pm \cos\beta. \end{aligned} \tag{2.9}$$

The neutral Goldstone boson and the physical pseudoscalar are calculated as linear combinations of the imaginary fields of the Higgs doublets

$$\begin{aligned} G^0 &= \eta_1^\pm \cos\beta + \eta_2^\pm \sin\beta \\ A &= -\eta_1^\pm \sin\beta + \eta_2^\pm \cos\beta. \end{aligned} \tag{2.10}$$

Finally the SM Higgs boson (the neutral CP-even Higgs field in Φ_1, when working in the Higgs basis) would be

$$h_{SM} = \rho_1 \cos\beta + \rho_2 \sin\beta \tag{2.11}$$

and the other CP-even state

$$h_2 = -\rho_1 \sin\beta + \rho_2 \cos\beta. \tag{2.12}$$

Making this basis rotation of the fields means that the parameters in the scalar potential also have to be redefined to the new basis. But as mentioned above, such a redefinition does not change the physics of the model.

The masses of the five Higgs fields can be calculated from the Higgs potential [48, 50]. For CP-odd state A and charged Higgs, the masses are given by

$$m_A^2 = \frac{m_{12}^2}{\sin\beta\cos\beta} - v^2\lambda_5 \tag{2.13}$$

$$m_{H^\pm} = m_A^2 + \frac{1}{2}v^2\left(\lambda_5 - \lambda_4\right). \tag{2.14}$$

The masses of the neutral CP-even Higgs have to be calculated from the diagonalisation of the

following squared mass matrix

$$\mathcal{M}^2 = \begin{pmatrix} (m_A^2 + \lambda_5 v^2)\sin^2\beta + \lambda_1 v^2 \cos\beta^2 & (-m_A^2 - \lambda_5 v^2 + \lambda_{345} v^2)\sin\beta\cos\beta \\ (-m_A^2 - \lambda_5 v^2 + \lambda_{345} v^2)\sin\beta\cos\beta & (m_A^2 + \lambda_5 v^2)\cos^2\beta + \lambda_2 v^2 \sin\beta^2 \end{pmatrix}. \quad (2.15)$$

Hence, the masses for the neutral CP-even Higgs bosons are

$$m^2_{H^0,h} = \frac{1}{2}\left[\mathcal{M}^2_{11} + \mathcal{M}^2_{22} \pm \sqrt{(\mathcal{M}^2_{11} - \mathcal{M}^2_{22}) + 4(\mathcal{M}^2_{12})^2}\right] \quad (2.16)$$

where H^0 and h are the mass eigenstates, $\mathcal{M}^2_{ij}$ corresponds to the ij entry of the $\mathcal{M}^2$ matrix. The initial Higgs ρ_1, ρ_2 and the mass eigenstates neutral Higgs bosons h, H^0 are related as follows

$$\begin{aligned} H^0 &= \rho_1 \cos\alpha + \rho_2 \sin\alpha \\ h &= -\rho_1 \sin\alpha + \rho_2 \cos\alpha. \end{aligned} \quad (2.17)$$

where α is the rotation angle which diagonalises $\mathcal{M}^2$. If one then calculates what would the SM Higgs boson be in terms of the mass eigenstates and the rotation angles α and β, one finds

$$h_{SM} = H^0 \cos(\beta - \alpha) + h \sin(\beta - \alpha) \quad (2.18)$$

therefore, h corresponds to the SM Higgs boson only when $\cos(\beta - \alpha) = 0$.

Yukawa Interactions

The interactions of the Higgs fields with fermions are contained in the Yukawa part of the Lagrangian. The Yukawa couplings in a general 2HDM take the form

$$-\mathcal{L}^{\text{Yuk}} = (Y_u^{(a)})_{ij} \bar{Q}_{Li} \tilde{\Phi}_a u_{Rj} + (Y_d^{(a)})_{ij} \bar{Q}_{Li} \Phi_a d_{Rj} + (Y_e^{(a)})_{ij} \bar{L}_{Li} \Phi_a e_{Rj} + \text{h.c.} \quad (2.19)$$

where $i, j = 1, 2, 3$ are flavour indices, $a = 1, 2$ is the Higgs index, $\tilde{\Phi}_a = i\tau_2 \Phi_a^*$ and $Y^{(a)}_{u,d,e}$ are the 3×3 Yukawa matrices for each fermion type. This part of the Lagrangian contains a large number of free parameters. These Yukawa interactions are the responsible for the Dirac masses of the fermion sector of the SM after spontaneous symmetry breaking, except for the neutrino sector. Assuming Φ_1 acquires all the vev, the quark and charged lepton masses are proportional to the singular values of the Yukawa interactions with Φ_1, exactly as for the SM Higgs presented in Chapter 1. The quark mixing matrix V_{CKM} is determined from the left-handed eigenvectors of the up and down Yukawa couplings.

The Yukawa sector of a general 2HDM induces tree level FCNCs. In the SM, the diagonalisation of the mass matrices automatically diagonalises the Yukawa interactions avoiding tree level FCNC. In the general 2HDM the Yukawa interactions with both Higgs in principle cannot be simultaneously diagonalised. In the Higgs basis, once the Yukawa couplings with Φ_1 are diagonalised as in eq. (1.3), the Yukawa couplings with Φ_2 also have to be rotated to the same

basis as follows

$$\widetilde{Y}_{\tilde{x}}^{(2)} = V_{\tilde{x}_L}^{\dagger} Y_{\tilde{x}}^{(2)} V_{\tilde{x}_R} \tag{2.20}$$

where $\tilde{x} = u, d, e$. Here $\widetilde{Y}_{\tilde{x}}^{(2)}$ is in general a non-diagonal matrix. Therefore, FCNCs quark-Higgs interactions at tree level arise from the non-diagonal entries in $\widetilde{Y}_{\tilde{x}}^{(2)}$. These couplings are strongly constrained by precision flavour observables and cannot be avoided unless some symmetry is imposed. The impact of the Yukawa couplings on flavour physics and methods to accommodate a 2HDM with the stringent experimental limits are discussed in more detail in Section 2.2. Finally, the Yukawa couplings are complex matrices. Hence, the couplings with Φ_2 carry new CP violating phases. CP violation in a general 2HDM is discussed in detail in Section 2.4.

Here it has been assumed that right-handed neutrinos do not exist and therefore there is no Dirac mass term for neutrinos. If right-handed neutrinos would couple to the Higgs bosons via Yukawa interactions and this would be the only coupling that generates neutrino masses, the flavour discussion for the lepton sector would be exactly equivalent to the quark flavour sector.

Gauge Bosons Interactions

Introducing new Higgs doublets in the model does not only generate new Yukawa couplings with the fermionic sector but also new couplings to the SM vector bosons. Nevertheless, not all combinations of Higgs bosons are allowed to couple with gauge bosons. For example, CP is conserved in the scalar sector at tree level. Therefore couplings such as ZhH are forbidden. Trilinear couplings with two identical Higgs bosons such as Zhh are forbidden due to Bose statistics. The allowed couplings for a 2HDM are summarised in Table (2.1) [51].

$\cos(\beta-\alpha)$	$\sin(\beta-\alpha)$	Angle Independent
$H^0W^+W^-$	hW^+W^-	$VV\phi\phi,\ VVAA,\ VVH^+H^-$
H^0ZZ	hZZ	γH^+H^-
ZAh	ZAH^0	ZH^+H^-
$W^\pm H^\mp h$	$W^\pm H^\mp H^0$	$W^\pm H^\mp A$
$ZW^\pm H^\mp h$	$ZW^\pm H^\mp H^0$	$ZW^\pm H^\mp A$
$\gamma W^\pm H^\mp h$	$\gamma W^\pm H^\mp H^0$	$\gamma W^\pm H^\mp A$

Table 2.1: Dependence of the couplings between gauge bosons and Higgs bosons in a 2HDM as a function of the mixing angles α and β. Here $\phi = h$ or H^0 and $VV = W^+W^-,\ ZZ,\ Z\gamma$, or $\gamma\gamma$.

It is important to remark that there are no couplings of the neutral Higgs to photons or gluons at tree level. Nevertheless, these couplings do appear at the one loop level and are particularly important for Higgs production at colliders via processes of gluon-gluon fusion or neutral Higgs detection via $\gamma\gamma$ decay.

2.2 Flavour Physics in a 2HDM

As previously explained, in a general 2HDM there is no way to simultaneously diagonalise both Yukawa matrices for a given type of quark. The off-diagonal elements of the Yukawa matrices lead to FCNCs processes which strongly constrain the parameter space of the model due to the stringent experimental limits. In this section an overview of the impact of a general 2HDM on flavour observables is presented. We can divide such processes into two types: tree level and loop processes. We assume we are working in the Higgs basis, hence all the flavour effects beyond the SM come from the Yukawa couplings with $\Phi^{(2)}$.

Tree Level Contributions

In the 2HDM there are two kind of processes that receive tree level contributions from the Yukawa couplings: FCNCs and charged current processes. First of all, a model with flavour changing neutral Yukawa couplings (with h, H^0 and A) at tree level gives rise to FCNCs processes at tree level. As experiments are in very good agreement with the SM, FCNCs are strongly constrained. Hence any kind of new physics which contributes to such processes must be strongly suppressed. We can divide the tree level FCNCs in two different kind of processes

- Muonic decays of neutral mesons such as $B_{s,d} \to \mu^+\mu^-$, $K_L \to \mu^+\mu^-$ or $\bar{D}^0 \to \mu^+\mu^-$. The Feynman diagram corresponding to these kind of processes is shown on the left panel in Fig. 2.1,
- $\Delta\mathrm{F} = 2$ processes such as $K - \bar{K}$, $D_0 - \bar{D}_0$ or $B_{s,d} - \bar{B}_{s,d}$ mixing. The Feynman diagram for these kind of processes is presented on the right panel in Fig 2.1.

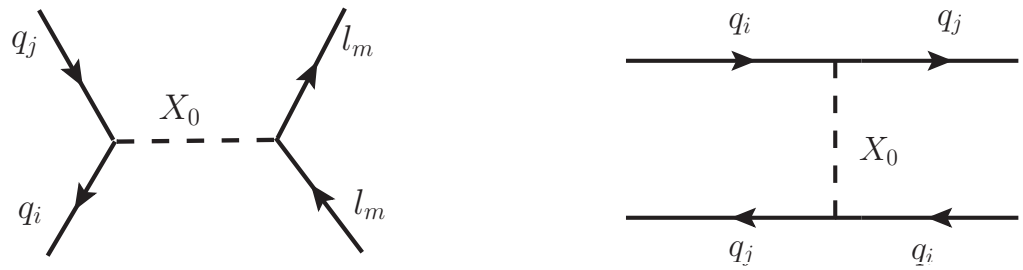

Figure 2.1: Tree level FCNCs processes generated via neutral Higgs Yukawa couplings in a general 2HDM. Left: Feynman diagram contributing to muonic neutral meson decays. Right: Feynman diagram contributing to ΔF=2 processes. X_0 corresponds to h, H^0 or A.

If the lepton sector is also taken into account, one can have a third kind of process from the coupling with neutral mesons.

- Flavour changing lepton decays such as $\tau \to \mu\mu\mu$ and $\mu \to eee$. The Feynman diagram corresponding to the first process is represented in Fig 2.2.

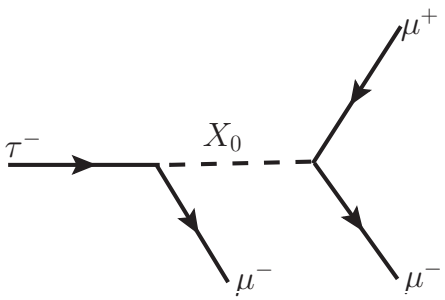

Figure 2.2: Feynman diagram in a general 2HDM contributing to LFV τ decay. X_0 corresponds to h, H^0 or A.

Second, the 2HDM also contributes at tree level to charged current processes. These kind of processes, already exist in the SM and are mediated by a W boson. Some examples are $B \to \tau\nu$, $B \to D\tau\nu$ or $D \to \tau\nu$. These kinds of meson decays are particularly interesting to study due to the large coupling of third generation of fermions to charged Higgs particles. Experimental results from the BABAR collaboration studying semileptonic B decays showed discrepancies with respect to the SM for different channels at 3.4 σ when combined [52]. If these results are confirmed, new physics is needed to explain them. The Feynman diagram of the charged Higgs contributing to the $B \to D\tau\nu$ processes as example is shown in Fig. 2.3.

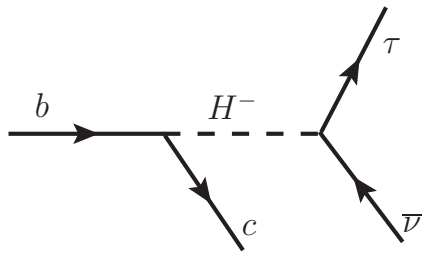

Figure 2.3: Feynman diagram of the $B \to D\tau\nu$ process via tree level Yukawa couplings.

Nevertheless, as such processes already exist in the SM at tree level, FCNCs are usually more interesting observables from a phenomenological point of view.

Loop Contributions

The good agreement of experiments with the SM predictions already constraints a large part of the parameter space of the 2HDM with the tree level processes described above. Nevertheless, there are also stringent constraints coming from one loop processes which give further information of the unconstrained area of the parameter space of the model. Even if the tree level processes previously discussed also receive a radiative corrections, in this part we only discuss processes which first appear at the one loop level. For the quark sector, the Yukawa couplings to the top quark remain unconstrained from tree level contributions. In Fig. 2.4 the $B \to X_s\gamma$ meson decay through a one loop contribution is shown. This decay is an example of a radiative process that

constraints part of the remaining parameter space.

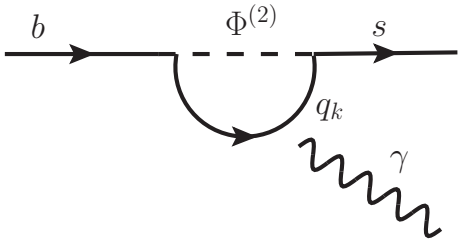

Figure 2.4: Feynman diagram contributing to $b \to s\gamma$ process via one loop process. Here $\Phi^{(2)}$ corresponds to h, H^0, A or H^-

In the lepton sector, processes such as $\mu \to e\gamma$ or the magnetic moment of a charged lepton, which appear at the loop level, can also strongly constraint the Yukawa sector. In particular, these kind of processes do not only receive contributions from one loop diagrams, but can have stronger contributions from a two loop diagram known as the Barr-Zee diagram [53] in some regions of the parameter space. The one and two loop diagrams for the $\mu \to e\gamma$ processes are shown in Fig. 2.5.

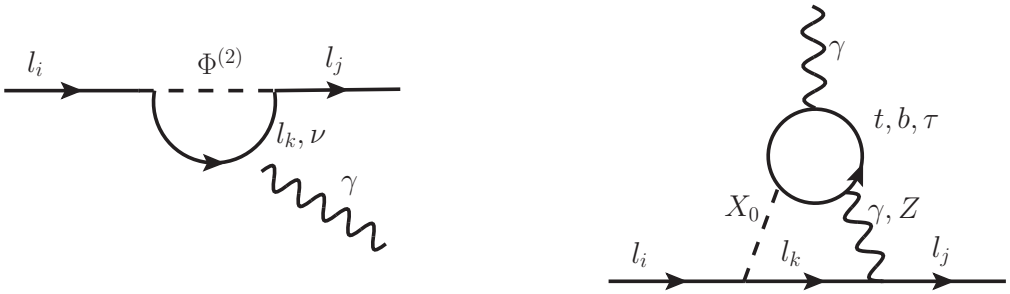

Figure 2.5: Radiative Feynman diagrams contributing to the $l \to l'\gamma$ process. The right panel shows the one loop diagram. The left panel shows the two loops (Barr-Zee) diagram. Here $\Phi^{(2)}$ corresponds to h, H^0, A or H^- and X_0 corresponds to h, H^0 or A

These are some of the flavour observables which receive significant contributions from new Yukawa interactions in a general 2HDM. Such processes are strongly constrained by the stringent flavour experimental constraints hence, need to be suppressed. In the next section, different methods to make new Yukawa couplings compatible with experimental data are discussed.

2.3 Suppressing Flavour Effects

We discuss here three different approaches to suppress large contributions to flavour observables from Yukawa couplings in a general 2HDM. These methods are natural scenarios with absence of fine-tuning in the Yukawa sector to accommodate flavour constraints. It is important to mention that LFV is absent because neutrinos are massless particles in the SM. However, it is known that neutrinos do have mass and the lepton sector mixes through weak interactions. Also, as we have

just seen, in a general 2HDM there are LFV processes that appear via Yukawa couplings with charged leptons. We keep the assumption of massless neutrinos for the discussion in this section and just focus on the quark sector. Nevertheless, this issue is addressed in the next chapters.

2.3.1 Type-I and II 2HDM

The most popular models that avoid FCNCs processes at tree level are the Type I and the Type II 2HDM. In the Type I 2HDM [54, 55] quarks couple to just one of the Higgs doublets. This can be achieved by imposing a Z_2 symmetry under which the two Higgs doublets transform as

$$(\Phi_1, \Phi_2) \xrightarrow{Z_2} (-\Phi_1, \Phi_2)\,. \tag{2.21}$$

Fermions are even under this symmetry. This is calculated in a general basis, therefore quarks just acquire their masses from the vev of Φ_2. Hence, the Yukawa Lagrangian reads

$$-\mathcal{L}^{\text{Yuk}} = (Y_u^{(2)})_{ij}\bar{q}_{Li}u_{Rj}\tilde{\Phi}_2 + (Y_d^{(2)})_{ij}\bar{q}_{Li}d_{Rj}\Phi_2 + (Y_e^{(2)})_{ij}\bar{L}_{Li}e_{Rj}\Phi_2 + \text{h.c.}. \tag{2.22}$$

The scalar Higgs potential also changes after imposing the Z_2 symmetry: the terms λ_6, λ_7 and m_{12}^2 do not appear in these models unless Z_2 is violated.

In the Type II 2HDM [55, 56], the right-handed up family couples to one of the Higgs doublet whereas the right-handed down family couples to the other one. This can be fulfilled by imposing a Z_2 symmetry, equivalent to the Type I 2HDM for the Higgs sector but

$$u_R \xrightarrow{Z_2} u_R \qquad \text{and} \qquad d_R \xrightarrow{Z_2} -d_R \tag{2.23}$$

for the fermion sector. This transformation can also be interchanged for up and down right-handed quarks.

As the Higgs fields transform equally for both models, the Higgs potential in the Type II 2HDM is the same as the Type I 2HDM. However, some models in the literature assume that the imposed Z_2 symmetry is softly broken by including the m_{12}^2 term in the Higgs potential. It is important to remark that Supersymmetric models have the same Yukawa couplings as the Type II model.

In general in the Type II 2HDM, for the lepton sector, it is assumed that charged right-handed leptons transform as the down sector. Yet, this is not a necessary condition and in the literature some models impose that leptons transform as up quarks under the Z_2 symmetry. These models are known as flipped 2HDM [57]. Also, lepton-specific models assume that quarks behave as a Type I scenario (therefore just couple to Φ_2) whereas leptons couple to Φ_1 [58, 59].

In conclusion, the Type I and Type II 2HDM assume that there is one single Yukawa matrix for each fermion, coupling just to one single Higgs doublet. As a consequence, all Yukawa matrices can be diagonalised at the same time and no FCNCs appear at tree level.

2.3.2 The Aligned 2HDM

The aligned limit for the 2HDM [60] is another scenario in which a new Higgs doublet is added to the SM without FCNCs at tree level. In these kind of models FCNCs are avoided by imposing that the Yukawa couplings of the two doublets are aligned in flavour space. In other words, the Yukawa matrices have to be proportional to each other (separately for $u,\ d$ type quarks and charged leptons)

$$Y_{\tilde{x}}^{(2)} = A_{\tilde{x}}^{(2)} Y_{\tilde{x}}^{(1)} \tag{2.24}$$

where $\tilde{x} = u,\ d,\ e$. Here $Y_{\tilde{x}}^{(1)},\ Y_{\tilde{x}}^{(2)}$ are the Yukawa couplings with Φ_1 and Φ_2, respectively, and $A_{\tilde{x}}^{(2)}$ are arbitrary complex numbers. This scenario guarantees that all Yukawa matrices can simultaneously be diagonalised, avoiding FCNCs at tree level. Of course, in the Higgs basis, the singular values of $Y_x^{(1)}$ are proportional to the masses of quarks and charged leptons. In such scenario, the only source of flavour violation comes from the CKM matrix, which does not only appear in weak interactions via the W boson, but also in the Yukawa couplings of the charged scalars in Φ_2. Nevertheless, quantum corrections spoil the alignment between the Yukawa couplings [61].

What makes these models particularly interesting is the freedom of the parameters $A_x^{(2)}$. The fact that the Yukawas are aligned avoids tree level FCNCs but $A_{\tilde{x}}^{(2)}$ are complex couplings which can acquire any value, leading to new sources of CP violation even in the absence of FCNCs at tree level. In this scenario, the Higgs potential is the same as the general 2HDM potential.

2.3.3 Ansatz on the Yukawa Textures

The suppression of FCNCs in a general 2HDM can be achieved by assuming a determined texture for the Yukawa matrices. In [62] Cheng-Sher proposed a framework where FCNCs are proportional to the square root of the masses of the quarks involved. The Cheng-Sher *ansatz* states that in the Higgs basis, the Yukawa matrices of quarks with Φ_2 take a hierarchical structure following

$$\left(Y_q^{(2)}\right)_{ij} = \Delta_{ij}^q \frac{\sqrt{m_i m_j}}{v} \tag{2.25}$$

where Δ_{ij}^q are Yukawa matrix parameters which determine the texture of the Yukawa coupling and are model dependent (see for example [63] for the six-texture form of the mass matrix or [64] for the four-flavour form). The bounds on Δ_{ij}^q can be derived from experimental limits and depend on the mass of the Higgs bosons.

This framework controls the FCNCs processes as, if one assumes $\Delta_{ij}^q \sim \mathcal{O}(1)$, the Yukawa couplings with the first two generations, which set the most stringent FCNCs bounds, become strongly suppressed. In contrast with the Type I, Type II and the alignment limit, using this *ansatz*, FCNC are not avoided at tree level, as the framework predicts non-vanishing non-diagonal entries in the Yukawa couplings with Φ_2 in the Higgs basis. This means that even if this scenario can fulfil the strong experimental constraints, experiments might be able to detect the small off-diagonal Yukawa couplings.

2.3.4 The Decoupling Limit

Another natural scenario to avoid large FCNCs processes arising from Yukawa couplings in a 2HDM is the decoupling limit [48, 50]. This limit does not eliminate FCNCs at tree level but instead suppresses them by increasing the new physics scale, making it much larger than the electroweak scale. In other words, this limit is accomplished by imposing the masses of the four Higgs $H^0,\ H^\pm,\ A$ are much larger than the mass of the h boson,

$$m_A \simeq m_{H^0} \simeq m_{H^\pm} \gg m_h \sim v. \tag{2.26}$$

In this limit, the effects of the heavy Higgs states are decoupled at low energies, relevant for current experiments. A consequence of the decoupling limit is that the mixing angles α and β defined above have to fulfil $\cos(\alpha-\beta) \simeq 0$. This can be shown as follows.

First, let us assume that the Higgs self-couplings are $\sim \mathcal{O}(1)$. Second, once $m_{H^0} \gg m_h$ is assumed, from eq. (2.16) one finds [48]

$$m_{H^0}^2 \simeq m_A^2 \tag{2.27}$$

$$m_h^2 \simeq f_{11}(\lambda_i)\cos^2\beta + f_{22}(\lambda_i)\sin^2\beta + f_{12}(\lambda_i)\sin 2\beta \sim \mathcal{O}(v^2) \tag{2.28}$$

where $f_{11,22,12}(\lambda_i)$ are the 11, 22, and 12 part of the matrix entries in eq. (2.15) which do not contain m_A^2, respectively. If one calculates the value of $\cos(\beta-\alpha)$ in this scenario one finds (see [48] for a detailed calculation)

$$\cos(\beta-\alpha) \simeq \mathcal{O}\left(\frac{m_h^2}{m_{H^0}^2}\right) \simeq 0. \tag{2.29}$$

Thus, in this limit the light field h behaves as the SM Higgs. This means that all the couplings with the gauge bosons summarized in Table 2.1 which are proportional to $\cos(\alpha-\beta)$ vanish.

As in the Cheng-Sher *ansatz*, the decoupling limit there is no basis in which all the Yukawa couplings can be simultaneously diagonalised. When rotating to the fermion mass basis, the only flavour violating couplings are contained in the Yukawa couplings with Φ_2. This can be seen from eq. (2.20). Not only do these Yukawa couplings generate tree level FCNCs but also new sources of CP violation. Even if new physics effects in the decoupling limit are suppressed by the square or even the fourth power of the mass of the heavy Higgs, they are phenomenologically interesting, as the Yukawa couplings to the new bosons generate new flavour and CP violating processes which could be detectable.

2.4 CP violation

In the SM, the hermiticity of the Higgs potential requires all its parameters to be real. This means that all the CP violation in the SM comes from the Yukawa sector. After the rotation of the fermion fields, just one CP violating phase remains physical for quarks (and one for leptons, assuming that neutrinos have Dirac masses). This is the CKM CP phase. In contrast to this

scenario, the general 2HDM contains further physical complex phases, not only in the Yukawa matrices but also in the Higgs potential. In this section CP violation in a general 2HDM is presented. Remember we chose the vev for both Higgs doublets to be real to avoid spontaneous CP violation.

The Scalar Sector

The scalar potential of a general 2HDM is written in eq. (2.1). The Higgs potential is hermitian, therefore the parameters $m_{11}^2,\ m_{22}^2,\ \lambda_1,\ \lambda_2,\ \lambda_3$ and λ_4 have to be real. The remaining parameters $m_{12}^2,\ \lambda_5,\ \lambda_6$ and λ_7 can be complex. The Higgs potential contains then a total of 14 parameters, 10 real and 4 complex. Let us now discuss how many of these parameters are actually physical.

The scalar doublets Φ_1 and Φ_2 can always be rotated to a new Higgs basis by a unitary transformation $\Phi'_a = U\Phi_a$ where U is a $U(2)$ matrix [44]:

$$U = e^{-i\psi}\begin{pmatrix} \cos\theta & e^{-i\xi}\sin\theta \\ -e^{i\chi}\sin\theta & e^{i(\chi-\xi)}\cos\theta \end{pmatrix}. \tag{2.30}$$

Of course, the parameters in the potential also have to be transformed when the fields are redefined. Such a transformation can therefore be used to absorb non-physical parameters from the potential. Here, the ψ phase does not change the scalar potential parameters as it is a global $U(1)$ rotation. Consequently, only the remaining three parameters in the U matrix can be used to absorb three parameters (2 complex and 1 real) from the potential, leaving the latter with only 11 physical parameters. In other words, one can rotate to the basis where the Higgs mass matrix is diagonal (m_{12}^2=0), eliminating two degrees of freedom (1 real and 1 complex) and then rephase Φ_2 (eliminating a further complex parameter), leaving the 2HDM potential with a total of two CP violating phases.

The Scalar-Fermion Sector

In this subsection new sources of CP violation coming from the scalar-fermion Yukawa interactions in a general 2HDM are presented. To begin with the discussion, we start calculating the CP violating phase coming from the SM Yukawa couplings in the quark sector. The SM quark Yukawa Lagrangian is in general a complex matrix. Nevertheless one can always rotate the quark fields to the mass basis

$$\begin{aligned} u_L &\to V_{u_L} u_L & \qquad d_L &\to V_{d_L} d_L \\ u_R &\to V_{u_R} u_R & \qquad d_R &\to V_{d_R} d_R. \end{aligned} \tag{2.31}$$

With such a field rotation the Yukawa matrices can be diagonalised with positive values in the diagonal. This means that the phases in the Yukawa sector disappear. Of course, the phases do not actually disappear but are transferred to the charged current couplings through the CKM matrix. The CKM matrix with 3 quark generations is a 3×3 unitary matrix, which can be parametrized with a total of 9 degrees of freedom (3 angles and 6 phases). Yet, one can still

rephase the quark fields in order to remove five of these phases, leaving the CP violating phase of the CKM matrix. The SM CP violating phase can be parametrized through the Jarlskog invariant defined in eq. (1.10).

Let us continue the discussion in the basis where just one CP violating phase appears in the CKM matrix with diagonal Yukawa couplings with Φ_1. Once Φ_2 is introduced, two new complex Yukawa couplings appear, $Y_u^{(2)}$ and $Y_d^{(2)}$. Each matrix contains 9 real and 9 complex parameters. None of the complex parameters can be eliminated with the rotation of the quark fields (unless some of the entries of the Yukawa couplings are 0 or assumed to be real). Else, new phases would appear in the SM sector. Therefore, a general 2HDM has 18 complex parameters in the scalar-fermion sector for quarks in addition to the CP violating CKM phase .

A similar description can be done for the lepton sector. However, as the nature of neutrino masses still remains undiscovered, the properties of CP violation in the lepton sector are unknown.

2.5 Direct searches for new Higgs bosons

In July 2012 the ATLAS and CMS collaborations announced the observation of a new particle compatible with the SM Higgs boson. This particle has a mass of about 125 GeV. After this discovery, the parameter space for 2HDM has been significantly constrained. Searches for new Higgs boson states had already been done by other experiments such as the LEP experiments or Tevatron. None of these experiments found signals of new physics and were only able to set limits in the parameter space. Nevertheless, with the second LHC run a new area of the parameter space in the 2HDM will be uncovered or even signals of physics beyond the SM compatible with new Higgs bosons might be detected.

In this section some of the latest results for new Higgs boson searches for both Run-I and Run-II of the LHC are presented to give an idea of the current experimental status of direct searches for new Higgs bosons.

ATLAS: Run I

In this part some of the latest results from the ATLAS collaboration for the Run-I at the LHC are summarised. The searches during the first run did not show any strong evidence for physics beyond the SM. The following studies have been done with an energy of $\sqrt{s} = 8$ TeV and integrated luminosity of 20.3 fb^{-1}.

Neutral Higgs boson

- The ATLAS collaboration has set an upper limit on $\sigma(gg \to A) \times \text{BR}(A \to Zh_{SM}) \times \text{BR}(h_{SM} \to f\bar{f})$, where h_{SM} corresponds to the Higgs boson detected with a mass of 125 GeV. The analysis has been done for A boson masses in a range from 220 to 1000 GeV, in the context of a general 2HDM. The results are 0.098 to 0.013 pb for $f = \tau$ and 0.57 to 0.014 pb for $f = b$ [65].

- Searches for neutral Higgs decays in different channels have been able to exclude regions of the 2HDM parameter space and set a lower limit pseudoscalar mass $m_A > 370$ GeV [66] in the context of the "h" Minimal Supersymmetric Standard Model (hMSSM) [67].

- The ATLAS collaboration has investigated the process $t \to h_{SM} q$ with $q = u$ or c. This process does not exist at tree level in the SM and is suppressed at higher orders due to the GIM mechanism. New particles inside the loops tend to enlarge the branching ratio of such processes. The ATLAS collaboration has set limits on the branching ratio of the process, leading to the most stringent bounds on the Yukawa couplings $y_{tc}^{(1)} < 0.13$ and $y_{tu}^{(1)} < 0.13$ [68].

Charged Higgs boson

- The existence of charged Higgs bosons has also been studied by the ATLAS collaboration. The latest study regarding these searches is presented in [69], through the decay $H^+ \to tb$ in the context of a general 2HDM. A mass range between $m_{H^\pm} = 200 - 600$ GeV has been explored with a production via $gb \to tH^+$, (with electron or muon final state). An excess of 2.4 standard deviations is found for values $m_{H^\pm} = 300$ and 400 GeV. For masses between 0.4 and 2.0 TeV (with electron or muon final state) and 1.5–3.0 TeV (for hadronic final state) the s-channel production $qq' \to H^\pm$. No significant excess is found and just upper limits on the $\sigma(qq' \to H^\pm) \times BR(H^+ \to tb)$ were set: 0.13 and 6.7 pb, 0.09 and 0.22 pb, respectively.

ATLAS: Run II

In December 2015 the ATLAS collaboration has released the first results for the second LHC run with searches of new neutral Higgs bosons in the context of the Minimal Supersymmetric Standard Model (MSSM) in the m_h^{mod} scenario, defined in [70], at 3.2 fb^{-1} luminosity. The study has been done in a mass range 200 GeV – 1.2 TeV for neutral Higgs boson decaying into $\tau\tau$ and $b\bar{b}$ [71]. No signal has been found for either of the searches and have just been able to set bounds on the parameter space. However ATLAS has observed an excess in the diphoton channel at 750 GeV with a local significance of 3.6 σ and a second excess at 1.6 TeV with a local significance of 2.8 σ [72].

CMS: Run I

The CMS collaboration results in Run-I regarding searches for Higgs bosons are in agreement with the ATLAS searches. There is no strong evidence for physics beyond the SM. Here we present the latest CMS results regarding searches for new scalar bosons during Run-I. The results correspond to pp collisions with a center-of-mass energy of $\sqrt{s} = 8$ TeV and luminosity of 19.7 fb^{-1}.

Neutral Higgs boson

- The CMS collaboration has presented the results of searches for heavy scalar bosons decaying via $H^0 \to h_{SM} h_{SM}$ in a mass range of $260 < m_{H^0} < 350$ GeV heavy pseudoscalar bosons decaying via $A \to Z\ h_{SM}$ in a mass range of $220 < m_A < 350$ GeV. The interpretation has been done in the MSSM with low $\tan\beta$ and 2HDM Type-II scenarios. The results have showed no excess, and CMS has just been able to set upper limits on the cross section of the process [73].

- Further searches for pseudoscalar Higgs bosons have been presented in [74] for the $A \to \tau\tau$ decay, produced in association with a $b\bar{b}$ pair, in the context of a Type-II 2HDM. The results are consistent with the SM predictions. A pseudoscalar Higgs with a mass below 80 GeV in a Type-II scenario (coupling to down-type quarks) is excluded.

Charged Higgs boson

- The process $t \to H^{\pm} b$ and $H^{\pm} \to c\bar{s}$ for light charged Higgs has been studied in the context of a general 2HDM [75]. No signal of such process has been found. Therefore just an upper limit on $\mathrm{Br}(t \to H^{\pm} b)$ of 1.2 to 6.5 % has been set for masses between 90 and 160 GeV (assuming a $\mathrm{Br}(H^{\pm} \to c\bar{s})$=100%).

CMS: Run-II

The CMS collaboration has presented a similar result to the one of the ATLAS collaboration of the signal on the two-photon final state with invariant mass of 760 GeV and local significance of 2.6 σ [76]. The search has been done with a luminosity of 2.6 fb^{-1}.

The Run-II ATLAS and CMS results have generated large interest in the theoretical particle community. Several theoretical scenarios can explain the diphoton excess. In particular, the 2HDM is one of the models which has been studied immediately after the signal was reported. For example in [77] (Type-I and Type-II) and [78] (Type-I in the decoupling limit) the 2HDM extended with a family of vector-like quarks and leptons is studied. The authors claim that these scenarios are capable of explaining the diphoton excess seen by both experiments. In [79], [80] and [81] a general 2HDM has been studied and the parameter space has been scanned in order to constraint such model. The authors claim that, in order to explain the diphoton excess, one has to add a considerable amount of additional degrees of freedom and large Yukawa couplings to generate large couplings to photons. This result is consistent with [77] and [78]. In [79] and [80] the authors consider vector-like quarks as new degrees of freedom in order to explain the signal. This shows the amount of interest that signals of physics beyond the SM generates in the scientific community, and in particular the interest of the 2HDM. Future Higgs searches made by the ATLAS and CMS collaboration might be able to prove whether the signal is a real sign of new physics or not.

Part II

The Flavour Sector with Extra Higgs Doublets

CHAPTER **3**

Generating the Quark Parameters in a Two Higgs Doublet Model

The origin of the hierarchies of fermion masses and mixing angles is one of the biggest mysteries in particle physics. In this chapter we present a mechanism to naturally generate the hierarchies in the quark sector by extending the SM with an extra Higgs doublet, following [1]. In this model, no new fermions or extra symmetries are introduced. For this study the lepton sector is neglected. As discussed in Chapter 2, a general 2HDM tends to generate large effects on flavour observables and usually discrete symmetries are used to avoid them. However, flavour violating effects can be suppressed in the decoupling limit, where the scale of new physics arises at a sufficiently large energy. This is the limit taken for the model discussed in this chapter.

3.1 Standard Model Flavour Structures in a 2HDM

The Yukawa Lagrangian of a general 2HDM is given in eq. (2.19). For convenience and without loss of generality, we choose to work in the Higgs basis, where Φ_1 acquires all of the vev. Hence, $\langle\Phi_1\rangle = v/\sqrt{2}$ with $v \simeq 246$ GeV and $\langle\Phi_2\rangle = 0$. This means that the fermion mass matrices are proportional to the Yukawa couplings with Φ_1.

3.1.1 The Rank-1 Limit

The main assumption taken in this model is that the tree level Yukawa couplings have very hierarchical singular values. In practice, the Yukawa matrices can be taken to be of rank-1 at tree level. After this assumption is made, by the proper transformation of the quark fields, the tree level Yukawa couplings with Φ_1 can be written at the cut-off scale Λ as

$$Y_u^{(1)}(\Lambda) = \begin{pmatrix} 0 & 0 & 0 \\ 0 & 0 & 0 \\ 0 & 0 & y_u^{(1)} \end{pmatrix} \ , \ Y_d^{(1)}(\Lambda) = \begin{pmatrix} 0 & 0 & 0 \\ 0 & 0 & \epsilon y_d^{(1)} \\ 0 & 0 & y_d^{(1)} \end{pmatrix} \ , \tag{3.1}$$

which generate the following masses for the top and bottom quarks, respectively

$$\begin{aligned} m_t|_{\text{tree}} &= y_u^{(1)} v/\sqrt{2}, \\ m_b|_{\text{tree}} &= y_d^{(1)} \sqrt{1+\epsilon^2} v/\sqrt{2}. \end{aligned} \tag{3.2}$$

As the Yukawa matrices are of rank-1, the remaining quark masses are zero at tree level in this scenario

$$\begin{aligned} m_c|_{\text{tree}} &= m_u|_{\text{tree}} = 0 \ , \\ m_s|_{\text{tree}} &= m_d|_{\text{tree}} = 0 \ . \end{aligned} \tag{3.3}$$

From the above tree level Yukawas, only the $|V_{tb}|$ term in the CKM matrix can be determined. The reason is that, as the Yukawa matrices are of rank-1, only the top and bottom mass eigenstates are fixed. As V_{CKM} contains the product of the matrices with the different left-handed mass eigenstates for both the up and the down sector, only the product of the top and bottom mass eigenstates is determined. The left-handed eigenstates for the first and second generation can be rotated leaving the Lagrangian invariant. Nevertheless, we know that the CKM matrix is a unitary matrix. Therefore

$$V_{CKM} V_{CKM}^{\dagger} = \mathbb{1}. \tag{3.4}$$

This means that even if the $|V_{ub}|$ and $|V_{cb}|$ terms are undetermined at tree level, they have to fulfil the following condition

$$|V_{ub}|^2 + |V_{cb}|^2 = \epsilon^2. \tag{3.5}$$

It is known from experiments that this combination has to be $\ll 1$. This means that one should take the limit $\epsilon \to 0$. This limit is assumed from now on. In this case, $|V_{tb}| = 1$. Thus, at tree level, the structure of the CKM matrix is

$$|V_{CKM}| = \begin{pmatrix} ? & ? & 0 \\ ? & ? & 0 \\ 0 & 0 & 1 \end{pmatrix} \tag{3.6}$$

where the "?" entries correspond to terms that cannot be determined from the tree level Yukawas and exclusively depend on the mixing between the first and second generation of left-handed quarks. This scenario is presented in Fig. 3.1, where a simplified graphical representation of the left-handed eigenstates at tree level is shown to better understand the outcome of the model. In this figure just the third generation of left-handed eigenvectors are determined. On the left panel, the scenario for $\epsilon \neq 0$ is shown. The first and second generation have degenerate eigenvalues (with value 0) and their eigenvectors are undetermined. Even so, they have to lay on the surface perpendicular to the third generation eigenvector (on the red surface for the up-type quarks and on the blue surface for the down-type quarks). On the right panel, the scenario with $\epsilon \to 0$ is shown. This limits imposes that the bottom and top left-handed mass eigenstates have to be

aligned. In this scenario, the surface where the first and second generation lay coincides for both quark types. In this way, the structure of the CKM matrix is consistent with the experimental values in a first approximation. The scenario for the right-handed sector is very similar. The eigenstates of the third generation are determined at tree level. Nevertheless, the misalignment between the top and the bottom right-handed eigenvectors has no physical consequence.

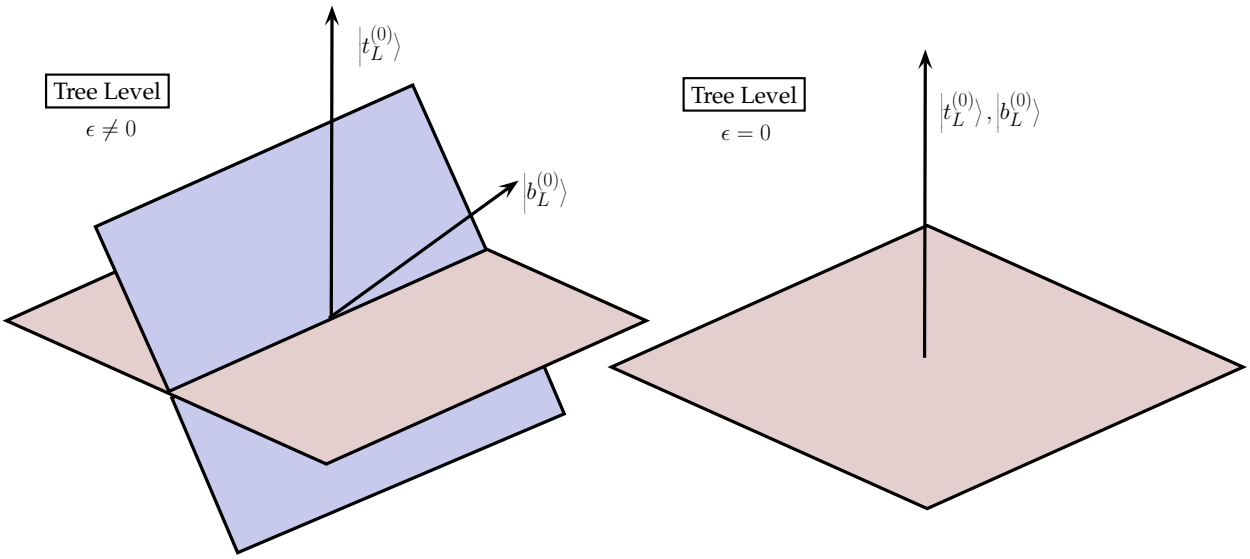

Figure 3.1: Tree level scenario for rank-1 Yukawa couplings. After imposing $\epsilon \to 0$, the top and bottom left-handed mass eigenstates are aligned. The first and second generation must lay on the surface perpendicular to them.

In this scenario, the couplings with Φ_2 are also taken to be of rank-1. As the quark fields have already been rotated to the basis where eq. (3.1) is fulfilled, the Yukawa couplings with Φ_2 have to take the most general rank-1 matrix form

$$Y_u^{(2)}(\Lambda) = U_L^\dagger \begin{pmatrix} 0 & 0 & 0 \\ 0 & 0 & 0 \\ 0 & 0 & y_u^{(2)} \end{pmatrix} U_R \ ,$$
$$Y_d^{(2)}(\Lambda) = D_L^\dagger \begin{pmatrix} 0 & 0 & 0 \\ 0 & 0 & 0 \\ 0 & 0 & y_d^{(2)} \end{pmatrix} D_R \ , \tag{3.7}$$

where $U_{L,R}$, $D_{L,R}$ are 3×3 unitary matrices. As in this case the Yukawa matrix elements are $(Y_u^{(2)})_{ij} = y_u^{(2)} (U_L)^*_{3i} (U_R)_{3j}$, $(Y_d^{(2)})_{ij} = y_d^{(2)} (D_L)^*_{3i} (D_R)_{3j}$, only the last row of the unitary matrices is relevant. We parametrise this row as

$$(U_L)_{31} = e^{i\rho_{u_L}} \sin\theta_{u_L} \sin\omega_{u_L} \ ,$$
$$(U_L)_{32} = e^{i\xi_{u_L}} \sin\theta_{u_L} \cos\omega_{u_L} \ ,$$
$$(U_L)_{33} = e^{i\chi_{u_L}} \cos\theta_{u_L} \ , \tag{3.8}$$

and equivalently for U_R, D_L, D_R. In this model we are just interested in reproducing the mass hierarchy pattern and the structure of the mixing matrices and not in understanding the origin or value of the CKM CP violating phase. We therefore neglect any of the complex phases of the model in this chapter for the sake of simplicity.

3.2 Quantum Corrections in Quark Sector

The rank-1 Yukawa matrices generate masses for the top and bottom quarks, leaving the first and second generation massless and the mixing between the latter completely undetermined. In this section, the results for the one loop corrections to the Yukawa couplings with Φ_1 using perturbation theory are presented. As will now be discussed, in this framework we are able to generate masses for the second generation of quarks and reproduce the hierarchical structure of the CKM matrix. In order to calculate the impact of loop corrections to the Yukawa couplings we use the leading-log approximation

$$\begin{aligned} Y_u^{(1)}|_{1-\text{loop}} &\simeq Y_u^{(1)}|_{\text{tree}} + \frac{1}{16\pi^2}\beta_u^{(1)} \log\frac{\Lambda}{M_H} \,, \\ Y_d^{(1)}|_{1-\text{loop}} &\simeq Y_d^{(1)}|_{\text{tree}} + \frac{1}{16\pi^2}\beta_d^{(1)} \log\frac{\Lambda}{M_H} \,, \end{aligned} \tag{3.9}$$

where M_H corresponds to the mass of the new Higgs (which is much larger than the SM Higgs mass) and $\beta_u^{(1)}$, $\beta_d^{(1)}$ are the beta-functions, defined in Appendix A.1.

3.2.1 Preliminaries: Degenerate Perturbation Theory

In this part the method used to calculate the masses and mixing angles for degenerate states is presented. The calculations done here are for the up-type quarks, but are completely analogous for the down sector. In order to determine the CKM matrix, we are just interested in calculating the left-handed rotation matrix V_{u_L}, defined in eq. (1.3). Therefore, our calculations are done using perturbation theory on $H_u^{(0)}$, defined as

$$H_u^{(0)} = Y_u^{(1)} Y_u^{(1)\dagger}\Big|_{\text{tree}} \tag{3.10}$$

and is diagonalised as

$$H_{u_{\text{diag}}}^{(0)} = V_{u_L}^\dagger H_u^{(0)} V_{u_L}. \tag{3.11}$$

This means that $H_u^{(0)}$ is a 3×3 matrix which just has one well defined eigenvector, $\left|t_L^{(0)}\right\rangle$, and eigenvalue, $\left(y_u^{(1)}\right)^2$. We now define $H_u^{(1)}$, which contains the perturbation corrections to $H_u^{(0)}$

$$H_u^{(1)} = H_u^{(0)} + \lambda_u\, \delta H_u^{(1)}\Big|_{\text{tree}} = \tag{3.12}$$

$$= Y_u^{(1)} Y_u^{(1)\dagger} + \lambda_u Y_u^{(1)} \delta Y_u^{(1)\dagger} + \lambda_u \delta Y_u^{(1)} Y_u^{(1)\dagger}\Big|_{\text{tree}} \tag{3.13}$$

where λ_u is a perturbation parameter, which in our case takes the value $\frac{1}{16\pi^2}\log\frac{\Lambda}{M_H}$, and $\delta Y_u^{(1)} = \beta_u^{(1)}$ corresponds to the loop corrections to the Yukawa coupling $Y_u^{(1)}$. Perturbation theory for non-degenerate states consists of calculating the series expansion around the initial eigenvalues and eigenstates. As in our case there are two degenerate eigenstates at tree level, zero-th order in perturbation theory[1] has to be used to calculate the undetermined eigenvectors. Their corresponding eigenvalues are calculated at first order in perturbation theory, as at tree level they are determined with value 0. The calculation is done as following these steps

- Define the projector operator P_u which defines the subspace perpendicular to $\left|t_L^{(0)}\right\rangle$

$$P_u = \mathbb{1} - \left|t_L^{(0)}\right\rangle\left\langle t_L^{(0)}\right|. \tag{3.14}$$

- Calculate the perturbation δH_u projected on the subspace perpendicular to $\left|t_L^{(0)}\right\rangle$

$$\delta\hat{H}_u^{(1)} = P_u \delta H_u^{(1)} P_u \tag{3.15}$$

- Calculate the eigenvalues and eigenvectors for $\lambda_u \delta\hat{H}_u^{(1)}$.

In our case the result still does not break degeneracy. Therefore, we have to consider higher order corrections. The next steps in our calculations are

- We add the corrections proportional to λ_u^2 and define $H_u^{(2)}$

$$\begin{aligned} H_u^{(2)} &= H_u^{(0)} + \lambda_u \delta H_u^{(1)} + \lambda_u^2 \delta H_u^{(2)} = & (3.16)\\ &= Y_u^{(1)} Y_u^{(1)\dagger} + \lambda_u Y_u^{(1)} \delta Y_u^{(1)\dagger} + \lambda_u \delta Y_u^{(1)} Y_u^{(1)\dagger} + \lambda_u^2 \delta Y_u^{(1)} \delta Y_u^{(1)\dagger}\Big|_{\text{tree}}. & (3.17) \end{aligned}$$

- As we are now taking terms proportional to λ_u^2, we also have take into account higher order corrections with terms which also contain λ_u^2. With all this, the matrix that one has to diagonalise is

$$\delta\hat{H}_u^{(2)} = P_u \delta H_u^{(2)} P_u - P_u \delta H_u^{(2)} \frac{\mathbb{1} - P_u}{y_u^{(1)^2}} \delta H_u^{(2)} P_u. \tag{3.18}$$

- We take the terms only up to order λ_u^2 in $\delta\hat{H}_u^{(2)}$.

[1] For a full Hamiltonian $H = H^{(0)} + \lambda\delta H$ with eigenvectors $|i_L\rangle$ and unperturbed eigenvectors $\left|i_L^{(0)}\right\rangle$, if there is a subset of degenerate unperturbed eigenstates, zero-th order in perturbation theory fixes them univocally, using the perturbation $\lambda\delta H$:

$$\left|i_L^{(0)}\right\rangle = \lim_{\lambda\to 0} |i_L\rangle$$

In our case, as $\left|t_L^{(0)}\right\rangle = (0,0,1)^T$, assuming that the Yukawa couplings are real parameters in the flavour basis, the matrix which has to be diagonalised is

$$\lambda_u^2 \delta\hat{H}_u^{(2)} = \lambda_u^2 \begin{pmatrix} \delta y_{11}^2 + \delta y_{12}^2 & \delta y_{21}\delta y_{11} + \delta y_{22}\delta y_{12} & 0 \\ \delta y_{21}\delta y_{11} + \delta y_{22}\delta y_{12} & \delta y_{21}^2 + \delta y_{22}^2 & 0 \\ 0 & 0 & 0 \end{pmatrix} \tag{3.19}$$

where δy_{ij} corresponds to the ij entry of the $\delta Y_u^{(1)}$ matrix. The eigenvalues and eigenvectors of $\lambda_u^2 \delta\hat{H}_u^{(2)}$ correspond to the first and second generation for the up-type quarks. The eigenvalues are then suppressed by a factor λ_u^2, as they are calculated at second order in perturbation theory. Therefore the corresponding Yukawa singular values for the first and second generation are suppressed by a λ_u factor. The eigenvectors contain no suppression and are of norm 1.

This solution is valid only if the eigenstate which is determined at tree level (in this case $\left|t_L^{(0)}\right\rangle$) is $(0,0,1)$. Nevertheless, if this is not the case, one can just rotate all the calculations to this basis, and do the inverse rotation to give the answer in the initial basis.

3.2.2 A Scenario with Rank-2 Yukawa Couplings

We have just seen how to use perturbation theory to calculate the eigenvalues and eigenvectors in a degenerate case. It is important to remark that in this scenario, the loop corrections increase the rank of the Yukawa couplings with Φ_1 to rank-2 at most. This can be proved as follows. If one takes the β functions in Appendix A.1, one can see that its structure for both up or down quark type always follows the pattern

$$\frac{1}{16\pi^2}\log\frac{\Lambda}{M_H}\beta_{u,d}^{(1)} = A_{u,d}^{(1)} Y_{u,d}^{(1)} + B_{u,d}^{(1)} Y_{u,d}^{(2)} \tag{3.20}$$

where $A_{u,d}^{(1)}$ and $B_{u,d}^{(1)}$ are combinations of the different Yukawa matrices and contain the loop suppression factor. The rank of $A_{u,d}^{(1)}$ and $B_{u,d}^{(1)}$ is not important for this discussion. As $Y_{u,d}^{(1)}$ and $Y_{u,d}^{(2)}$ are rank-1 matrices, one can write them as the outer product of two vectors

$$\frac{1}{16\pi^2}\log\frac{\Lambda}{M_H}\beta_{u,d}^{(1)} = A_{u,d}^{(1)}\left|y_{u,d_L}^{(1)}\right\rangle\left\langle y_{u,d_R}^{(1)}\right| + B_{u,d}^{(1)}\left|y_{u,d_L}^{(2)}\right\rangle\left\langle y_{u,d_R}^{(2)}\right| = \left|\delta\tilde{y}_{u,d_L}^{(1)}\right\rangle\left\langle y_{u,d_R}^{(1)}\right| + \left|\delta\tilde{y}_{u,d_L}^{(2)}\right\rangle\left\langle y_{u,d_R}^{(2)}\right| \tag{3.21}$$

where $\left|y_{u,d_L}^{(1)}\right\rangle$ has been redefined to $\left|\delta\tilde{y}_{u,d_L}^{(1)}\right\rangle$ to absorb matrices $A_{u,d}^{(1)}$ and $B_{u,d}^{(1)}$ in order to simplify the discussion. If now the β functions are used to calculate the 1-loop Yukawa couplings $Y_{u,d}^{(1)}$, one finds

$$Y_{u,d}^{(1)}|_{1-\text{loop}} \simeq \left|y_{u,d_L}^{(1)}\right\rangle\left\langle y_{u,d_R}^{(1)}\right| + \left|\delta\tilde{y}_{u,d_L}^{(1)}\right\rangle\left\langle y_{u,d_R}^{(1)}\right| + \left|\delta\tilde{y}_{u,d_L}^{(2)}\right\rangle\left\langle y_{u,d_R}^{(2)}\right| = \left|y_{u,d_L}^{\prime(1)}\right\rangle\left\langle y_{u,d_R}^{(1)}\right| + \left|\delta\tilde{y}_{u,d_L}^{(2)}\right\rangle\left\langle y_{u,d_R}^{(2)}\right| \tag{3.22}$$

where $\left|y_{u,d_L}^{\prime(1)}\right\rangle = \left|y_{u,d_L}^{(1)}\right\rangle + \left|\delta\tilde{y}_{u,d_L}^{(1)}\right\rangle$. As the one loop Yukawa couplings with Φ_1 can be written as a linear combination of two outer products, the rank of the matrix can be at most of rank-2. This discussion is valid at any loop.

Physical Parameters

As the Yukawa matrices can be at most of rank-2 after including radiative corrections, the first generation of quarks remains massless in this model. Therefore, not all of the parameters presented in eqs. (3.1) and (3.7) are physical. One way of counting how many initial parameters are actually physical is through the following rule [82]

$$\#\text{Physical Parameters} = \#\text{Total Parameters} - \#\text{Broken Generators}. \tag{3.23}$$

A rank-1 Yukawa coupling in a general basis contains a total of 5 real parameters and 5 phases. In the absence of Yukawa couplings, there is a global $U(3)^3$ symmetry. This symmetry breaks to a $U(1)^3$ when including the Yukawa matrices when the first generation of quarks remains massless. In other words

$$U(3)_{Q_L} \times U(3)_{u_R} \times U(3)_{d_R} \longrightarrow U(1)_{u_R} \times U(1)_{d_R} \times U(1)_B \tag{3.24}$$

The number of generators for $U(3)$ are 9. A $U(3)$ matrix contains 3 real parameters and 6 phases. Instead $U(1)$ has only one generator, which corresponds to a phase. Therefore

$$20\ \mathbb{R}\ \text{Parameters} - 9\ \text{Broken}\ \mathbb{R}\ \text{Parameters} = 11\ \mathbb{R}\ \text{Physical Parameters}$$
$$20\ \text{Phases} - 15\ \text{Broken Phases} = 5\ \text{Physical Phases}$$

Thus, the model contains a total of 16 physical parameters. The non-physical parameters in eqs. (3.1) and (3.7) with real Yukawa couplings correspond to ω_{u_R} and ω_{d_R}, which parametrise the $U(1)$ transformation for the first generation of right-handed quarks. This will be discussed later in detail.

3.2.3 Masses for the Second Generation of Quarks

The values of the quark masses for the second generation can now be calculated at one loop, using the results in Section 3.2.1. The Feynman diagrams which contribute to increase the Yukawa matrix rank using perturbation theory are shown in Fig. 3.2. In both cases, the coupling of quarks with Φ_2 must generate a new direction in flavour space.

To simplify the results, one can use the assumption $y_d^{(1)}, y_d^{(2)} \ll y_u^{(1)}, y_u^{(2)}$. This is a reasonable assumption as it is known from observations that $y_d^{(1)} \ll y_u^{(1)}$. One finds that

$$y_{c,s}^2(M_H) \simeq \left(\frac{1}{16\pi^2}\log\frac{\Lambda}{M_H}\right)^2 \sum_{i,j=1}^{2} \left(\beta_{u,d_{ij}}^{(1)}(\Lambda)\right)^2 \tag{3.25}$$

where $\beta_{u,d_{ij}}^{(1)}$ is the ij entry of the $\beta_{u,d}^{(1)}$ matrices. Hence, at one loop the approximate ratio between

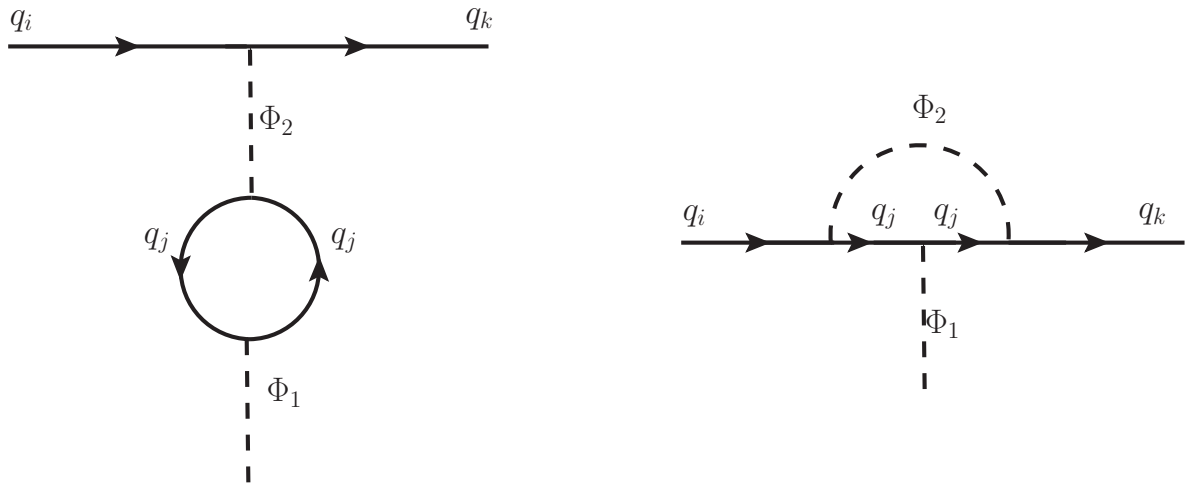

Figure 3.2: One loop Feynman diagrams in $\beta^{(1)}_{u,d}$ which generate a mass for the second generation of quarks.

the Yukawa couplings of the second and third generation of quarks are [1]

$$\frac{y_c}{y_t} \simeq \left(\frac{1}{16\pi^2}\log\frac{\Lambda}{M_H}\right)\frac{3}{4}(y_u^{(2)})^2 \sin 2\theta_{u_L}\sin 2\theta_{u_R}\ , \tag{3.26}$$

$$\frac{y_s}{y_b} \simeq \left(\frac{1}{16\pi^2}\log\frac{\Lambda}{M_H}\right)\frac{y_u^{(1)}y_u^{(2)}y_d^{(2)}}{y_d^{(1)}}\cos\theta_{u_R}\sin\theta_{d_R}N_d\ , \tag{3.27}$$

where

$$N_d = \left[9\sin^2\theta_{d_L}\cos^2\theta_{u_L} + 4\cos^2\theta_{d_L}\sin^2\theta_{u_L} - 3\sin 2\theta_{d_L}\sin 2\theta_{u_L}\cos(\omega_{d_L}-\omega_{u_L})\right]^{1/2}\ . \tag{3.28}$$

As one can see from eq. (3.27), all of the Yukawa couplings of the second generation contain a loop suppression which immediately generates a smaller value for them with respect to the third generation. Nevertheless, the logarithmic term enhances the value of the second generation masses, as in principle the cut-off scale can be much larger than the heavy Higgs mass.

Let us now discuss in detail the dependence of the masses with respect to the Yukawa parameters. After taking the assumption $y_d^{(1)}, y_d^{(2)} \ll y_u^{(1)}, y_u^{(2)}$, the Feynman diagram which mainly contributes to the radiative generation of the charm mass is the left diagram in Fig. 3.2. The only way for the charm quark to radiatively couple to Φ_1 is through Φ_2, which at the same time has to couple to the top quark. This diagram corresponds to the wave-function renormalization diagram proportional to $\mathrm{Tr}(Y_u^{(1)}Y_u^{(2)\dagger})Y_u^{(2)}$ in $\beta_u^{(1)}$. This can also be seen from eq. (3.27). In order to generate the charm mass, one needs non-vanishing $\cos\theta_{u_L}\cos\theta_{u_R}$ and $\sin\theta_{u_L}\sin\theta_{u_R}$. These two terms parametrise the mixing between the top quark and the lightest generations through Φ_2. This mixing is the only way to transfer the electroweak symmetry breaking from the third to the second generation.

In the case of the strange quark mass, the dependence with the parameters of the model is

more sophisticated. The reason is that both the wave-function renormalization and the vertex diagram in Fig. 3.2, contribute to generate the strange mass. These diagrams are proportional to $\mathrm{Tr}(Y_u^{(2)}Y_u^{(1)\dagger})Y_d^{(2)}$ and $Y_u^{(2)}Y_u^{(1)\dagger}Y_d^{(2)}$ in $\beta_d^{(1)}$, respectively. The first term, which corresponds to the left Feynman diagram in Fig. 3.2, requires similar conditions to the ones needed to generate the charm mass. In this case the non-vanishing terms have to be $\cos\theta_{u_L}\cos\theta_{u_R}$ and $\sin\theta_{d_L}\sin\theta_{d_R}$. Here, $\cos\theta_{u_L}\cos\theta_{u_R}$ implies that the Higgs Φ_2 has to couple to the top quark, whereas $\sin\theta_{d_L}\sin\theta_{d_R}$ means that Φ_2 has to couple to the lightest generations of the down-type quarks. This corresponds to the Feynman diagram where the top quark is inside the loop. On the other hand, $Y_u^{(2)}Y_u^{(1)\dagger}Y_d^{(2)}$ corresponds to the right diagram in Fig. 3.2. For this term to contribute to the generation of the strange quark mass, $\cos\theta_{u_R}\sin\theta_{u_L}\neq 0$ and $\cos\theta_{d_L}\sin\theta_{d_R}\neq 0$. Here $\cos\theta_{u_R}\sin\theta_{u_L}\neq 0$ means that the left-handed doublet of the light quarks has to couple to the right-handed top quark through Φ_2 and $\cos\theta_{d_L}\sin\theta_{d_R}\neq 0$ indicates that the left-handed doublet of the third generation of quarks has to couple to the right-handed light down type quarks also through Φ_2. In other words, the third generation of quarks has to be the inside the loop, coupling to both Φ_1 and Φ_2.

In this scenario, as the Yukawa matrices with Φ_1 can be at most of rank-2, the first generation of quarks remains massless. Nevertheless, as will later be discussed, by introducing additional flavour structures to the model, as for example introducing extra Higgs doublets or taking rank-2 matrices at tree level, one can generate a non-vanishing mass for the first generation. In the latter case, radiative corrections to the masses of the second generation can be larger than the tree level contribution. Hence, in this case, the results deduced from rank-1 Yukawa couplings are still a good approximation.

Finally, the effects of such a model on precision flavour observables are negligible as the decoupling limit is taken for this analysis. Nevertheless, the masses which are generated radiatively depend logarithmically on the mass of the heavy Higgs and therefore, modifying the scale of new physics barely changes the predictions in the quark sector.

3.2.4 Radiative Effects on the CKM Matrix

At tree level, the mixing between the first and second generation of quarks is completely undetermined. This can be resolved using perturbation theory of degenerate states. The mixing between the first and second generation for each quark type can be parametrised with a mixing angle $\zeta_{u,d}$, such that the mixing matrix for each quark type is

$$V_{u,d_L} = \begin{pmatrix} \cos\zeta_{u,d} & \sin\zeta_{u,d} & 0 \\ -\sin\zeta_{u,d} & \cos\zeta_{u,d} & 0 \\ 0 & 0 & 1 \end{pmatrix}. \tag{3.29}$$

Using the result in eq. (3.19) one finds

$$\zeta_{u,d} = \tan^{-1}\left(\frac{\beta^{(1)}_{u,d_{11}}\beta^{(1)}_{u,d_{21}} + \beta^{(1)}_{u,d_{12}}\beta^{(1)}_{u,d_{22}}}{(\beta^{(1)}_{u,d_{21}})^2 + (\beta^{(1)}_{u,d_{22}})^2}\right). \tag{3.30}$$

Knowing that $V_{CKM} = V_{u_L}^{\dagger} V_{d_L}$, the Cabibbo angle can be calculated

$$V_{us} \simeq -V_{cd} \simeq \frac{3 \sin\theta_{d_L} \cos\theta_{u_L} \sin(\omega_{d_L} - \omega_{u_L})}{N_d} \tag{3.31}$$

and the value for the remaining diagonal element is

$$V_{ud} \simeq V_{cs} \simeq \sqrt{1 - V_{us}^2}. \tag{3.32}$$

It is interesting that the masses of the second generation of quarks arise at one loop and hence contain a loop suppression factor which naturally generates the hierarchy between the second and third generation of quarks. But even if the Cabibbo angle is generated by the one loop corrections, it contains no loop suppression factor. Figure 3.3 shows a simplified graphical representation of the left-handed eigenstates at one loop to better understand the outcome of the model. As we have seen in Section 3.1, at tree level, just the third generation eigenvectors are determined. The first and second generation have to lay on the surface perpendicular to the latter. The top and bottom left-handed eigenstates are imposed to be aligned at tree level. Once the one loop corrections are included, the degeneracy between the first and second generation is broken if the correction has some misalignment with respect to the third generation eigenvector. In Fig 3.3, $|\delta\tilde{y}_{u,d_L}\rangle$ represents the left-handed part of the loop correction, defined in eq. (3.22). The second generation eigenvalue is proportional to the length of the projection on the perturbation of the surface perpendicular to the third generation. It is therefore loop suppressed. The direction projection of the perturbation $|\delta\tilde{y}_{u,d_L}\rangle$ on the surface perpendicular to the third generation, determines the direction of the second generation eigenvector. As this eigenvector was undetermined at tree level, even if the loop eigenvalue is very small, it breaks the tree level degeneracy between first and second generation, leaving the eigenvectors totally determined. If the perturbation breaks the degeneracy, the vectors which are generated contain no loop suppression. Therefore, the Cabibbo angle is not loop suppressed. In perturbation theory language, the Cabibbo angle is generated at zero-th order. This mechanism was actually noted in previous works [83–85] for the mixing in the neutrino sector with degenerate mass eigenvalues. Note that the Cabibbo angle depends only on left-handed parameters. The necessary condition to to generate a non-vanishing Cabibbo angle is that the left-handed charm and strange eigenvectors have to be misaligned, therefore $\sin(\omega_{d_L} - \omega_{u_L}) \neq 0$.

After the one loop corrections, at zero-th order in perturbation theory, the structure of the CKM matrix is

$$|V_{CKM}| = \begin{pmatrix} V_{ud} & V_{us} & 0 \\ V_{cd} & V_{cs} & 0 \\ 0 & 0 & 1 \end{pmatrix} \tag{3.33}$$

Once the eigenvectors are determined at zero-th order in perturbation theory, one can use first order perturbation theory to calculate higher order corrections of all the CKM matrix elements. In this case we are interested in calculating the corrections to the terms which are zero. The result are

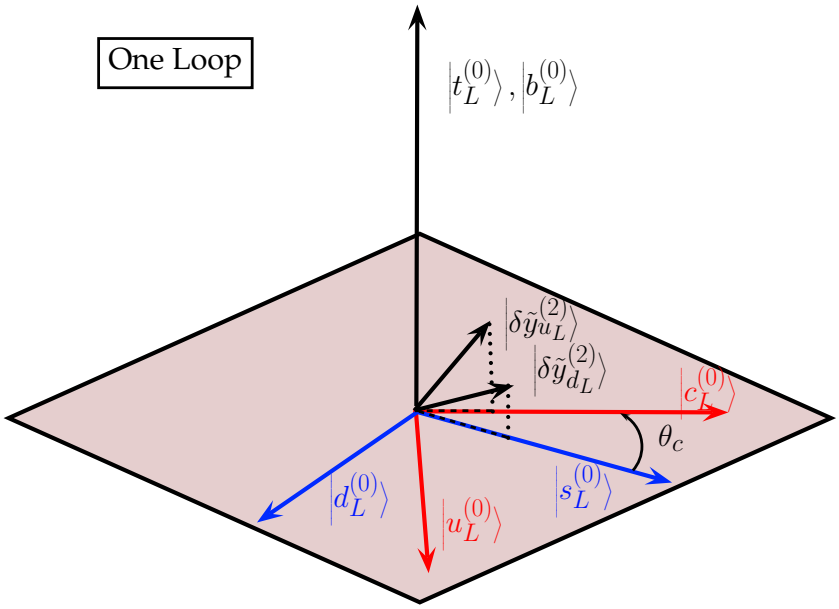

Figure 3.3: Graphical representation of the left-handed quark mass eigenstates after introducing the one loop corrections. The small perturbations $|\delta\tilde{y}_{u,d_L}\rangle$ determine a new direction in space and generate a non-zero eigenvalue for the second generation of quarks. The misalignment between the projector of these two vectors determines the value of the Cabibbo angle, θ_c.

$$
\begin{aligned}
V_{ub} &\simeq \left(\frac{1}{16\pi^2}\log\frac{\Lambda}{M_H}\right)\frac{3y_u^{(1)}y_u^{(2)}y_d^{(2)}}{y_d^{(1)}}\sin\theta_{d_L}\cos\theta_{d_R}\cos\theta_{u_L}\cos\theta_{u_R}\sin(\omega_{d_L}-\omega_{u_L})\,,\\
V_{cb} &\simeq \left(\frac{1}{16\pi^2}\log\frac{\Lambda}{M_H}\right)\frac{y_u^{(1)}y_u^{(2)}y_d^{(2)}}{y_d^{(1)}}\left\{\frac{1}{4}\frac{y_d^{(1)}y_u^{(2)}}{y_d^{(2)}y_u^{(1)}}\sin 2\theta_{u_L}(3\cos 2\theta_{u_R}+2)\right.\\
&\left.+\cos\theta_{d_R}\cos\theta_{u_R}\left[2\cos\theta_{d_L}\sin\theta_{u_L}-3\sin\theta_{d_L}\cos\theta_{u_L}\cos(\omega_{d_L}-\omega_{u_L})\right]\right\}\,.
\end{aligned}
\tag{3.34}
$$

Of course these terms do contain the loop-suppression factor and now the right-handed parameters contribute to the first order perturbation corrections. This is because we are calculating the corrections of a vector which is already determined.

It is important to mention that some of the parameters of this model are univocally determined. In this scenario we have two massless particles, the up and the down quark. There is hence an unbroken $U(1)_{u_R}\times U(1)_{d_R}$ symmetry. As explained above, this means that the couplings of the right-handed part of the first generation of quarks have no physical meaning. This can also be seen as follows. If one calculates the Yukawa couplings in the mass basis, one finds

$$
\widetilde{Y}_{u,d}^{(2)}(M_H)\simeq y_{u,d}^{(2)}\begin{pmatrix}0 & -\sin\theta_{u,d_L}\sin\theta_{u,d_R}\sin\left(\zeta_{u,d_L}-\omega_{u,d_L}\right) & -\cos\theta_{u,d_R}\sin\theta_{u,d_L}\sin\left(\zeta_{u,d_L}-\omega_{u,d_L}\right)\\ 0 & \sin\theta_{u,d_L}\sin\theta_{u,d_R}\cos\left(\zeta_{u,d_L}-\omega_{u,d_L}\right) & \cos\theta_{u,d_R}\sin\theta_{u,d_L}\cos\left(\zeta_{u,d_L}-\omega_{u,d_L}\right)\\ 0 & \cos\theta_{u,d_L}\sin\theta_{u,d_R} & \cos\theta_{u,d_L}\cos\theta_{u,d_R}\end{pmatrix}\,.
\tag{3.35}
$$

As expected, ω_{u,d_R} do not appear in $\widetilde{Y}_{u,d}^{(2)}$. One can then set $\omega_{u,d_R}=0$. Furthermore, the

approximate values for the right-handed angles θ_{u,d_R} can be calculated from the following quark parameters

$$\begin{aligned} \frac{y_s}{y_b}\frac{V_{us}}{V_{ub}} &\simeq \tan\theta_{d_R} \ , \\ \frac{y_c}{y_t}\frac{V_{us}}{V_{td}} &\simeq \frac{3\sin 2\theta_{u_R}}{2+3\cos 2\theta_{u_R}} \ , \end{aligned} \tag{3.36}$$

which gives $\theta_{u_R} \approx 0.16$, $\theta_{d_R} \approx 1.06$.

Of course, there are degeneracies between the remaining parameters. Nevertheless, under the assumption that the couplings for each quark-type are of the same order, and the mixing angles are of $\mathcal{O}(1)$, one can naturally reproduce the experimental values for the second and third generation of masses and the mixing in the quark sector. Still, this is not a predictive model and unfortunately contains a large number of free parameters.

CHAPTER 4

Lepton Masses and Mixing Angles in a 2HDM see-saw

In the previous chapter we have presented the results of the quantum effects on the masses and mixing angles in the quark sector in a context of a 2HDM with rank-1 Yukawa couplings at tree level. In this chapter the results for the lepton sector are presented, following the discussion in [2]. The masses of the charged lepton sector follow a similar pattern to the quark sector. Nevertheless, as neutrinos are massless in the SM, the picture completely changes, as physics beyond the 2HDM has to be introduced to generate neutrino masses. In what follows we assume neutrino masses arise from the see-saw mechanism by adding right-handed neutrinos. In this scenario, one can also generate a completely anarchical PMNS matrix.

4.1 Tree Level Results

In this section we present the tree level results for charged leptons and neutrino masses together with the lepton mixing matrix in the context of a general 2HDM. In contrast with the quark sector, not only a new extra Higgs doublet is introduced but also right-handed neutrinos in order to generate neutrino masses in the see-saw framework. Here, the Yukawa couplings are also assumed to be rank-1 at a cut-off scale Λ. The decoupling limit is taken again for the analysis, in order to make the model compatible with experimental constraints. In the second part of this section, we present the results in a simplified scenario, where the 2HDM is extended by just one right-handed neutrino.

4.1.1 The General Framework

Following the description presented in Chapter 1, the flavour dependent part of the see-saw mechanism extended with an extra Higgs doublet is described by the following Lagrangian

$$-\mathcal{L}^{lep} = Y^{(a)}_{e,ij}\bar{l}_{Li}\Phi_a e_{Rj} + Y^{(a)}_{\nu,ij}\bar{l}_{Li}\tilde{\Phi}_a\nu_{Rj} - \frac{1}{2}M_{\mathrm{M},ij}\bar{\nu}^C_{Ri}\nu_{Rj} + \mathrm{h.c.} \tag{4.1}$$

where $i, j = 1, 2, 3$ are flavour indices, $a = 1, 2$ is a Higgs index and $\tilde{\Phi}_a = i\tau_2 \Phi_a^*$. As for the quark sector, we also work in the Higgs basis for convenience. Hence $\langle \Phi_1^0 \rangle = v/\sqrt{2}$, with $v \simeq 246$ GeV and $\langle \Phi_2^0 \rangle = 0$. This means that the charged lepton and neutrino Dirac masses are proportional to the singular values of $Y_e^{(1)}$ and $Y_\nu^{(1)}$, respectively. Here $M_{\rm M}$ is the Majorana mass matrix for the right-handed neutrinos, and its singular values $M_1, ..., M_N$, correspond to the Majorana masses for N right-handed neutrinos.

The first assumption taken in this part is that the Majorana mass scale is much larger than the mass of the extra Higgs bosons, as the former does not arise from electroweak symmetry breaking. As for the previous chapter, we denote the masses of the four new Higgs states, H^0, A^0 and $H^\pm$, as M_H. At the scale of the lightest right-handed neutrino, M_1, it is useful to describe the Lagrangian in eq. (4.1) with the following effective Lagrangian

$$-\mathcal{L}^{\nu,\text{eff}} = Y_{e,ij}^{(a)} \bar{l}_{Li} e_{Rj} \Phi_a + \frac{1}{2} \kappa_{ij}^{(ab)} (\bar{l}_{Li} \tilde{\Phi}_a)(\tilde{\Phi}_b^T l_{Lj}^C) + \text{h.c.}. \tag{4.2}$$

In this case, the dimension five operators are

$$\kappa^{(ab)}(M_1) = (Y_\nu^{(a)} M_{\rm M}^{-1} Y_\nu^{(b)T})(M_1) \, . \tag{4.3}$$

As the only Higgs that acquires a vev is Φ_1, the neutrino mass matrix, defined in eq. (1.25) at this scale is

$$\mathcal{M}_\nu(M_1) = \frac{v^2}{2} \kappa^{(11)}(M_1) \, , \tag{4.4}$$

and is diagonalised following eq. (1.26). This is valid for any number of right-handed neutrinos.

4.1.2 The Tree Level See-Saw with one Right-Handed Neutrino

Following the framework used for the quark sector, here the Yukawa matrices are also assumed to be of rank-1. To simplify this scenario, we assume the model contains just one right-handed neutrino with mass $M_{\rm M} \gg M_H$. Nevertheless, this discussion can be extended to a model with N right-handed neutrinos.

Physical Parameters

Before computing the tree level results, we calculate how many of the parameters of the model are indeed physical. As happened in the quark sector, in this scenario there is one massless charged lepton which generates a $U(1)$ symmetry in the model. The symmetry group in the lepton sector before and after introducing the Yukawa couplings is

$$U(3)_{L_L} \times U(3)_{e_R} \longrightarrow U(1) e_R. \tag{4.5}$$

The number of initial parameters in the charged lepton sector is counted as for any of the quark type: 5 real parameters and 5 phases for each Yukawa coupling. The Yukawa coupling for the neutrino sector is assumed to be a dimension-3 vector. Therefore each neutrino Yukawa vector

contains a total of 3 real parameters and 3 phases. Using eq. (3.23), the number of physical parameters is calculated as follows

$$16\ \mathbb{R}\text{ Parameters} - 6\text{ Broken }\mathbb{R}\text{ Parameters} = 10\ \mathbb{R}\text{ Physical Parameters}$$
$$16\text{ Phases} - 11\text{ Broken Phases} = 5\text{ Physical Phases.}$$

This means that the model contains a total of 15 physical parameters.

Analytical Results

As some of the parameters of the model are not physical, they can be rotated away by redefining the lepton fields. We chose to work in the charged leptons mass basis for simplicity. The Yukawa couplings with Φ_1 in this basis are written, at the cut-off scale Λ, as

$$Y_e^{(1)}(\Lambda) = \begin{pmatrix} 0 & 0 & 0 \\ 0 & 0 & 0 \\ 0 & 0 & y_e^{(1)} \end{pmatrix} \ , \ Y_\nu^{(1)}(\Lambda) = y_\nu^{(1)} \begin{pmatrix} 0 \\ \sin\alpha \\ \cos\alpha \end{pmatrix}. \tag{4.6}$$

As the Yukawa matrices are of rank-1, only the third generation has a non-vanishing mass. Therefore

$$m_\tau|_{\text{tree}} = \frac{v}{\sqrt{2}}\, y_e^{(1)}, \qquad m_\mu|_{\text{tree}} = m_e|_{\text{tree}} = 0 \tag{4.7}$$

$$m_3|_{\text{tree}} = \frac{v^2}{2}\, \frac{y_\nu^{(1)2}}{M_{\text{M}}}, \qquad m_2|_{\text{tree}} = m_1|_{\text{tree}} = 0 \tag{4.8}$$

Note that the misalignment in the quark sector between the up and down tree level Yukawa couplings with Φ_1 was parametrised with the ϵ parameter, which was later assumed $\epsilon \to 0$. This limit was taken to mimic the hierarchical structure of the CKM matrix. We will now see that this assumption should not be imposed for the lepton sector. The PMNS matrix at tree level has the following structure

$$U_{PMNS} = \begin{pmatrix} ? & ? & ? \\ ? & ? & ? \\ ? & ? & \cos\alpha \end{pmatrix} \tag{4.9}$$

where "?" indicates the unknown parameters due to the undetermined eigenvectors of the first and second generation. In this scenario, even if only $U_{\tau 3}$ is determined at tree level, U_{e3} and $U_{\mu 3}$ have to fulfil

$$U_{e3}^2 + U_{\mu 3}^2 = \sin^2\alpha. \tag{4.10}$$

As the PMNS matrix has a completely anarchical, we have to keep $\alpha > 0$. Beyond the generation of neutrino masses, this assumption is the key difference between the quark and the lepton sector. This discussion is represented in Fig 4.1. In this scenario the tree level Yukawa couplings with Φ_1 determine the eigenvectors of the third generation and their corresponding eigenvalues. The first and second generation are undetermined, but as for the quark sector, they have to lay on

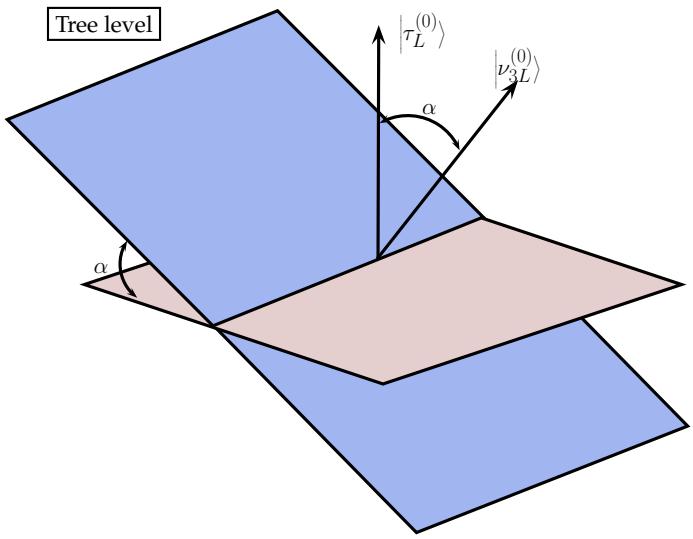

Figure 4.1: Tree level scenario for a 2HDM extended with one right-handed neutrino. The third generation eigenvalues and eigenvectors of leptons are determined. The misalignment between them is parametrised by the angle α. The red and blue surfaces represent the subspaces where the first and second generation of charged leptons and neutrinos have to lay on, respectively.

the surface perpendicular to the third generation (the red surface corresponds to charged leptons and the blue surface corresponds to neutrinos). The misalignment between the eigenstates of the third generation is parametrised by α.

The Yukawa interactions of leptons with Φ_2 are also rank-1. Hence, for the charged lepton sector the corresponding matrix in this basis is

$$Y_e^{(2)}(\Lambda) = E_L^\dagger \begin{pmatrix} 0 & 0 & 0 \\ 0 & 0 & 0 \\ 0 & 0 & y_e^{(2)} \end{pmatrix} E_R. \tag{4.11}$$

$E_{L,R}$ are 3×3 matrices, analogous to eq. (3.8). Due to the residual $U(1)_{e_R}$ symmetry discussed above, ω_{e_R} is not a physical parameter and therefore can be set to zero in this scenario.

The Yukawa coupling of neutrinos with Φ_2 takes a vector form

$$Y_\nu^{(2)}(\Lambda) = y_\nu^{(2)} \begin{pmatrix} e^{i\rho_\nu} \sin\theta_\nu \sin\omega_\nu \\ e^{i\xi_\nu} \sin\theta_\nu \cos\omega_\nu \\ e^{i\chi_\nu} \cos\theta_\nu \end{pmatrix} . \tag{4.12}$$

In the following sections we neglect any phase contribution for simplicity.

4.2 Quantum Corrections in the Lepton Sector

In this section we present results of the quantum corrections to the Yukawa couplings in the lepton sector. As for the quark sector, we are able to radiatively generate the masses of the second generation of leptons and determine univocally the entries of the PMNS matrix.

4.2.1 Radiative Corrections at $M_{\rm M}$ Scale

The analysis done in this part is completely analogous to the results presented in Section 3.2. The leading-log approximation is used to calculate the one loop Yukawa couplings for charged leptons and neutrinos. At the scale of decoupling of the right-handed neutrinos, taking the leading-log approximation, the Yukawa couplings are

$$\begin{aligned} Y_{e,ij}^{(a)}(M_{\rm M}) &\simeq Y_{e,ij}^{(a)}(\Lambda) + \frac{1}{16\pi^2}\beta_{e,ij}^{(a)}(\Lambda)\log\frac{\Lambda}{M_{\rm M}}\,, \\ Y_{\nu,i}^{(a)}(M_{\rm M}) &\simeq Y_{\nu,i}^{(a)}(\Lambda) + \frac{1}{16\pi^2}\beta_{\nu,i}^{(a)}(\Lambda)\log\frac{\Lambda}{M_{\rm M}}\,, \end{aligned} \tag{4.13}$$

respectively. The beta-functions $\beta_e^{(a)}$, $\beta_\nu^{(a)}$ can be found in Appendix A.1. Note that in this case, the scale at which the Yukawa couplings are calculated at one loop is $M_{\rm M}$.

As discussed in Section 3.2.2, the radiative corrections contained in the beta functions leads at most to Yukawa couplings of rank-2. This is indeed the case for charged leptons. The corresponding Feynman diagrams to generate charged lepton masses are exactly the same as for the quark sector, shown in Fig. 3.2, changing quarks by leptons. In this case the Yukawa couplings for the second generation of charged leptons can be calculated at $M_{\rm M}$ as

$$y_\mu^2(M_{\rm M}) \simeq \left(\frac{1}{16\pi^2}\log\frac{\Lambda}{M_{\rm M}}\right)^2 \sum_{i,j=1}^{2}\left(\beta_{e,ij}^{(1)}(\Lambda)\right)^2\,. \tag{4.14}$$

Once the mass degeneracy between the first and second generation of charged leptons is broken, the corresponding eigenvectors become unambiguously fixed. They can also be calculated using the results in Section 3.2.1. Following the notation in eq. (1.3), the unitary matrices V_{e_L} and V_{e_R},

$$V_{e_L}(M_{\rm M}) \simeq \begin{pmatrix} \cos\zeta_{e_L} & \sin\zeta_{e_L} & 0 \\ -\sin\zeta_{e_L} & \cos\zeta_{e_L} & 0 \\ 0 & 0 & 1 \end{pmatrix}, \qquad V_{e_R}(M_{\rm M}) \simeq \begin{pmatrix} \cos\zeta_{e_R} & \sin\zeta_{e_R} & 0 \\ -\sin\zeta_{e_R} & \cos\zeta_{e_R} & 0 \\ 0 & 0 & 1 \end{pmatrix}\,, \tag{4.15}$$

where

$$\tan\zeta_{e_L} = \left(\frac{\beta_{e,11}^{(1)}\beta_{e,21}^{(1)} + \beta_{e,12}^{(1)}\beta_{e,22}^{(1)}}{(\beta_{e,21}^{(1)})^2 + (\beta_{e,22}^{(1)})^2}\right)\Bigg|_\Lambda\,, \quad \tan\zeta_{e_R} = \left.\frac{\beta_{e,11}^{(1)}\beta_{e,12}^{(1)} + \beta_{e,21}^{(1)}\beta_{e,22}^{(1)}}{(\beta_{e,12}^{(1)})^2 + (\beta_{e,22}^{(1)})^2}\right|_\Lambda\,. \tag{4.16}$$

For convenience, at the $M_{\rm M}$ scale we rotate the lepton fields to the basis where the Yukawa coupling of charged leptons with Φ_1 is diagonal. We call the Yukawa coupling in this new basis

$\widetilde{Y}_e^{(a)}(M_{\rm M})$ which is calculated as

$$\widetilde{Y}_e^{(a)}(M_{\rm M}) = (V_{e_L}^\dagger Y_e^{(a)} V_{e_R})(M_{\rm M}). \tag{4.17}$$

For the neutrino sector the scenario is slightly different. It is also useful to define the neutrino Yukawa couplings in the basis where $\widetilde{Y}_e^{(1)}(M_{\rm M})$ is diagonal

$$\widetilde{Y}_\nu^{(a)}(M_{\rm M}) = (V_{e_L}^\dagger Y_\nu^{(a)})(M_{\rm M})\ . \tag{4.18}$$

At the $M_{\rm M}$ scale, the neutrino Yukawa couplings receive quantum corrections following eq. (4.13). If one introduces the one loop corrections to calculate the effective couplings $\kappa^{(ab)}$, one finds that at the $M_{\rm M}$ scale

$$\kappa_{ij}^{(ab)}(M_{\rm M}) = \frac{1}{M_{\rm M}}\ \widetilde{Y}_{\nu,i}^{(a)} \widetilde{Y}_{\nu,j}^{(b)}\Big|_{M_{\rm M}}\ . \tag{4.19}$$

As one can see, these couplings are still a rank-1 matrices. As left-handed neutrino masses are generated by $\kappa^{(11)}$, at this energy scale, the first and second generation of left-handed neutrinos remain massless.

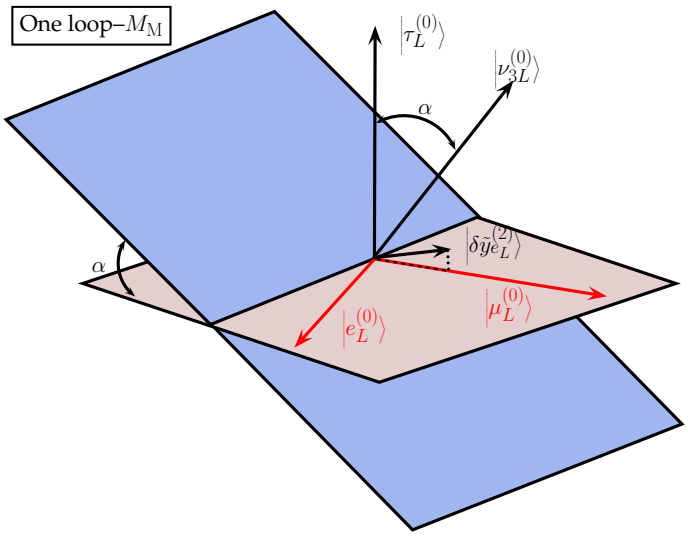

Figure 4.2: Graphical representation of the left-handed eigenvectors in the lepton sector at an energy scale $M_{\rm M}$. At this scale, the eigenvectors for the first and second generation of charged leptons are determined. This is not the case for the left-handed neutrinos, as the radiative corrections do not generate a new direction in flavour space.

This scenario is shown in a graphical representation in Fig 4.2. For charged leptons, at an energy scale $M_{\rm M}$ the loop correction generates a new direction in flavour space which breaks the degeneracy between the first and second generation. The eigenvalue is directly proportional to the projection of the perturbation on the subspace perpendicular to $\left|\tau_L^{(0)}\right\rangle$, and defines the direction of the eigenvector. The same situation has to happen in the right-handed sector, as the Dirac mass connects the left- and right-handed eigenstates.

As the corrections to the neutrino Yukawa couplings do not determine a new direction in flavour space, there is no way to determine the left-handed eigenstates of the corresponding first and second generations.

4.2.2 Determining the Lepton Parameters at the M_H Scale

The Yukawa couplings $Y_e^{(1)}$ is subject to quantum corrections between the scale $M_{\rm M}$ and M_H. Using the leading-log approximation one finds

$$Y_{e,ij}^{(a)}(M_H) \simeq Y_{e,ij}^{(a)}(M_{\rm M}) + \frac{1}{16\pi^2}\beta_{e,ij}^{(a)}(M_{\rm M}) \log\frac{M_{\rm M}}{M_H}. \tag{4.20}$$

With this, one can calculate the Yukawa couplings for the charged lepton sector at an energy scale M_H. The corresponding Yukawa singular values are

$$\begin{aligned} y_\tau(M_H) &\simeq y_e^{(1)} \\ y_\mu(M_H) &\simeq \frac{1}{16\pi^2}\left\{\left[\sum_{i,j=1}^{2}\left(\beta_{e,ij}^{(1)}(\Lambda)\right)^2\right]^{1/2}\log\frac{\Lambda}{M_{\rm M}} + \left[\sum_{i,j=1}^{2}\left(\beta_{e,ij}^{(1)}(M_{\rm M})\right)^2\right]^{1/2}\log\frac{M_{\rm M}}{M_H}\right\}, \\ y_e(M_H) &= 0\,. \end{aligned} \tag{4.21}$$

Taking these results, if one calculates the ratio between the muon and tau masses, finds

$$\frac{m_\mu}{m_\tau} \simeq \frac{1}{16\pi^2}\frac{y_e^{(2)}}{y_e^{(1)}}(P^2+Q^2)^{1/2}\,, \tag{4.22}$$

where P and Q are defined as

$$P \equiv y_\nu^{(1)}y_\nu^{(2)}p_\nu \log\left(\frac{\Lambda}{M_{\rm M}}\right) + \sum_{x=e,u,d} y_x^{(1)}y_x^{(2)}p_x \log\left(\frac{M_{\rm M}}{M_H}\right)\,, \tag{4.23}$$

$$Q \equiv y_\nu^{(1)}y_\nu^{(2)}q_\nu \log\left(\frac{\Lambda}{M_{\rm M}}\right) + \sum_{x=e,u,d} y_x^{(1)}y_x^{(2)}q_x \log\left(\frac{M_{\rm M}}{M_H}\right)\,, \tag{4.24}$$

and p_x, q_x are functions of the angles inside the Yukawa matrices $Y_x^{(2)}(\Lambda)$. They are given in Appendix A.2. In this framework the first generation remains massless even if the Yukawa couplings at a scale $M_{\rm M}$ are already of rank-2. This is because there is no new direction in flavour space added to the model which can generate a mass for the first generation. Therefore, the discussion in Section 3.2.2 remains valid for charged leptons at this energy scale.

It is possible to estimate the value of the mass ratio between the second and third generation of charged leptons, even if it depends on several parameters. Here, p_x and q_x exclusively depend on the mixing angles inside the Yukawa couplings with Φ_2. If one takes generic values for these angles, p_x and q_x acquire values $\mathcal{O}(0.1)$. Furthermore, it is also reasonable to assume $y_x^{(2)} \sim y_x^{(1)}$. With this, the main contribution to the muon mass comes from the neutrino Yukawa coupling or from the up-type Yukawa coupling. In the latter case, as the $M_{\rm M} \gg M_H$, the mass ratio

is enhanced by the logarithm. For example, if one sets $\Lambda = 10^{19}$ GeV, $M_{\rm M} = 10^{14}$ GeV and $M_H = 10^4$ GeV, one gets $\log(\Lambda/M_{\rm M}) \sim 10$ and $\log(\Lambda/M_H) \sim 30$. Therefore, the ratio between the muon and the tau mass can be approximated to

$$\frac{m_\mu}{m_\tau} \sim (0.01 - 0.1)\frac{y_e^{(2)}}{y_e^{(1)}} \max\left\{y_\nu^{(1)} y_\nu^{(2)}, 3 y_u^{(1)} y_u^{(2)}\right\} \ . \tag{4.25}$$

In Fig. 4.3 we show the probability distribution of this mass ratio with the assumptions mentioned above and a flat linear distribution for the Yukawa mixing angles in $Y_x^{(2)}$, between 0 and 2π. The blue histogram contains the quantum effects generated only by neutrinos, fixing $y_\nu^{(1)} = y_\nu^{(2)} = 1$, whereas the red histogram shows the results for the quantum effects generated only by the top quark, with $y_u^{(1)} = y_u^{(2)} = 1$. If changing the values of the Yukawa couplings, the probability distribution would be rescaled on the horizontal axis. The experimental value for the muon and tau masses shows a large hierarchy between them. This suggests that the generation of the muon mass is dominated by the diagram with the right-handed neutrino inside the loop. Nevertheless, the proper ratio between the masses can be generated from the top loop diagram by the appropriate choice of the parameters of the model.

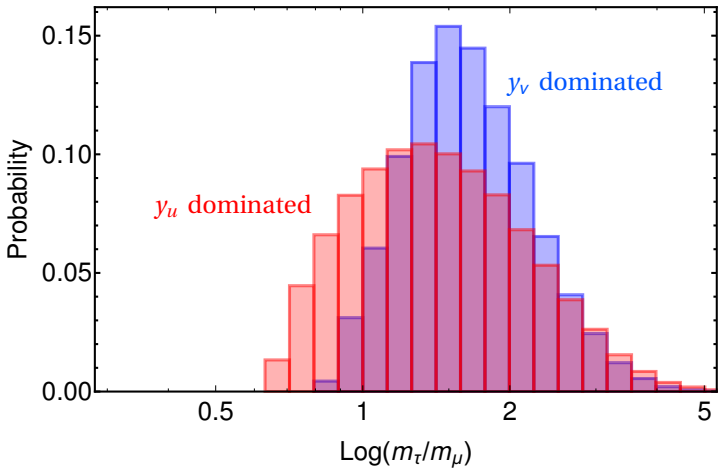

Figure 4.3: Probability distribution for m_μ/m_τ from a random scan of the angles in the model. The blue curve only contains the effects generated by neutrinos, whereas the blue curve only contains the contribution of the top quark.

For the charged lepton mixing sector, as the matrices which diagonalise the Yukawa couplings with Φ_1 are already determined at $M_{\rm M}$, at the M_H scale they only receive loop suppressed corrections. Hence, they approximately read as eq. (4.15). For the neutrino sector, $\kappa^{(11)}(M_{\rm M})$ is of rank-1. Therefore there are two degenerate, vanishing masses. Nevertheless, below $M_{\rm M}$, $\kappa_{ij}^{(ab)}$ is also subject to radiative corrections

$$\kappa_{ij}^{(ab)}(M_H) \simeq \kappa_{ij}^{(ab)}(M_{\rm M}) + \frac{1}{16\pi^2}\beta^{(a)}_{\kappa^{(ab)},ij}(M_{\rm M}) \log\frac{M_{\rm M}}{M_H} \tag{4.26}$$

where $\beta_{\kappa^{(ab)}}$ is contained in Appendix A.1. As was already noted in [86], there is only one term in the β function which generates a radiative mass for the second generation of left-handed neutrinos in such a scenario. It is contained in the last term in eq. (A.6), and corresponds to

$$2\lambda_5 \frac{\widetilde{Y}_\nu^{(2)} \widetilde{Y}_\nu^{(2)T}}{M_{\rm M}}, \tag{4.27}$$

where λ_5 is a coupling constant in the potential presented in eq. (2.1). The corresponding Feynman diagram, which contributes to induce a mass for the second generation, is shown in Fig. 4.4.

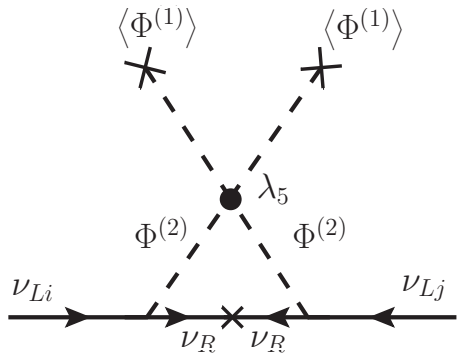

Figure 4.4: One loop Feynman diagram which generates a non-vanishing mass for ν_{L_2}.

With all this, one finds that the neutrino masses at the M_H scale, neglecting subdominant effects, are

$$m_3(M_H) \simeq \frac{v^2}{2M_{\rm M}} |\widetilde{Y}_\nu^{(1)}|^2 \,, \tag{4.28}$$

$$m_2(M_H) \simeq \frac{1}{16\pi^2} \frac{\lambda_5 v^2}{M_{\rm M}} \left[|\widetilde{Y}_\nu^{(2)}|^2 - \frac{(\widetilde{Y}_\nu^{(2)T} \widetilde{Y}_\nu^{(1)})^2}{|\widetilde{Y}_\nu^{(1)}|^2} \right] \log \frac{M_{\rm M}}{m_H} \,, \tag{4.29}$$

$$m_1(M_H) \simeq 0. \tag{4.30}$$

The ratio between the masses of the second and third generation is then

$$\frac{m_2}{m_3} \simeq \frac{\lambda_5}{8\pi^2} \left(\frac{y_\nu^{(2)}}{y_\nu^{(1)}} \right)^2 (1 - \cos^2\psi) \log \frac{M_{\rm M}}{m_H} \,. \tag{4.31}$$

Here, $\cos\psi \equiv \cos\alpha \cos\theta_\nu + \sin\alpha \sin\theta_\nu \cos\omega_\nu$ determines the misalignment between $Y_\nu^{(1)}$ and $Y_\nu^{(2)}$. This outcome is quite intuitive, as to generate a non-vanishing neutrino mass for the second generation, there must be a Yukawa coupling pointing in a new direction in flavour space. Therefore, $\sin\psi > 0$ to generate $m_2 \neq 0$. This scenario is slightly different from the quark sector, as the right-handed neutrinos are Majorana particles and the mass term for the left-handed sector is generated in the see-saw mechanism. Here, $m_1(M_H)$ can be approximated to be zero. Nevertheless, the latter is not exactly zero, but receives corrections from two loop diagrams [87].

The discussion in Section 3.2.2 is therefore not valid for the neutrino sector if taking into account higher loop corrections.

As done for charged leptons, we want to estimate the magnitude of the neutrino mass ratio in this scenario. If we again take generic values for the Yukawa mixing angles on gets $\cos\psi = \mathcal{O}(0.1)$ and with $\Lambda = 10^{19}$ GeV and $M_{\rm M} = 10^{14}$ GeV (therefore, $\log(\Lambda/M_{\rm M}) \sim 10$), one finds

$$\frac{m_2}{m_3} \simeq (0.1 - 1)\,\lambda_5 \left(\frac{y_\nu^{(2)}}{y_\nu^{(1)}}\right)^2 . \tag{4.32}$$

In Fig. 4.5 we show the probability distribution for the mass ratio m_2/m_3. For this plot $y_u^{(1)} \simeq y_u^{(2)}$ and $\lambda_5 = 1$ have been assumed. A flat linear distribution for the mixing angles inside the Yukawa couplings with Φ_2 has been taken. One can see that indeed, $m_2/m_3 = \mathcal{O}(0.1)$, which is in agreement with experimental data.

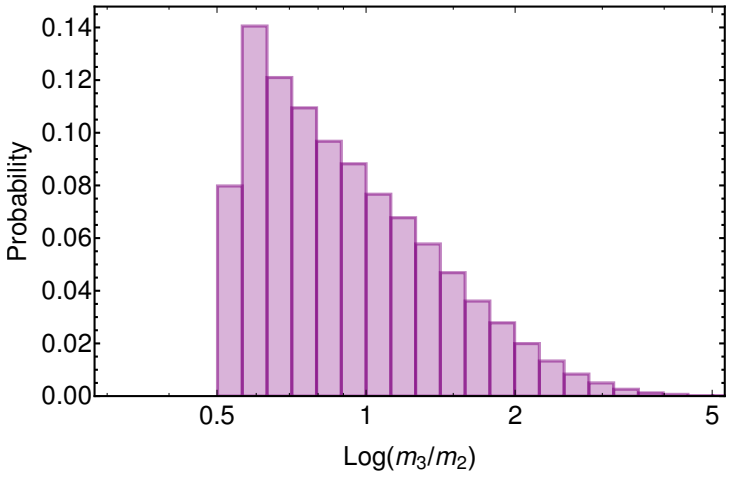

Figure 4.5: Probability distribution ofm_2/m_3 using a flat linear random scan of Yukawa angles at the cut-off scale.

Now, as the degeneracy between the first and second generation is broken, the neutrino mixing matrix is univocally determined. Its second and third column, neglecting subleading effects, read

$$\begin{aligned} V_{\nu,i3}(m_H) &\simeq \frac{\widetilde{Y}_{\nu i}^{(1)}}{|\widetilde{Y}_\nu^{(1)}|} , \\ V_{\nu,i2}(m_H) &\simeq \frac{1}{N_2}\left[\widetilde{Y}_\nu^{(2)} - \frac{\widetilde{Y}_\nu^{(2)T}\widetilde{Y}_\nu^{(1)}}{|\widetilde{Y}_\nu^{(1)}|^2}\widetilde{Y}_\nu^{(1)}\right] , \end{aligned} \tag{4.33}$$

with $|\widetilde{Y}_\nu^{(a)}|^2 = \sum_i (\widetilde{Y}_{\nu i}^{(a)})^2$ and

$$N_2 \equiv \left[\widetilde{Y}_\nu^{(2)T}\widetilde{Y}_\nu^{(2)} - \frac{(\widetilde{Y}_\nu^{(2)T}\widetilde{Y}_\nu^{(1)})^2}{|\widetilde{Y}_\nu^{(1)}|^2}\right]^{1/2} , \tag{4.34}$$

where the neutrino Yukawa couplings $\widetilde{Y}_\nu^{(a)}$ are all evaluated at the scale $M_{\rm M}$.

With the flavour basis to the mass basis rotation well determined, the PMNS matrix can be calculated. The PMNS mixing angles approximately read

$$\begin{aligned}
\tan\theta_{12} &\simeq \frac{\sin\zeta_{e_L}\cos\alpha\,(\cos\alpha\sin\theta_\nu\cos\omega_\nu-\sin\alpha\cos\theta_\nu)-\cos\zeta_{e_L}\sin\theta_\nu\sin\omega_\nu}{\cos\alpha\sin\theta_\nu\,(\cos\zeta_{e_L}\cos\omega_\nu+\sin\zeta_{e_L}\sin\omega_\nu)-\cos\zeta_{e_L}\sin\alpha\cos\theta_\nu}\,,\\
\sin\theta_{13} &\simeq -\sin\zeta_{e_L}\sin\alpha\,,\\
\tan\theta_{23} &\simeq \cos\zeta_{e_L}\tan\alpha\,,
\end{aligned} \tag{4.35}$$

where ζ_{e_L} is defined in eq. (4.16). From these results it can be seen that in the limit $\alpha \to 0$, one gets a hierarchical PMNS matrix, as happened for the CKM matrix. Therefore, the amount of misalignment between the rank-1 Yukawa couplings at tree level determines the complete structure of the mixing matrix.

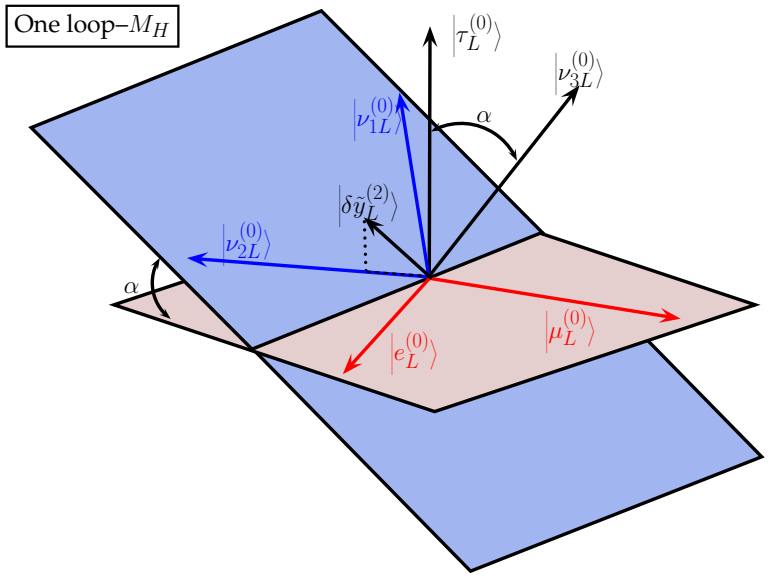

Figure 4.6: One loop scenario at the M_H scale for the lepton sector. The eigenstates of the charged leptons were already determined at $M_{\rm M}$ and now only receive loop suppressed corrections (not plotted here, for simplicity). A small correction to $\kappa^{(11)}$ generates a new direction in flavour space in the neutrino sector, which determines the eigenvector for the second generation.

The scenario at the M_H scale is represented in Fig 4.6. At the $M_{\rm M}$ scale, the left- and right-handed eigenvectors for the charged leptons are already known whereas for the left-handed neutrinos are completely undetermined. At the M_H scale, the former only receive corrections which are loop suppressed. In the case of neutrinos, they receive radiative corrections which generate a small perturbation in flavour space, determining the eigenvalue and eigenvector for the second generation. The eigenvalue is proportional to the projection of the perturbation on the blue surface squared and the same projection determines the direction of the corresponding eigenvector. Thus, all eigenstates are now determined for the lepton sector.

Let us mention that the angle ζ_{e_L} is in general neither maximal nor minimal. Therefore the contribution of charged leptons to the neutrino mixing is in principle not negligible. In this scenario the PMNS matrix has in principle an anarchical structure.

From the model it is possible to univocally determine the parameters α and ζ_{e_L} in terms of the angles θ_{12} and θ_{13}

$$\sin^2\alpha \simeq \frac{\sin^2\theta_{13} + \tan^2\theta_{23}}{1 + \tan^2\theta_{23}}\,, \tag{4.36}$$

$$\sin^2\zeta_{e_L} \simeq \frac{\sin^2\theta_{13}(1 + \tan^2\theta_{23})}{\sin^2\theta_{13} + \tan^2\theta_{23}}\,. \tag{4.37}$$

Taking the known experimental values for the mixing angles, one obtains $|\sin\alpha| \simeq 0.65$, $|\sin\zeta_{e_L}| \simeq 0.23$. Furthermore, the angles θ_ν and ω_ν also are constrained to fulfil the following expression

$$\tan\theta_\nu \simeq \frac{\sin\alpha(\tan\theta_{12}\cos\zeta_{e_L} - \cos\alpha\sin\zeta_{e_L})}{\tan\theta_{12}\cos\alpha\cos(\zeta_{e_L} - \omega_\nu) - \cos^2\alpha\cos\omega_\nu\sin\zeta_{e_L} + \cos\zeta_{e_L}\sin\omega_\nu}\,. \tag{4.38}$$

In this framework, both the values for the masses of the second and third generation of leptons and the lepton mixing angles can be naturally accommodated. Nevertheless, the first generation remains massless and the number of physical parameters is too large to make the model predictive. As was already mentioned in Chapter 3, including new flavour structures, therefore a new direction for each lepton type in Fig. 4.6, can generate a radiative mass for the first generation.

CHAPTER **5**

Fermion Masses in a Three Higgs Doublet Model

In the previous chapters a framework to generate the masses and mixing angles of quarks and leptons in a general 2HDM has been presented. With the assumption of rank-1 Yukawa matrices, the hierarchies between the second and third generation of masses can naturally be reproduced. Furthermore, the mixing matrices for both quark and lepton sectors can be generated with the correct structure through radiative corrections. Even if the model is an appealing scenario to describe the fermion parameters, it has a strong drawback: the first generation of fermions is still massless. This is of course in disagreement with experiments.

In this chapter the analytical results for the SM fermion masses in the context of a 3HDM are presented. The analysis is basis independent and follows the calculations in Chapters 3 and 4.

5.1 The Flavour Structure at Tree Level

In this part the fermion parameters are calculated at tree level in a 3HDM. The model consists in adding two new Higgs doublets to the SM, with the same quantum numbers as the SM Higgs. For the neutrino sector, the masses are generated in the see-saw framework. Hence, one has to add at least one right-handed neutrino to the model.

The Higgs potential for a 3HDM is given by [88, 89]

$$V = m_{ab}^2 \left(\phi_a^\dagger \phi_b\right) + \frac{1}{2}\lambda_{abcd} \left(\phi_a^\dagger \phi_b\right) \left(\phi_c^\dagger \phi_d\right) \tag{5.1}$$

with $a, b, c, d = 1, 2, 3$. Note that for $a, b, c, d = 1, 2$, one recovers the 2HDM potential in eq. (2.1).

The Yukawa and neutrino parts of the Lagrangian are completely analogous to eq. (2.19) and eq. (4.1), respectively, with $a = 1, 2, 3$. Following the analysis in the previous chapters, we take the limit of rank-1 Yukawa couplings at a cut-off scale Λ. To make a basis independent analysis, we write the Yukawa matrices as an outer product of two dimension-3 vectors

$$Y_{\tilde{x}}^{(a)}(\Lambda) = \left|y_{\tilde{x}_L}^{(a)}\right\rangle \left\langle y_{\tilde{x}_R}^{(a)}\right|, \tag{5.2}$$

where $\tilde{x} = u, d$ and e. To simplify the scenario, we just add one right-handed neutrino to the model. Therefore the corresponding neutrino Yukawa couplings are

$$Y_\nu^{(a)}(\Lambda) = \left| y_{\nu_L}^{(a)} \right\rangle . \tag{5.3}$$

To make the model compatible with the current experimental constraints, we take the decoupling limit. Therefore the bosons in Φ_2 and Φ_3 take masses much larger than the SM Higgs mass. For simplicity we collectively denote the heavy masses by M_H.

Physical Parameters

It has already been discussed, that the amount of parameters in the Yukawa sector of the 2HDM is too large to make the model predictive. In the 3HDM we are adding one new Yukawa coupling for each fermion type, increasing the number of parameters by 20 in the quark sector and 16 in the lepton sector. Furthermore, as we will now see, one can generate the masses for all fermions in this scenario. Here we calculate how many of the parameters in the model are indeed physical.

For the quark sector, in the absence of Yukawa couplings, there is a global $U(3)^3$ symmetry which breaks into $U(1)_B$ once the quarks masses are introduced

$$U(3)_{Q_L} \times U(3)_{u_R} \times U(3)_{d_R} \longrightarrow U(1)_B \tag{5.4}$$

Following rule in eq. (3.23), this means that the number of physical parameters are

$$30\ \mathbb{R}\text{ Parameters} - 9\text{ Broken }\mathbb{R}\text{ Parameters} = 21\ \mathbb{R}\text{ Physical Parameters}$$
$$30\text{ Phases} - 17\text{ Broken Phases} = 13\text{ Physical Phases}$$

For the lepton sector the group that breaks is

$$U(3)_{L_L} \times U(3)_{e_R} \tag{5.5}$$

The neutrino Yukawa couplings are assumed to be dimension 3 vectors. Hence, the number of physical parameters in the lepton sector is calculated as

$$24\ \mathbb{R}\text{ Parameters} - 6\text{ Broken }\mathbb{R}\text{ Parameters} = 18\ \mathbb{R}\text{ Physical Parameters}$$
$$24\text{ Phases} - 12\text{ Broken Phases} = 12\text{ Physical Phases}$$

Therefore, for the Yukawa quark sector, from the total of 60 parameters in the model, there are only 34 which are physical. The Yukawa lepton sector contains a total of 48 parameters. But only 30 of them are physical. This means that, as for the 2HDM, this model is also non-predictive.

Tree Level Masses

Following the previous chapters, for simplicity and without loss of generality we chose to work in the basis where just one of the Higgs doublets acquires a vev. Therefore $\langle \Phi_1^0 \rangle = v/\sqrt{2}$ and

$\langle \Phi_2^0 \rangle = \langle \Phi_3^0 \rangle = 0$. From the rank-1 Yukawa matrices presented in eq. (5.2), the masses at tree level are completely analogous to the ones in the 2HDM. They are calculated as follows

$$m_{\tilde{x}_3}^{(0)}|_{\text{tree}} = \frac{v}{\sqrt{2}} \sqrt{\left\langle y_{\tilde{x}_L}^{(1)} \middle| y_{\tilde{x}_L}^{(1)} \right\rangle \left\langle y_{\tilde{x}_R}^{(1)} \middle| y_{\tilde{x}_R}^{(1)} \right\rangle}\,, \tag{5.6}$$

for $\tilde{x} = u, d, e$. As we want to generate neutrino masses in the see-saw scenario, one has to take into account that there is a Majorana mass term for right-handed neutrinos. Therefore the neutrino mass Lagrangian follows eqs. (4.1–4.3). Taking the Yukawa coupling in eq. (5.3), the mass for the third generation neutrino is

$$m_{\nu_3}^{(0)}|_{\text{tree}} = \frac{v^2}{2} \frac{\left\langle y_{\nu_L}^{(1)} \middle| y_{\nu_L}^{(1)} \right\rangle}{M_{\text{M}}}. \tag{5.7}$$

As in the 2HDM, the first and second generation of fermions remain massless at tree level.

5.2 Basis Independent Quantum Corrections

In order to calculate the one loop corrections to the Yukawa couplings in a 3HDM, we use the leading-log approximation defined in eq. (3.9) for the quark sector and eqs. (4.13), (4.20) for the lepton sector. The corresponding β functions are defined in Appendix A.1.

5.2.1 Generating Rank-3 Yukawa Couplings

In the framework of a 2HDM with rank-1 Yukawa couplings there are only two determined directions in flavour space. This means that one can generate at most one radiative mass, leaving the first generation of fermions massless. In a 3HDM, one Yukawa coupling is added for each fermion type with respect to the 2HDM. Therefore, following the discussion in Section 3.2.2, in a 3HDM, the one loop corrections can be written as

$$\begin{aligned} \frac{1}{16\pi^2} \log \frac{E_1}{E_2} \beta_x^{(1)}(E_1) &= A_x \left| y_{x_L}^{(1)} \right\rangle \left\langle y_{x_R}^{(1)} \right| + B_x \left| y_{x_L}^{(2)} \right\rangle \left\langle y_{x_R}^{(2)} \right| + C_x \left| y_{x_L}^{(3)} \right\rangle \left\langle y_{x_R}^{(3)} \right| \\ &= \left| \delta\tilde{y}_{x_L}^{(1)} \right\rangle \left\langle y_{x_R}^{(1)} \right| + \left| \delta\tilde{y}_{x_L}^{(2)} \right\rangle \left\langle y_{x_R}^{(2)} \right| + \left| \delta\tilde{y}_{x_L}^{(3)} \right\rangle \left\langle y_{x_R}^{(3)} \right| \end{aligned} \tag{5.8}$$

with $\frac{E_1}{E_2} = \frac{\Lambda}{M_H}$ for quarks, at M_{M}, $\frac{E_1}{E_2} = \frac{\Lambda}{M_{\text{M}}}$ for charged leptons and at M_H, $\frac{E_1}{E_2} = \frac{M_{\text{M}}}{M_H}$ for leptons. Hence, following eq. (3.22), the Yukawa couplings with Φ_1 at one loop are

$$\begin{aligned} Y_x^{(1)}|_{1-\text{loop}} &\simeq \left| y_{x_L}^{(1)} \right\rangle \left\langle y_{x_R}^{(1)} \right| + \left| \delta\tilde{y}_{x_L}^{(1)} \right\rangle \left\langle y_{x_R}^{(1)} \right| + \left| \delta\tilde{y}_{x_L}^{(2)} \right\rangle \left\langle y_{x_R}^{(2)} \right| + \left| \delta\tilde{y}_{x_L}^{(3)} \right\rangle \left\langle y_{x_R}^{(3)} \right| \\ &= \left| y_{x_L}^{\prime(1)} \right\rangle \left\langle y_{x_R}^{(1)} \right| + \left| \delta\tilde{y}_{x_L}^{(2)} \right\rangle \left\langle y_{x_R}^{(2)} \right| + \left| \delta\tilde{y}_{x_L}^{(3)} \right\rangle \left\langle y_{x_R}^{(3)} \right|. \end{aligned} \tag{5.9}$$

This corresponds to a rank-3 matrix. As there are three different rank-1 Yukawa matrices for each fermion type, the model generates three different directions in flavour space. Hence the masses of the first and second generations of fermions are both induced through radiative corrections in this scenario. A completely analogous scenario is to assume that in a 2HDM, at least one of the

Yukawa matrices is of rank-2, for each fermion type. In such case, the model would also contain three different directions in flavour space for each fermion type and thus generate masses for all fermion generations.

5.2.2 Fermion Masses at One Loop

We now present the analytical results for the radiative fermion masses. Using the result in eq. (3.19), one finds that the corresponding eigenvalues y_{x2}^2 and y_{x1}^2, generated at zero-th order in perturbation theory in a basis independent analysis are

$$y_{x2}^2 + y_{x1}^2 \simeq \mathrm{Tr}(\mathbb{P}_x \mathbb{Q}_x), \tag{5.10}$$

$$y_{x2}^2 y_{x1}^2 \simeq \mathrm{Det}(\mathbb{P}_x)\mathrm{Det}(\mathbb{Q}_x) \tag{5.11}$$

where $\mathbb{P}_{x_{a,b}}$ and $\mathbb{Q}_{x_{a,b}}$ correspond to the ab entry of the 2×2 $\mathbb{P}_x$ and $\mathbb{Q}_x$ matrices, defined as

$$\mathbb{P}_{x_{a,b}} = \left\langle \delta\tilde{y}_{x_L}^{(a+1)} \right| P_{x_L} \left| \delta\tilde{y}_{x_L}^{(b+1)} \right\rangle, \tag{5.12}$$

$$\mathbb{Q}_{x_{a,b}} = \left\langle y_{x_R}^{(a+1)} \right| P_{x_R} \left| y_{x_R}^{(b+1)} \right\rangle. \tag{5.13}$$

Furthermore, P_{x_L} and P_{x_R} are the operators that project any vector to the subspace perpendicular to $\left|y_{x_L}^{(1)}\right\rangle$ and $\left|y_{x_R}^{(1)}\right\rangle$, respectively

$$P_{x_{L,R}} = \mathbb{1} - \frac{\left|y_{x_{L,R}}^{(1)}\right\rangle \left\langle y_{x_{L,R}}^{(1)}\right|}{\left\langle y_{x_{L,R}}^{(1)} \middle| y_{x_{L,R}}^{(1)} \right\rangle}. \tag{5.14}$$

Here, $\left|\delta\tilde{y}_{x_L}^{(2,3)}\right\rangle$ are vectors which are loop suppressed. The loop suppression generates smaller masses for both first and second generation with respect to the third generation. These vectors are calculated at the M_H scale. The corresponding expressions can be found in Appendix A.3. Note that for the neutrino sector, to calculate the masses we want to find the singular values of $\kappa^{(11)}$. This means that here $y_{\nu 2}^2$ and $y_{\nu 1}^2$ should not be the eigenvalues of the Yukawa matrix with Φ_1 but of $\kappa^{(11)}\kappa^{(11)*}$. Therefore, for the neutrino sector, this discussion is only valid when changing $R \to L$. Hence, $\mathbb{Q}_\nu$ is defined as

$$\mathbb{Q}_{\nu_{a,b}} = \left\langle y_{b_L}^{(a+1)} \right| P_{x_L} \left| y_{\nu_L}^{(b+1)} \right\rangle. \tag{5.15}$$

Thus, the masses of the first and second generation of neutrinos are calculated as follows

$$m_{\nu 1,2} = \frac{v^2}{2} y_{\nu 1,2}. \tag{5.16}$$

In Fig. 5.1 the graphical representation of the Yukawa sector following the results in eqs. (5.10) and (5.11) at the M_H scale is shown. On the left (right) panel, the left- (right-) handed sector is represented. For the left-handed sector, the vectors $\left|y_{x_L}^{(1)}\right\rangle$ determine the left-handed eigenvalues of the third generation of fermions, exactly as for the 2HDM. The one loop corrections induce two

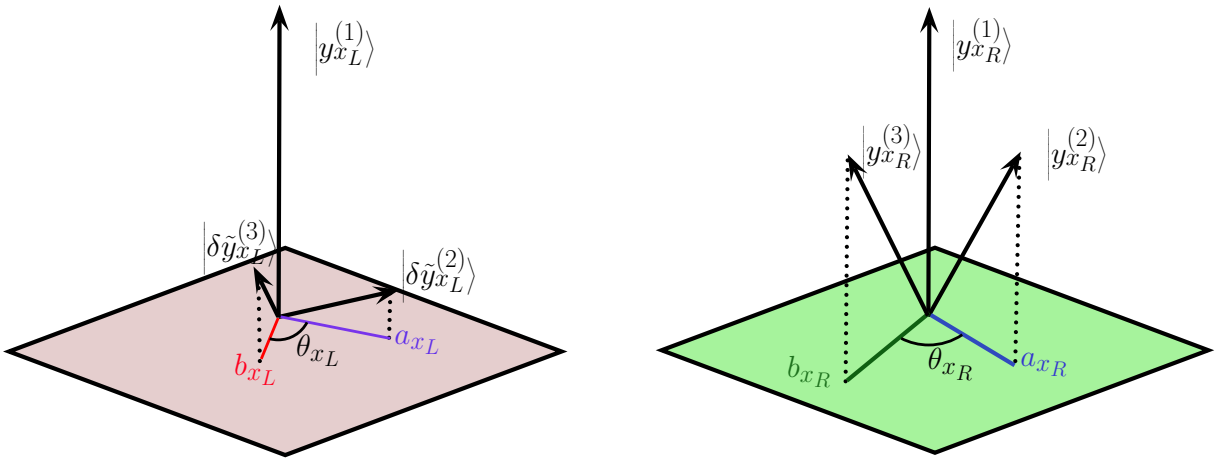

Figure 5.1: Graphical representation of the one loop scenario in a 3HDM for both left- and right-handed sectors at the M_H scale. See text for details.

new vectors in flavour space, $\left|\delta\tilde{y}^{(2)}_{x_L}\right\rangle$ and $\left|\delta\tilde{y}^{(3)}_{x_L}\right\rangle$. Each one of these vectors generates a projection in the surface perpendicular to $\left|y^{(1)}_{x_L}\right\rangle$, which we call a_{x_L} and b_{x_L}. The angle between the latter is θ_{x_L}. A similar situation happens for the right-handed sector. In this case, the two vectors which generate two new directions in space with respect to $\left|y^{(1)}_{x_R}\right\rangle$ are $\left|y^{(2)}_{x_R}\right\rangle$ and $\left|y^{(3)}_{x_R}\right\rangle$. These vectors are not loop suppressed. The projections on the subspace perpendicular to $\left|y^{(1)}_{x_R}\right\rangle$ are named a_{x_R} and b_{x_R}. These projections are misaligned by an angle θ_{x_R}. Hence, using eqs. (5.10), (5.11), the Yukawa couplings of the second and first generation are written in terms of these new parameters as

$$(y^2_{x_2} + y^2_{x_1})(M_H) \simeq \left[a^2_{x_L} a^2_{x_R} + b^2_{x_L} b^2_{x_R} + 2\left(a_{x_L} b_{x_L} \cos\theta_{x_L}\right)\left(a_{x_R} b_{x_R} \cos\theta_{x_R}\right)\right] \tag{5.17}$$

$$(y^2_{x_2} y^2_{x_1})(M_H) \simeq \left[\left(a^2_{x_L} b^2_{x_L} \sin^2\theta_{x_L}\right)\left(a^2_{x_R} b^2_{x_R} \sin^2\theta_{x_R}\right)\right]. \tag{5.18}$$

It is straightforward to see which are the conditions needed to generate radiative masses for the lightest generations. To induce the masses for the second generation of fermions one needs at least

- $\left|\delta\tilde{y}^{(2)}_{x_L}\right\rangle$ or $\left|\delta\tilde{y}^{(3)}_{x_L}\right\rangle$ misaligned from $\left|y^{(1)}_{x_L}\right\rangle$ and
- $\left|y^{(2)}_{x_R}\right\rangle$ or $\left|y^{(3)}_{x_R}\right\rangle$ misaligned from $\left|y^{(1)}_{x_R}\right\rangle$.

For the first generation to acquire a mass, a misalignment of the projections is needed for both left- and right-handed sectors. This means that

- both $\left|\delta\tilde{y}^{(2)}_{x_L}\right\rangle$ and $\left|\delta\tilde{y}^{(3)}_{x_L}\right\rangle$ have to be misaligned from $\left|y^{(1)}_{x_L}\right\rangle$,
- both $\left|y^{(2)}_{x_R}\right\rangle$ and $\left|y^{(3)}_{x_R}\right\rangle$ have to be misaligned from $\left|y^{(1)}_{x_R}\right\rangle$ and

- both angles θ_{x_L} and θ_{x_R} have to be larger than zero.

Both masses are loop suppressed, as a_{x_L} and b_{x_L} contain the corresponding loop factor. As mentioned above, for the neutrino sector one has to change $R \to L$.

It is known from experiments that one of these two Yukawa singular values has to be larger than the other one, due to the hierarchies between the first and second generation of masses. We assign y_{x1} to the smallest eigenvalue and y_{x2} to the next-to-smallest eigenvalue. This means that the Yukawa couplings of the first and second generation at the M_H scale approximately read

$$y_{x2}^2(M_H) \simeq \mathrm{Tr}(\mathbb{P}_x \mathbb{Q}_x)|_{M_H}\,, \tag{5.19}$$

$$y_{x1}^2(M_H) \simeq \mathrm{Det}(\mathbb{P}_x)\mathrm{Det}(\mathbb{Q}_x) y_{x2}^{-2}\Big|_{M_H}\,. \tag{5.20}$$

Using the simplified expressions in eqs. (5.17), (5.18), one can calculate the ratio between the first and second generation of masses. Assuming for simplicity $a_{x_{L,R}} \sim b_{x_{L,R}}$, one finds

$$\frac{m_{x_1}}{m_{x_2}} \simeq \frac{\sin\theta_{x_L}\sin\theta_{x_R}}{2 + 2\cos\theta_{x_L}\cos\theta_{x_R}}. \tag{5.21}$$

This means that the hierarchy between the first and second generation of fermions is fixed by the misalignment parametrised by $\theta_{x_{L,R}}$. Taking a misalignment of $\theta_{x_{L,R}} \sim \mathcal{O}(0.1)$, one gets $m_{x_1}/m_{x_2} \sim \mathcal{O}(10^{-3})$. Therefore, in this scenario, without strong assumptions we are generating the masses for the third generation of fermions at tree level and radiative masses for the first and second generation, with a hierarchy between them determined by the distribution of the Yukawa couplings in flavour space.

Of course, one can always take the 2HDM limit, in which at least one of the following conditions is fulfilled

- $a_{x_L} \gg b_{x_L}$ and/or
- $a_{x_R} \gg b_{x_R}$

or vice versa. With at least one of these assumptions one also generates a strong hierarchy between both masses

$$\frac{m_{x_1}}{m_{x_2}} \simeq \frac{b_{x_L} b_{x_R}\sin\theta_{x_L}\sin\theta_{x_R}}{a_{x_L} a_{x_R}} \ll 1. \tag{5.22}$$

In this limit, the expression for m_{x_2} is the same as for the 2HDM.

CHAPTER **6**

Constraints from Flavour Physics

In the previous chapters we have presented different extensions of the SM with extra Higgs doublets to explain the hierarchies between the masses and the pattern of the mixing angles in the fermion sector. In order to make the models compatible with the current experimental constraints, we have taken the decoupling limit. As explained in Chapter 2, this limit does not avoid FCNCs or new sources of CP violation, but suppresses new physics effects by assuming that the scale of new physics is much higher than the electroweak scale.

In this chapter we make a phenomenological analysis of a general 2HDM with rank-1 Yukawa couplings, following Chapters 3 and 4 . We study the impact of new physics on flavour observables in order to understand which observables are most sensitive to the model and to set a limit on the scale of new physics.

6.1 The $\Delta F = 2$ Observables: Basic formulae

This part contains a description of the basic formulae for the $\Delta F = 2$ observables in $K - \bar{K}$ and $B^0_{s,d} - \bar{B}^0_{s,d}$ mixing systems and rare K and B meson decays. In particular, the observables discussed are ΔM_s, ΔM_d, $S_{\psi\phi}$ and $S_{\psi K_S}$ for the B sector, and ΔM_K and ε_K for the K sector.

6.1.1 $\Delta F = 2$ within the Standard Model

B Physics

In the SM, the $B^0_{d,s}$ and $\bar{B}^0_{d,s}$ mesons mix. The mixing happens because their mass eigenstates are a linear combination of the flavour eigenstates. In the SM, the dominant contribution comes from box diagrams as the one in Fig. 1.1. The mixing is parametrised through the difference between the two mass eigenvalues, which is proportional to the absolute value of the off-diagonal 12 entry of the B meson mass matrix, defined as [90]

$$M_{12(d,s)} = \frac{G_F^2}{12\pi^2} M_W^2 m_{B_{(d,s)}} \left(\lambda_t^{(d,s)}\right)^2 F^2_{B_{(d,s)}} \hat{B}_{B_{(d,s)}} \eta_B S_0(B_{(d,s)}) \,, \tag{6.1}$$

where the relevant CKM factors that enter meson mixing are defined as

$$\lambda_t^{(d)} = V_{tb}^* V_{td}, \qquad \lambda_t^{(s)} = V_{tb}^* V_{ts} \ . \tag{6.2}$$

Here, M_W corresponds to the W boson mass, $F_{B_{d,s}}$ are meson constants, η_B contains short distance QCD corrections, $\hat{B}_{B_{(d,s)}}$ are SM non-perturbative factors given in [90] and $S_0(x_t)$ is the flavour universal real valued function which describes the top contribution to the one-loop box function, and is defined as [91, 92]

$$S_0(x_t) = \frac{4x_t - 11x_t^2 + x_t^3}{4(1-x_t)^2} - \frac{3x_t^2 \log x_t}{2(1-x_t)^3} \ , \tag{6.3}$$

where $x_t = m_t^2/M_W^2$. The $\Delta B = 2$ mass differences for the $B_{d,s}$ systems are [93]

$$\Delta M_{d,s} = M_{d,s}^H - M_{d,s}^L = 2|M_{12(d,s)}| \ , \tag{6.4}$$

where H and L denote heavy and light, respectively. Using then eq. (6.1), one finds

$$\Delta M_d = \frac{G_F^2}{6\pi^2} M_W^2 m_{B_d} |\lambda_t^{(d)}|^2 F_{B_d}^2 \hat{B}_{B_d} \eta_B S_0(x_t) \, , \tag{6.5}$$

$$\Delta M_s = \frac{G_F^2}{6\pi^2} M_W^2 m_{B_s} |\lambda_t^{(s)}|^2 F_{B_s}^2 \hat{B}_{B_s} \eta_B S_0(x_t) \, . \tag{6.6}$$

The numerical calculations for the SM predictions in [94] give

$$\Delta M_d = (0.53 \pm 0.02) \text{ ps}^{-1} \qquad \text{and} \qquad \Delta M_s = (20.31 \pm 3.25) \text{ ps}^{-1} \tag{6.7}$$

and the current experimental values are [95, 96]

$$\Delta M_d = (0.5050 \pm 0.0021 \pm 0.0010) \text{ ps}^{-1} \qquad \text{and} \qquad \Delta M_s = (17.757 \pm 0.021) \text{ ps}^{-1} \ . \tag{6.8}$$

Furthermore, the mixing induced CP violation for the $B_{d,s}$ system is parametrised by $S_{\psi\phi}$ and $S_{\psi K_S}$. This asymmetry is given by given by [6]

$$S_{\psi X} \sin(\Delta M_{d,s} t) = \frac{\Gamma(\bar{B}_{d,s} \to J/\psi X) - \Gamma(B_{d,s} \to J/\psi X)}{\Gamma(\bar{B}_{d,s} \to J/\psi X) + \Gamma(B_{d,s} \to J/\psi X)} \tag{6.9}$$

where X corresponds to ϕ or K_S. In the SM $S_{\psi\phi}$ is parametrised in terms of the β_s phase, $V_{ts} = |V_{ts}| \, e^{-i\beta_s}$, as follows

$$S_{\psi\phi} = \sin(2|\beta_s|). \tag{6.10}$$

The current experimental value measured by the LHCb collaboration [97] and the SM prediction [98] are

$$\sin^{-1} S_{\psi\phi}^{exp} = -0.058 \pm 0.050 \text{ rad} \qquad \text{and} \qquad \sin^{-1} S_{\psi\phi}^{SM} = -0.036 \pm 0.002 \text{ rad}, \tag{6.11}$$

respectively. In the SM, $S_{\psi K_S}$ is parametrised in terms of the β phase

$$S_{\psi K_S} = \sin(2\beta) \tag{6.12}$$

with $V_{td} = |V_{td}|\, e^{-i\beta}$. The corresponding experimental value measured by the Heavy Flavour Averaging Group [99] and the SM prediction [100] are

$$S^{exp}_{\psi K_S} = 0.682 \pm 0.019 \qquad \text{and} \qquad S^{SM}_{\psi K_S} = 0.832^{+0.013}_{-0.033}, \tag{6.13}$$

respectively. As one can see, the experimental results for $S_{\psi\phi}$ are in good agreement with the SM predictions whereas $S_{\psi K_S}$ shows a 2.7σ deviation from the SM [100]. It is therefore interesting to study the contribution of new physics which might change the theoretical predictions of these observables.

K Physics

Just as for B mesons, the K meson mass eigenstates, K_S and K_L, are a mixture of the CP eigenstates K_1 and K_2 [93]

$$K_{S,L} = \frac{K_{1,2} + \varepsilon_K K_{2,1}}{\sqrt{1 + |\varepsilon_K|^2}}. \tag{6.14}$$

Here, ε_K is the parametrisation of indirect CP violation in kaon decay

$$\varepsilon_K = \frac{\langle(\pi\pi)_{I=0}|K_L\rangle}{\langle(\pi\pi)_{I=0}|K_S\rangle} = \frac{\kappa_\epsilon e^{i\varphi_\epsilon}}{\sqrt{2}(\Delta M_K)_{\text{exp}}} \left[\Im\left(M_{12}^K\right)\right], \tag{6.15}$$

where $\varphi_\epsilon = (43.5 \pm 0.05)^\circ$ is a superweak phase defined as [101]

$$\varphi_\epsilon = \arctan\left(\frac{2\Delta M_K}{\Delta\Gamma_K}\right) \tag{6.16}$$

with $\Delta\Gamma_K = \Gamma_S - \Gamma_L$ being the difference between decay widths and $\kappa_\epsilon = 0.94 \pm 0.02$ is a suppression factor which takes into account $\varphi_\epsilon \neq 45^\circ$ and includes long distance effects [102, 103]. Here, ΔM_K is the mass difference between the two mass eigenstates, and is defined as

$$\Delta M_K = 2\Re\left(M_{12}^K\right), \tag{6.17}$$

where M_{12}^K is the 12 entry of the mass matrix for the flavour eigenstates, completely analogous to the B system (with $x_c = m_c^2/M_W^2$),

$$\left(M_{12}^K\right)^* = \frac{G_F^2}{12\pi^2} F_K^2 \hat{B}_K m_K M_W^2 \left[\lambda_c^2 \eta_1 S_0(x_c) + \lambda_t^2 \eta_2 S_0(x_t) + 2\lambda_c\lambda_t \eta_3 S_0(x_c, x_t)\right], \tag{6.18}$$

and

$$\lambda_i = V_{is}^* V_{id}\,. \tag{6.19}$$

The η_i factors are QCD corrections evaluated at the NLO level in [104–108]. For η_1 and η_3 also NNLO corrections are known [109, 110]. Here $S_0(x_c, x_t)$ is a one-loop box function [92]

$$S_0(x_c,x_t) = \frac{-3x_t x_c}{4(-1+x_t)(-1+x_c)} - \frac{x_t(4-8x_t+x_t^2)x_c \log x_t}{4(-1+x_t)^2(-x_t+x_c)} + \frac{x_t x_c(4-8x_c+x_c^2)\log x_c}{4(-1+x_c)^2(-x_t+x_c)}. \tag{6.20}$$

As K_L and K_S are not CP eigenstates, both can decay into CP even (for example, $(\pi\pi)_{I=0}$) and CP odd (for example, $(\pi\pi\pi)_{I=0}$) final states via K_1 and K_2, respectively. The ε_K parameter determines the probability of K_L and K_S of decaying into a CP even or a CP odd final state. The experimental value [6] and the SM prediction [110] are

$$|\varepsilon_K|^{exp} = (2.228 \pm 0.011) \times 10^{-3} \qquad |\varepsilon_K|^{SM} = (1.81 \pm 0.28) \times 10^{-3}, \tag{6.21}$$

respectively. From these two results one can see that in principle there is a slight tension between the theoretical prediction and experimental data. As experiments become more precise, we will be able to determine whether this tension is due to statistical fluctuations or new physics. Furthermore, the SM prediction for the $K_L - K_S$ mass difference calculated in [110] is

$$\Delta M_K^{SM} = (0.47 \pm 0.18) \times 10^{-2} \text{ps}^{-1} \tag{6.22}$$

whereas the current experimental value is [6]

$$\Delta M_K^{exp} = (0.5292 \pm 0.0009) \times 10^{-2} \text{ps}^{-1}. \tag{6.23}$$

As for the B sector, any contribution of new physics might change the theoretical prediction for these observables. Nevertheless, they have to be compatible with the experimental results. In the next part we present the parametrisation of new physics to all the observables presented here.

6.1.2 New Physics on $\Delta F = 2$ Observables

We have just presented the formulas for different $\Delta F = 2$ observables within the SM. As it has already been mentioned, new physics might contribute to change the value of these observables. In such case, the expressions presented above have to be redefined. For the B sector, we redefine $S_{\psi K_S}$ and $S_{\psi\phi}$ as follows

$$S_{\psi K_S} = \sin(2\beta + 2\varphi_{B_d}), \qquad S_{\psi\phi} = \sin(2|\beta_s| - 2\varphi_{B_s}), \tag{6.24}$$

where φ_{B_d} and φ_{B_s} contain the new physics contribution and are directly related to the phases of the functions $S(B_q)$

$$2\varphi_{B_q} = -\text{Arg}(S(B_q)), \quad q = s, d. \tag{6.25}$$

where

$$S(B_{d,s}) = S_0(x_t) + \Delta S(B_{d,s}). \tag{6.26}$$

Here $\Delta S(B_{d,s})$ contains the information of new physics. Furthermore

$$\Delta M_d = \frac{G_F^2}{6\pi^2} M_W^2 m_{B_d} |\lambda_t^{(d)}|^2 F_{B_d}^2 \hat{B}_{B_d} \eta_B |S(B_d)|\,, \tag{6.27}$$

$$\Delta M_s = \frac{G_F^2}{6\pi^2} M_W^2 m_{B_s} |\lambda_t^{(s)}|^2 F_{B_s}^2 \hat{B}_{B_s} \eta_B |S(B_s)|\,. \tag{6.28}$$

For the K sector, M_{12}^K is redefined as

$$\left(M_{12}^K\right)^* = \frac{G_F^2}{12\pi^2} F_K^2 \hat{B}_K m_K M_W^2 \left[\lambda_c^2 \eta_1 S_0(x_c) + \lambda_t^2 \eta_2 S(K) + 2\lambda_c \lambda_t \eta_3 S_0(x_c, x_t)\right], \tag{6.29}$$

with

$$S(K) = S_0(x_t) + \Delta S(K)\,. \tag{6.30}$$

where $\Delta S(K)$ contains the contribution of new physics. The explicit expressions in the general case for $\Delta S(B_{d,s})$ and $\Delta S(K)$ can be found in Sec. 3.2 of [111]. The general structure for these corrections is

$$\Delta S(M) \sim \sum_{X,Y=L,R} \frac{\Delta_X^{ij} \Delta_Y^{ij}}{M_H^2} \sum_k C_{kXY}(\mu_H) \langle Q_{kXY}(\mu_H, M)\rangle\,. \tag{6.31}$$

with $M = B_{d,s}, K$. Here, $C_{kXY}(\mu_H)$ correspond to the different Wilson coefficients and $\langle Q_{kXY}(\mu_H, M)\rangle$ are the hadronic matrix elements between two different states. There are several operators which can contribute to change the theoretical value of these observables which are not included in the SM. In the following section we present the contributing new operators in the context of a general 2HDM with rank-1 Yukawa matrices together with the numerical analysis on the different $\Delta F = 2$ observables.

6.2 $\Delta F = 2$ Observables Analysis

In this section we present the flavour analysis made for a general 2HDM with rank-1 Yukawa couplings, following Chapters 3 and 4.

6.2.1 Preliminaries

In order to make the analysis for the different flavour observables presented above, the model is rotated to the mass basis at the M_H scale, following eq. (2.20). As already explained, the off-diagonal elements in $\widetilde{Y}_d^{(2)}$ generate flavour changing currents at tree level. The translation between the notation in the previous chapters and previous studies in the literature, such as [111],

is

$$\Delta_R^{ij} = -\left(\widetilde{Y}_d^{(2)}\right)_{ij} = \left(\Delta_L^{ji}\right)^* . \tag{6.32}$$

Hence

$$\widetilde{Y}_d^{(2)} = -\begin{pmatrix} * & \left(\Delta_L^{sd}\right)^* & \left(\Delta_L^{bd}\right)^* \\ \Delta_R^{sd} & * & \left(\Delta_L^{bs}\right)^* \\ \Delta_R^{bd} & \Delta_R^{bs} & * \end{pmatrix} . \tag{6.33}$$

In [111] the authors distinguish these four scenarios:

1. Left-handed scenario (LHS) with complex $\Delta_L^{ij} \neq 0$ and $\Delta_R^{ij} = 0$,
2. Right-handed scenario (RHS) with complex $\Delta_R^{ij} \neq 0$ and $\Delta_L^{ij} = 0$,
3. Left-Right symmetric scenario (LRS) with complex $\Delta_L^{ij} = \Delta_R^{ij} \neq 0$,
4. Left-Right asymmetric scenario (ALRS) with complex $\Delta_L^{ij} = -\Delta_R^{ij} \neq 0$,

As explained in Chapter 3, the mass of the lightest quarks vanishes and makes the first column of $\widetilde{Y}_d^{(2)}$ zero. This means that we have $\Delta_R^{sd,bd} = 0$ and thus

- LHS for B_d and K sector
- mixed scenario for B_s: both LH and RH couplings but with different strength (neither LRS nor ALRS).

The diagonal entries are flavour conserving and are not particularly interesting to study in this analysis. Nevertheless, they contribute to change the value of the masses and the mixing angles in the quark sector and have to be taken into account for the numerical analysis.

The operators which are not present in the SM but contribute to the $B_q^0 - \bar{B}_q^0$ mixing ($q = s, d$) here are

$$Q_1^{\mathrm{SLL}} = \left(\bar{b}P_L q\right)\left(\bar{b}P_L q\right) , \tag{6.34a}$$

$$Q_2^{\mathrm{SLL}} = \left(\bar{b}\sigma_{\mu\nu}P_L q\right)\left(\bar{b}\sigma^{\mu\nu}P_L q\right) , \tag{6.34b}$$

where $P_{R,L} = (1 \pm \gamma_5)/2$ and the colour indices are suppressed. For $K^0 - \bar{K}^0$ mixing the two new operators are

$$Q_1^{\mathrm{SLL}} = (\bar{s}P_L d)\,(\bar{s}P_L d) , \tag{6.35a}$$

$$Q_2^{\mathrm{SLL}} = (\bar{s}\sigma_{\mu\nu}P_L d)\,(\bar{s}\sigma^{\mu\nu}P_L d) . \tag{6.35b}$$

$$\tag{6.35c}$$

In order to calculate $\Delta S(M)$ in this model we define

$$T(B_q) = \frac{G_F^2}{12\pi^2} F_{B_q}^2 \hat{B}_{B_q} m_{B_q} M_W^2 \left(\lambda_t^{(q)}\right)^2 \eta_B, \tag{6.36}$$

$$T(K) = \frac{G_F^2}{12\pi^2} F_K^2 \hat{B}_K m_K M_W^2 \left(\lambda_t^{(K)}\right)^2 \eta_2. \tag{6.37}$$

Then

$$T(B_q)[\Delta S(B_q)]_{\rm SLL} = -\frac{(\Delta_L^{bq}(H))^2}{2M_H^2}\left[C_1^{\rm SLL}(\mu_H)\langle Q_1^{\rm SLL}(\mu_H, B_q)\rangle + C_2^{\rm SLL}(\mu_H)\langle Q_2^{\rm SLL}(\mu_H, B_q)\rangle\right] \tag{6.38}$$

$$T(B_q)[\Delta S(B_q)]_{\rm LR} = -\frac{\Delta_L^{bq}(H)\Delta_R^{bq}(H)}{M_H^2}\left[C_1^{\rm LR}(\mu_H)\langle Q_1^{\rm LR}(\mu_H, B_q)\rangle + C_2^{\rm LR}(\mu_H)\langle Q_2^{\rm LR}(\mu_H, B_q)\rangle\right], \tag{6.39}$$

where the Wilson coefficients $C_i^a(\mu_H)$ including NLO QCD corrections are given by [112]

$$\begin{aligned} C_1^{\rm SLL}(\mu) = C_1^{\rm SRR}(\mu) &= 1 + \frac{\alpha_s}{4\pi}\left(-3\log\frac{M_H^2}{\mu^2} + \frac{9}{2}\right), \\ C_2^{\rm SLL}(\mu) = C_2^{\rm SRR}(\mu) &= \frac{\alpha_s}{4\pi}\left(-\frac{1}{12}\log\frac{M_H^2}{\mu^2} + \frac{1}{8}\right), \\ C_1^{\rm LR}(\mu) &= -\frac{3}{2}\frac{\alpha_s}{4\pi}, \\ C_2^{\rm LR}(\mu) &= 1 - \frac{\alpha_s}{4\pi}\frac{3}{N} = 1 - \frac{\alpha_s}{4\pi}, \end{aligned} \tag{6.40}$$

and the matrix elements are given by

$$\langle Q_i^a(\mu_H, B_q)\rangle \equiv \frac{m_{B_q} F_{B_q}^2}{3} P_i^a(\mu_H, B_q). \tag{6.41}$$

They are evaluated at the matching scale $\mu_H = \mathcal{O}(M_H)$ and P_i^a are the coefficients introduced in [113]. In the K sector we have

$$T(K)[\Delta S(K)]_{\rm SLL} = -\frac{(\Delta_L^{sd}(H))^2}{2M_H^2}\left[C_1^{\rm SLL}(\mu_H)\langle Q_1^{\rm SLL}(\mu_H, K)\rangle + C_2^{\rm SLL}(\mu_H)\langle Q_2^{\rm SLL}(\mu_H, K)\rangle\right]. \tag{6.42}$$

The matrix elements are given as

$$\langle Q_i^a(\mu_H, K)\rangle \equiv \frac{m_K F_K^2}{3} P_i^a(\mu_H, K) \tag{6.43}$$

and the Wilson coefficients are as in eq. (6.40) in the B_q sector.

Usually lattice calculations give $\langle Q_i^a(\mu)\rangle$ at scales $\mu \sim 2$ GeV. As we want to study the contribution of the new couplings to the different flavour observables, $\langle Q_i^a(\mu)\rangle$ have to be calculated at the new physics scale. This is done by using the corresponding Renormalization Group Equations (RGEs). The analytic expressions are given in [113]. In Table 6.1 we summarise

the central values of $\langle Q_i^a(\mu_H)\rangle$, for $\mu_H = 100$ TeV, given in the $\overline{\text{MS}}$-NDR scheme. The results are based on the lattice calculations in [114] for the $B^0_{s,d}$-$\bar{B}^0_{s,d}$ system and in [115, 116] for the K^0-$\bar{K}^0$ system.

	$\langle Q_1^{\text{SLL}}(\mu_H)\rangle$	$\langle Q_2^{\text{SLL}}(\mu_H)\rangle$
K^0-$\bar{K}^0$	-0.097	-0.174
B^0_d-$\bar{B}^0_d$	-0.11	-0.20
B^0_s-$\bar{B}^0_s$	-0.16	0.30
	$\langle Q_1^{\text{LR}}(\mu_H)\rangle$	$\langle Q_2^{\text{LR}}(\mu_H)\rangle$
B^0_s-$\bar{B}^0_s$	-0.33	0.45

Table 6.1: Hadronic matrix elements $\langle Q_i^a(\mu_H)\rangle$ in units of GeV^3 at $\mu_H = 100$ TeV.

6.2.2 Numerical Results

In this part we present the numerical results for the $\Delta F = 2$ observables discussed above in the context of a general 2HDM with rank-1 Yukawa couplings. The model studied here contains in general a total of 11 real and 5 complex parameters for the quark sector. The large amount of paramenters makes very challenging to find an analytical expression for each one of the flavour observables. For this reason we do a numerical study of the model. The $\Delta F = 2$ observables can constrain the following ratios of the model

$$\Delta^{sd}_{L,R}/M_H, \qquad \Delta^{bd}_{L,R}/M_H, \qquad \Delta^{bs}_{L,R}/M_H\,. \tag{6.44}$$

In the model, the elements of $\widetilde{Y}_d^{(2)}$ are not independent of each other. Therefore, the B and the K sector cannot be treated separately. The study made in [111] showed that the constraints on the ratios in eq. (6.44) were of the order of $\mathcal{O}(10^{-3}/\text{TeV})$ for B_s system, $\mathcal{O}(10^{-4}/\text{TeV})$ for B_d system and $\mathcal{O}(10^{-5}/\text{TeV})$ for K system. As in principle there is no hierarchy between the elements in $\widetilde{Y}_d^{(2)}$, we expect the strongest constraints from ε_K and ΔM_K. One also has to check if the CP asymmetry $S_{\psi\phi}$ puts further constraints on the phases in $\Delta^{bs}_{L,R}$. Note that the observable which gives the strongest constraint, can strongly depend on the model. As an example, the model studied in [117] shows the strongest new physics constraints coming from B meson decays.

The new physics effects in $\Delta M_{d,s}$ and $|\varepsilon_K|$ scale like $\simeq 1/M_H^2$ whereas the entries in $\widetilde{Y}_d^{(2)}$ depend logarithmically on M_H. In order to find a lower bound on M_H to make the $\Delta F = 2$ observables compatible with the current experimental constraints, we first have a look at the off-diagonal elements in $\widetilde{Y}_d^{(2)}$. In Fig. 6.1 we show the result in [111] for the allowed region for $\Delta^{sd}_L/M_H = -\tilde{s}_{12}e^{i\delta_{12}}/M_H$ using $|V_{ub}| = 3.1\times10^{-3}$ (left plot) $|V_{ub}| = 4.0\times10^{-3}$ (right plot) and $|V_{cb}| = 0.0406$ for both plots, with $M_H = 1$ TeV and the following ε_K and ΔM_K constraints

$$0.75 \le \frac{\Delta M_K}{(\Delta M_K)_{\text{SM}}} \le 1.25, \qquad 2.0\times10^{-3} \le |\varepsilon_K| \le 2.5\times10^{-3}. \tag{6.45}$$

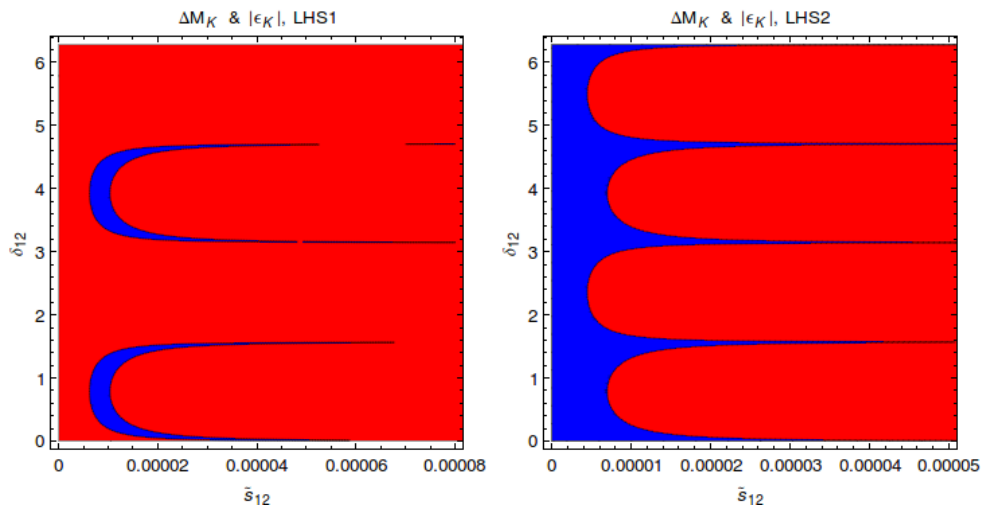

Figure 6.1: Allowed ranges for ΔM_K (red) and ε_k (blue) in eq. 6.45, with $|V_{ub}| = 3.1 \times 10^{-3}$ (left plot) $|V_{ub}| = 4.0 \times 10^{-3}$ (right plot) and $|V_{cb}| = 0.0406$ for both plots at $M_H = 1$ TeV. The results are taken from [111].

Even if in our case, $|V_{ub}|$ and $|V_{cb}|$ are not completely fixed but vary within a certain range, the shape of the allowed region shown in Fig. 6.1 should not vary significantly but would just be slightly shifted. The allowed region corresponds to $\tilde{s}_{12}/M_H \approx 10^{-5}/\text{TeV}$. Doing different scans with the model studied here we have found that the typical values for the real and imaginary part of Δ_L^{sd} (which, as mentioned above, does not strongly vary with M_H, as its dependence is logarithmic) is of the order of $\mathcal{O}(10^{-3}) - \mathcal{O}(10^{-2})$ (see Fig. 6.2). This means that the large deviations from the SM arise for $M_H \lesssim 100$ TeV. For this reason, for the following flavour analysis, the scale of new physics is fixed at $M_H = 100$ TeV.

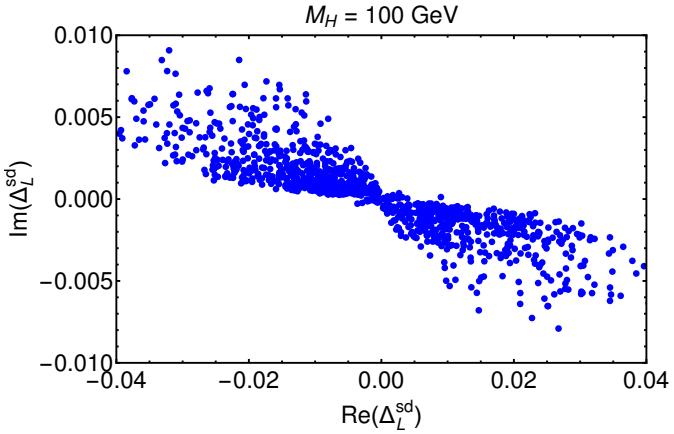

Figure 6.2: Δ_L^{sd} for $M_H = 100$ TeV.

The numerical analysis is divided in three different steps. First, we calculate points in the parameter space of the model which fulfil the constraints of the masses and mixing angles values at $M_H = 100$ TeV. The CP violating phase in the CKM has to be reproduced in this analysis. Therefore we take the phase $\rho_{u_L} \neq 0$ (see eq. (3.8)). In order to reduce the number of parameters

we fix the couplings with Φ_1

$$y_u^{(1)} = 1.09, \qquad y_d^{(1)} = 0.04 \tag{6.46}$$

and we constraint the couplings with Φ_2

$$0.2 < y_u^{(2)} < 1.5, \qquad 0 < y_d^{(2)} < 0.24. \tag{6.47}$$

The mass values used to constrain the parameters in this first part have been calculated using RunDec [118], running the mass values in [6] to 100 TeV. The masses for the second and third generation of quarks are constrained to

$$\begin{aligned} 470 \text{ MeV} < m_c < 680 \text{ MeV}, \qquad & 55 \text{ MeV} < m_s < 100 \text{ MeV} \\ 107 \text{ GeV} < m_t < 145 \text{ GeV}, \qquad & 1600 \text{ MeV} < m_b < 2800 \text{ MeV}. \end{aligned} \tag{6.48}$$

Instead, the CKM matrix elements used are the results in [6]. The complex phase of the CKM is calculated using the Jarlskog invariant. The error bars used for the first constraining analysis are $3 \times 1\sigma$ error bars in [6] for each element of the CKM sector.

Second, using each set of points which fulfil all of the mass, mixing angles and CP phase constraints, we calculate $\widetilde{Y}_d^{(2)}$. In Fig. 6.3 the values of the real and imaginary parts for $\Delta_{L,R}^{sd}$, $\Delta_{L,R}^{bd}$ and $\Delta_{L,R}^{bs}$ are shown. As one can see, there is no strong hierarchy between any of the entries, which means that a priori all the contribution of new physics are of the same order for each observable.

Finally, the results are used to calculate the $\Delta F = 2$ observables previously discussed. The range for each one of the observables which the points have to fulfil to be considered compatible with experimental constraints are

$$\begin{aligned} 16\,\text{ps}^{-1} \leq \Delta M_s \leq 20\,\text{ps}^{-1} \\ 0.46\,\text{ps}^{-1} \leq \Delta M_d \leq 0.56\,\text{ps}^{-1} \\ 0.004\,\text{ps}^{-1} \leq \Delta M_K \leq 0.0066\,\text{ps}^{-1} \\ 0.0019 \leq |\varepsilon_K| \leq 0.0025 \\ -0.14 \leq S_{\psi\phi} \leq 0.14 \\ 0.64 \leq S_{\psi K_S} \leq 0.72 \end{aligned} \tag{6.49}$$

As one can see, we use very large errors to take into account the theory and CKM uncertainties. Since the strongest constraints come from the K sector, smaller errors in the B sector do not change the outcome.

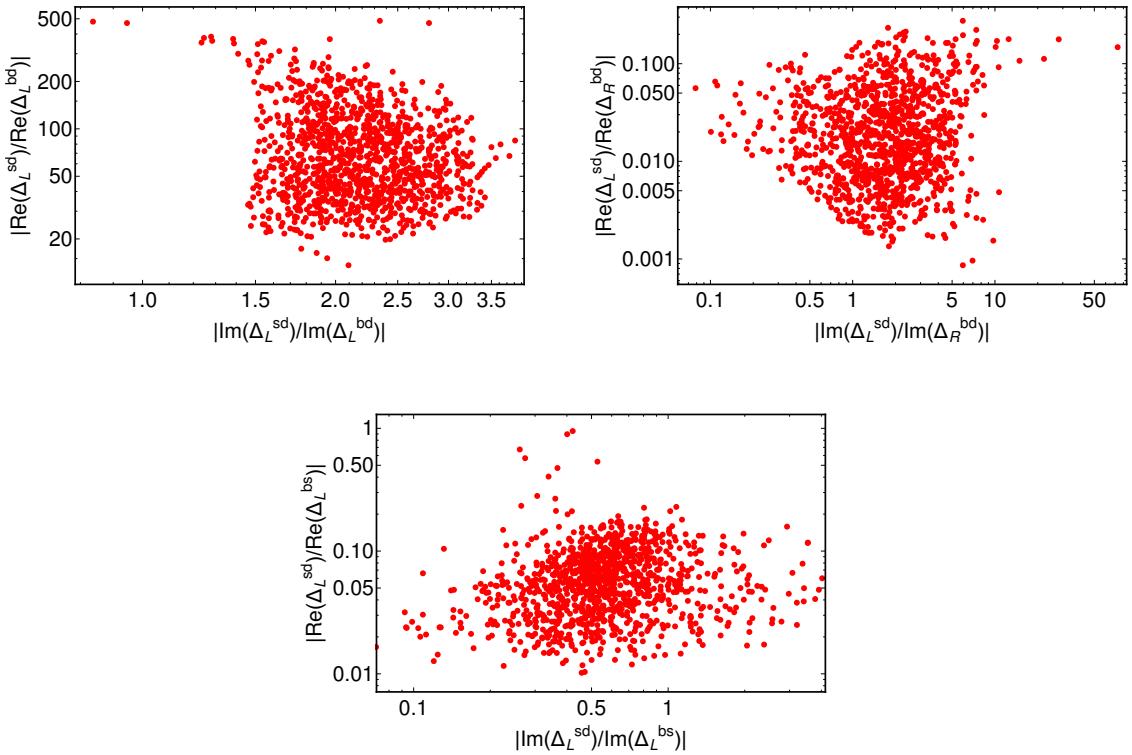

Figure 6.3: Comparison of the real and imaginary parts of $\Delta^{sd}_{L,R}$, $\Delta^{bd}_{L,R}$ and $\Delta^{bs}_{L,R}$.

The correlation between different $\Delta F = 2$ observables is shown in Fig. 6.4. The total number of initial points is 1173. The red points indicate the SM predictions. This means that the value for each observable is calculated using exclusively the CKM matrix prediction and neglecting any new physics contributions. The blue points correspond to the results containing new physics, hence both the CKM matrix and $\widetilde{Y}_d^{(2)}$ contributions. The yellow points indicate the SM points (red points) which fulfil all the $\Delta F = 2$ constraints indicated in eq. (6.49). There is a small amount of the SM points which fulfil the $\Delta F = 2$ constraints: from the 1173 initial points, only 180 pass the ε_K constraint and 189 the $S_{\psi K_S}$ constraint. The green points indicate the new physics points (blue points) which fulfil all the $\Delta F = 2$ constraints. From the blue points, 190 pass the $S_{\psi K_S}$ constraint and only 12 pass the ε_K constraint. Only 3 points pass all of the $\Delta F = 2$ constraints. We do not identify any typical correlation between observables, as the new physics effects are very small for all observables except for ε_K and ΔM_K, as predicted from the beginning.

Finally in Fig. 6.5 we show the correlations between ε_K, $S_{\psi K_S}$ and $|V_{ub,cb}|$. As one can see, the model can generate both inclusive and exclusive values for $|V_{ub,cb}|$. Nevertheless, due to the constraints coming from ε_K, the points which fulfil all the constraints belong to values $|V_{cb}| \approx 0.04$.

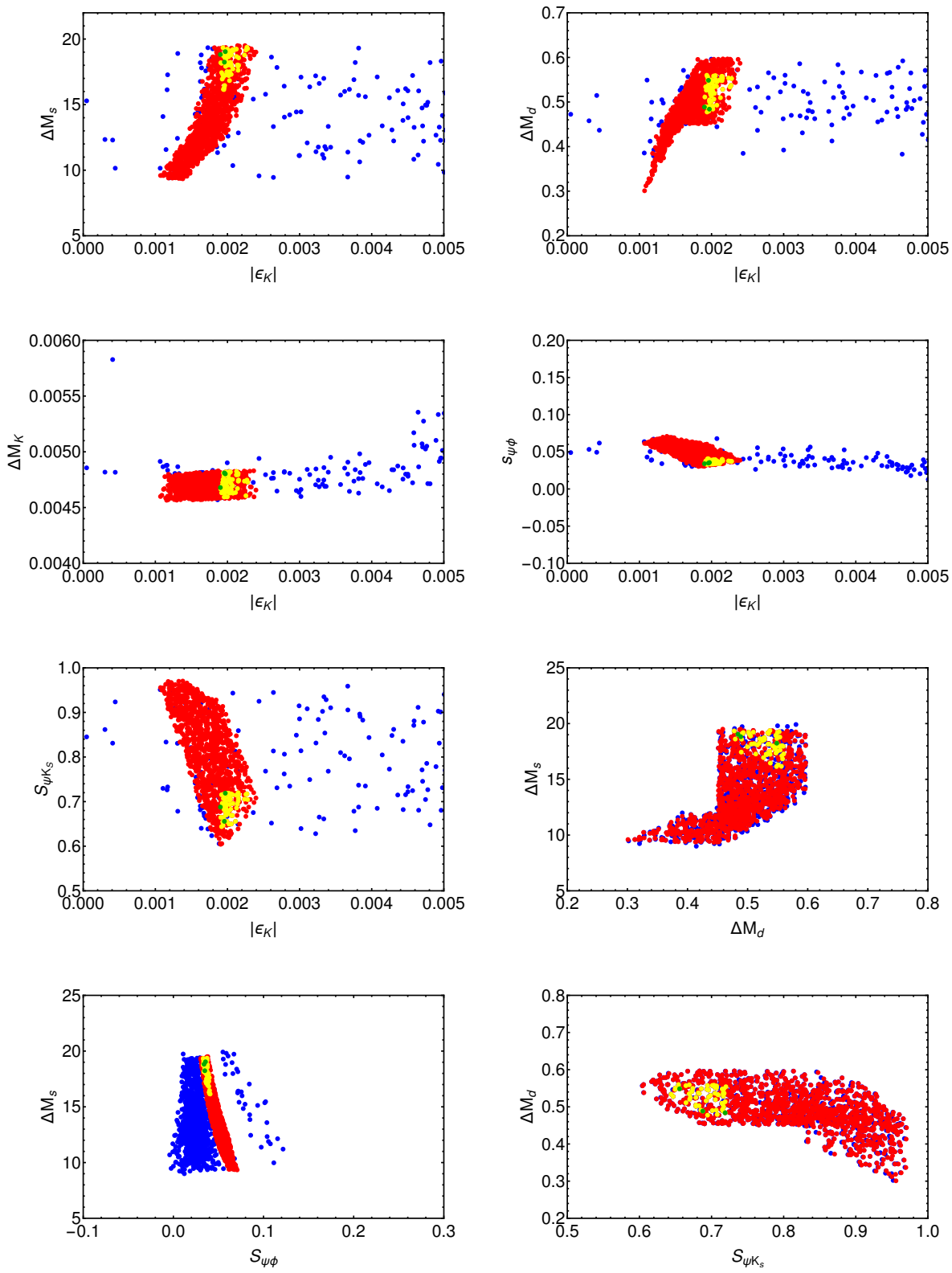

Figure 6.4: Correlation between various $\Delta F = 2$ flavour observables for $M_H = 100$ TeV. Red: SM points; blue: SM and new physics points; yellow: SM points that pass all constraints; green: SM and new physics points that pass all constraints.

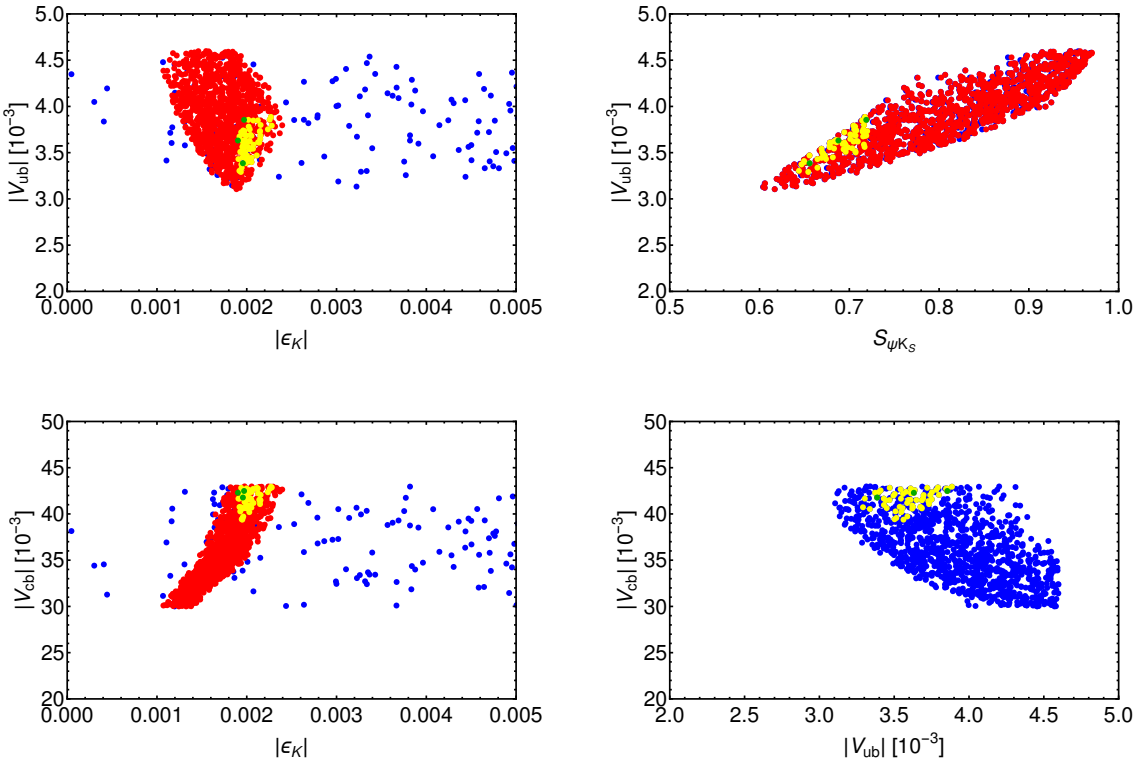

Figure 6.5: Correlations between ε_K, $S_{\psi K_S}$ and $|V_{ub,cb}|$. Colour code as in Fig. 6.4.

To summarise the results in this section, we have found that the new physics contributions to the different flavour observables for masses $M_H \lesssim 100$ TeV are too large to make the model compatible with experimental constraints. We have made a numerical analysis for several $\Delta F = 2$ observables, taking $M_H = 100$ TeV. For this mass value we have been able to find a small amount of points which survive all the constraints. At this scale the effects on the $B_{s,d}$ sector are very SM-like. The observable which gets the largest effects from new physics is ε_K. If in the future the experimental results of ε_K continue to disagree with the SM prediction, this model might be able to cure the tension. Nevertheless if there is some disagreement in the B sector, the model cannot help improve the theoretical agreement with the data.

6.3 $\Delta F = 1$ Observables Analysis

In the last section we have studied in detail the impact of a 2HDM with rank-1 Yukawa couplings on $\Delta F = 2$ observables at $M_H = 100$ TeV. In this section a first analysis to study the impact of this model on $\Delta F = 1$ observables is made. It is assumed that the main contribution to generate a radiative muon mass comes from the top quark (see left panel in Fig. 3.2). The points which fulfil all the quark masses and mixing constraints from the previous section, are reused for the analysis in this part. The parameters of the model are constrained to fulfil

$$y_e^{(1)} < 0.01, \qquad y_e^{(2)} < 0.1 \tag{6.50}$$

As for the quark sector, there is also a residual symmetry due to the massless electron which makes the first column of $\widetilde{Y}_e^{(2)}$ be zero. To simplify the scenario, CP violation is neglected in the lepton sector. Following the steps of the previous section, we take the points that fulfil following the muon and tau mass constraints

$$17.5 \text{ MeV} < m_\mu < 315 \text{ MeV}, \qquad 296 \text{ MeV} < m_\tau < 5330 \text{ MeV}. \tag{6.51}$$

One can see that these constraints are very flexible, as the analysis in this part is just a first approach to understand if the impact of the model on $\Delta F = 1$ observables can be stronger than for $\Delta F = 2$ observables. We do not impose any constraints on the mixing sector. This is because neutrinos play no role in this analysis and the strength of their contribution cannot be fixed. In principle $B_{s,d} \to \mu^+\mu^-$ is one of the observables which can be most sensitive to these kind of scenarios.

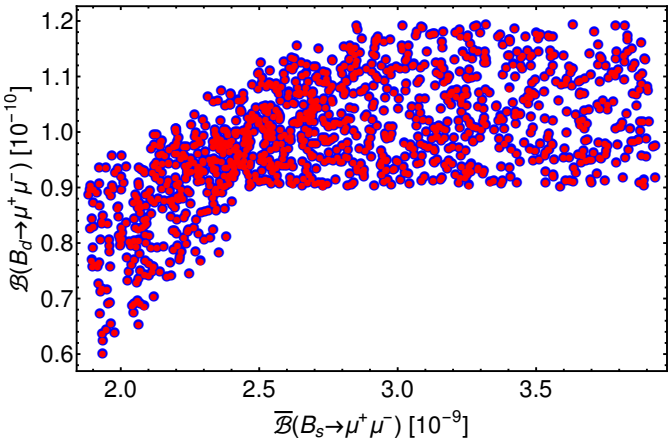

Figure 6.6: Numerical results for $\overline{\mathcal{B}}(B_s \to \mu^+\mu^-)$ and $\mathcal{B}(B_d \to \mu^+\mu^-)$. Colour code as in Fig. 6.4.

The results from this analysis are shown in Fig. 6.6. The values obtained for these branching ratios are not fixed but vary between the values

$$\overline{\mathcal{B}}(B_s \to \mu^+\mu^-) \in [1.9,\, 4.0] \cdot 10^{-9}\,, \tag{6.52}$$

$$\mathcal{B}(B_d \to \mu^+\mu^-) \in [0.6,\, 1.2] \cdot 10^{-10}\,. \tag{6.53}$$

Here, $\overline{\mathcal{B}}$ corresponds to the time-integrated branching ratio, which takes into account the non-vanishing $\Delta\Gamma_s = \Gamma_L^s - \Gamma_H^s$.

The new physics contribution are negligible for $B_{s,d} \to \mu^+\mu^-$ in this scenario, as we find that the effects are below 0.1% on both observables. The current experimental values for these two observables are [119]

$$\overline{\mathcal{B}}(B_s \to \mu^+\mu^-)_{\text{exp}} = \left(2.8^{+0.7}_{-0.6}\right) \cdot 10^{-9}\,, \tag{6.54}$$

$$\mathcal{B}(B_d \to \mu^+\mu^-)_{\text{exp}} = \left(3.9^{+1.6}_{-1.4}\right) \cdot 10^{-10}. \tag{6.55}$$

One can see that SM points for both observables are below the current experimental values and the contribution of new physics is too small to cure this effect.

From this analysis we can conclude the most sensitive observable to new physics contributions in this model is still ε_K.

Part III

Conclusions

Conclusions

One of the most striking features of the fermion sector in the SM are the strong hierarchies between the different masses together with the hierarchical mixing pattern for quarks. Such a structure for the SM fermion parameters suggests the existence of new physics. Furthermore, the evidence of massive neutrinos and mixing in the lepton sector is one of the main indications for the need of physics beyond the SM.

In this thesis we have worked in the framework of a general 2HDM to explain these issues. First we have presented the impact on the quark masses and mixing angles. The main assumption made is tree level Yukawa couplings are of rank-1. In this scenario we have shown that quantum effects can generate the correct mass hierarchy between the second and third generation of quarks. By imposing the third generation of left-handed quarks to be aligned at tree-level, we are able to reproduce the hierarchical structure of the CKM matrix once the radiative corrections are introduced. The most interesting point is that, even if the Cabibbo angle is generated due to quantum effects, its value is not loop suppressed, in contrast with masses generated radiatively. To avoid the stringent constraints coming from flavour physics, we have taken the decoupling limit. This limit assumes that the masses of the new Higgs bosons, collectively denoted by M_H, are much larger than the electroweak scale. This limit has small effects on the parameters which are radiatively generated and depend on M_H, as their dependence on the new physics scale is logarithmic.

We have also calculated the lepton parameters in the context of the see-saw model extended with one extra Higgs doublet. As for the quark sector, we have assumed that all tree level Yukawa couplings are of rank-1 at the Λ cut-off scale. We have also taken the decoupling limit to avoid flavour constraints. To simplify the scenario we have introduced just one right-handed neutrino for the see-saw mechanism, even if the discussion is valid for any number of right-handed neutrinos. The Majorana mass of the right-handed neutrino is taken to be much larger than M_H. The masses of the third generation of leptons arise at tree level. Furthermore, the anarchical structure of the PMNS matrix is already fixed by the tree level misalignment between the left-handed eigenvectors of the third generation of leptons. Nevertheless, at this scale, only the 33 entry of the PMNS matrix can be determined. When taking into account the quantum corrections at the Majorana scale, the second generation of charged lepton acquires a mass. It is not until the M_H scale that the degeneracy between the masses of the first and second generation of neutrinos is broken. The hierarchy between the second and third generation of lepton masses can be correctly reproduced in this model. Indeed, the model tends to generate a milder hierarchy

for the neutrino sector than for all other fermions, in agreement with experiments. At this scale, the PMNS matrix is univocally determined. In contrast to the quark sector, keeping the misalignment between the third generation of leptons makes the PMNS elements take completely anarchical values.

In the framework of a general rank-1 2HDM, the first generation of fermions remains massless. To fix this issue, a basis independent analysis in the context of a 3HDM has been presented. In this scenario, the third generation of fermions acquire their masses at tree level whereas the first and second generation of masses appear from radiative corrections. The hierarchy between the masses of the first and second generation can be naturally reproduced by the proper choice of misalignment between the different Yukawa matrices.

The main drawback of these kind of models is that due to the large number of physical parameters, they are not predictive scenarios. Nevertheless, they are attractive frameworks in which one can naturally explain the structure of the parameters in the SM fermion sector. Furthermore they open new interesting doors to the phenomenology in the flavour sector. Even if the decoupling limit ensures that the heavy Higgs mass scale can be large enough to suppress the contribution to new physics, new phenomena might be observed in future experiments. A numerical study to understand the impact of a 2HDM with rank-1 Yukawa couplings on different B and K physics observables and set a lower scale for M_H has been made. The results show that the observable which is most sensitive to the model is ε_K. The impact on the B sector is mainly SM-like in this scenario. The analysis shows that for $M_H \lesssim \mathcal{O}(100)$ TeV the deviations from the SM are too large to make the model compatible with current experimental constraints.

APPENDIX A

Renormalization Group Equations

A.1 Beta functions in NHDM Extended with Right-Handed Neutrinos

We present in this part the RGEs of the different Yukawa couplings $Y^{(a)}_{u,d,e,\nu}$ in the context of a general N-Higgs Doublet Model (NHDM) extended with right-handed neutrinos. The RGE of a Yukawa coupling is calculated through the β function as

$$\mu \frac{dY^{(a)}_{u,d,e,\nu}(\mu)}{d\mu} = \frac{1}{16\pi^2}\beta^{(a)}_{u,d,e,\nu}(\mu) \tag{A.1}$$

where $a = 1, ..., N$.

A.1.1 Below $M_{\rm M}$

The beta-functions for the SM extended by multi-Higgs doublets calculated in [120–122]. For energy scales below the right-handed neutrino Majorana mass they are given by

$$\begin{aligned}
\beta^{(a)}_u &= \left(-8g_s^2 - \frac{9}{4}\,g^2 - \frac{17}{12}\,g'^2\right) Y^{(a)}_u + \sum_b \mathrm{Tr}\left(3Y^{(a)}_d Y^{(b)\dagger}_d + 3Y^{(a)\dagger}_u Y^{(b)}_u + Y^{(a)}_e Y^{(b)\dagger}_e\right)^* Y^{(b)}_u \\
&\quad + \sum_b \left(-2\,Y^{(b)}_d Y^{(a)\dagger}_d Y^{(b)}_u + \frac{1}{2} Y^{(b)}_d Y^{(b)\dagger}_d Y^{(a)}_u + Y^{(a)}_u Y^{(b)\dagger}_u Y^{(b)}_u + \frac{1}{2} Y^{(b)}_u Y^{(b)\dagger}_u Y^{(a)}_u\right), \qquad \text{(A.2)} \\
\beta^{(a)}_d &= \left(-8g_s^2 - \frac{9}{4}\,g^2 - \frac{5}{12}\,g'^2\right) Y^{(a)}_d + \sum_b \mathrm{Tr}\left(3Y^{(a)}_d Y^{(b)\dagger}_d + 3Y^{(a)\dagger}_u Y^{(b)}_u + Y^{(a)}_e Y^{(b)\dagger}_e\right) Y^{(b)}_d \\
&\quad + \sum_b \left(-2\,Y^{(b)}_u Y^{(a)\dagger}_u Y^{(b)}_d + \frac{1}{2} Y^{(b)}_u Y^{(b)\dagger}_u Y^{(a)}_d + Y^{(a)}_d Y^{(b)\dagger}_d Y^{(b)}_d + \frac{1}{2} Y^{(b)}_d Y^{(b)\dagger}_d Y^{(a)}_d\right) \qquad \text{(A.3)} \\
\beta^{(a)}_e &= \left(-\frac{9}{4}g^2 - \frac{15}{4}g'^2\right) Y^{(a)}_e + \sum_b \left[3\mathrm{Tr}\left(Y^{(a)\dagger}_u Y^{(b)}_u + Y^{(a)}_d Y^{(b)\dagger}_d\right) + \mathrm{Tr}\left(Y^{(a)}_e Y^{(b)\dagger}_e\right)\right] Y^{(b)}_e \\
&\quad + \sum_b Y^{(a)}_e Y^{(b)\dagger}_e Y^{(b)}_e + \sum_b \frac{1}{2} Y^{(b)}_e Y^{(b)\dagger}_e Y^{(a)}_e \qquad \text{(A.4)}
\end{aligned}$$

where g_s, g and g' stand for the $SU(3)_C$, $SU(2)_L$ and $U(1)_Y$ gauge coupling constants, respectively.

Below $M_{\rm M}$, neutrino masses are described by the dimension five operators $\kappa^{(ab)}$. Here $a, b = 1, ..., N$. The renormalization group equations for the couplings $\kappa^{(ab)}$ are

$$\mu \frac{d\kappa^{(ab)}}{d\mu} = \frac{1}{16\pi^2} \beta_\kappa^{(ab)}(\mu) \tag{A.5}$$

where the corresponding beta functions were also calculated in [120] and read

$$\begin{aligned}
\beta_\kappa^{(ab)} = & \sum_c \frac{1}{2} \left[Y_e^{(c)} Y_e^{(c)\dagger} \kappa^{(ab)} + \kappa^{(ab)} \left(Y_e^{(c)} Y_e^{(c)\dagger} \right)^T \right] \\
& + \sum_c 2 \left[Y_e^{(c)} Y_e^{(b)\dagger} \kappa^{(ac)} + \kappa^{(cb)} \left(Y_e^{(c)} Y_e^{(a)\dagger} \right)^T \right] \\
& - \sum_c 2 \left[Y_e^{(c)} Y_e^{(a)\dagger} (\kappa^{(cb)} + \kappa^{(bc)}) + (\kappa^{(ac)} + \kappa^{(ca)}) \left(Y_e^{(c)} Y_e^{(b)\dagger} \right)^T \right] \\
& + \sum_c \left[3\mathrm{Tr}(Y_u^{(a)} Y_u^{(c)\dagger} + Y_d^{(a)\dagger} Y_d^{(c)}) + \mathrm{Tr}(Y_e^{(a)\dagger} Y_e^{(c)}) \right] \kappa^{(cb)} \\
& + \sum_c \kappa^{(ac)} \left[3\mathrm{Tr}(Y_u^{(b)} Y_u^{(c)\dagger} + Y_d^{(b)\dagger} Y_d^{(c)}) + \mathrm{Tr}(Y_e^{(b)\dagger} Y_e^{(c)}) \right] \\
& - 3g^2 \kappa^{(ab)} + \sum_{c,d} 2\lambda_{acbd} \kappa^{(cd)} \, .
\end{aligned} \tag{A.6}$$

Here the quartic couplings λ_{acbd} are defined in eq. (5.1).

A.1.2 Above $M_{\rm M}$

If a multi-Higgs doublet model is extended with right-handed neutrinos in the context of the see-saw mechanism, above the Majorana mass $M_{\rm M}$, the β functions read

$$\beta_{u,d}^{(a)M_{\rm M}} = \beta_{u,d}^{(a)} + \sum_b \mathrm{Tr}(Y_\nu^{(a)\dagger} Y_\nu^{(b)}) Y_{u,d}^{(b)}, \tag{A.7}$$

$$\beta_e^{(a)M_{\rm M}} = \beta_e^{(a)} + \sum_b \left[\mathrm{Tr}(Y_\nu^{(a)\dagger} Y_\nu^{(c)}) Y_e^{(b)} - 2 Y_\nu^{(b)} Y_\nu^{(a)\dagger} Y_e^{(b)} + \frac{1}{2} Y_\nu^{(b)} Y_\nu^{(c)\dagger} Y_e^{(a)} \right], \tag{A.8}$$

$$\begin{aligned}
\beta_\nu^{(a)M_{\rm M}} = & \left[-\frac{9}{4} g^2 - \frac{3}{4} g'^2 \right] Y_\nu^{(a)} + \sum_b \left[3\mathrm{Tr}(Y_u^{(a)} Y_u^{(b)\dagger} + Y_d^{(a)\dagger} Y_d^{(b)}) + \mathrm{Tr}(Y_\nu^{(a)} Y_\nu^{(b)\dagger} + Y_e^{(a)\dagger} Y_e^{(b)}) \right] Y_\nu^{(b)} \\
& + \sum_b \left[-2 Y_e^{(b)} Y_e^{(a)\dagger} Y_\nu^{(b)} + Y_\nu^{(a)} Y_\nu^{(b)\dagger} Y_\nu^{(b)} + \frac{1}{2} Y_e^{(b)} Y_e^{(b)\dagger} Y_\nu^{(a)} + \frac{1}{2} Y_\nu^{(b)} Y_\nu^{(b)\dagger} Y_\nu^{(a)} \right].
\end{aligned} \tag{A.9}$$

A.2 P and Q Functions in the Lepton Sector

The functions P and Q, defined in eqs. (4.24), determine the ratio between the muon and the tau mass, eq. (4.22). They are a linear combination of the functions p_x and q_x, with $x = e, \nu, u, d$,

which are explicitly given by

$$\begin{aligned} p_e &= \frac{1}{4}\sin 2\theta_{eL}\sin 2\theta_{eR}\sin\omega_{eL}\ , \\ q_e &= \frac{1}{4}\sin 2\theta_{eL}\sin 2\theta_{eR}\cos\omega_{eL}\ , \end{aligned} \tag{A.10}$$

$$\begin{aligned} p_\nu = &-2\cos\theta_{eL}\sin\theta_{e_R}\cos\alpha\sin\theta_\nu\sin\omega_\nu \\ &+\sin\theta_{eL}\sin\theta_{e_R}\left(\cos\alpha\sin\omega_{eL}\cos\theta_\nu+\sin\alpha\sin\theta_\nu\left(\sin\omega_{eL}\cos\omega_\nu-2\cos\omega_{eL}\sin\omega_\nu\right)\right)\ , \\ q_\nu = &-2\cos\theta_{eL}\sin\theta_{e_R}\cos\alpha\sin\theta_\nu\cos\omega_\nu \\ &+\sin\theta_{eL}\sin\theta_{e_R}\cos\omega_{eL}\left(\cos\alpha\cos\theta_\nu-\sin\alpha\sin\theta_\nu\cos\omega_\nu\right)\ , \end{aligned} \tag{A.11}$$

$$\begin{aligned} p_u &= 3\cos\theta_{uL}\cos\theta_{uR}\sin\theta_{e_L}\sin\theta_{e_R}\sin\omega_{eL}\ , \\ q_u &= 3\cos\theta_{uL}\cos\theta_{uR}\sin\theta_{e_L}\sin\theta_{e_R}\cos\omega_{eL}\ , \end{aligned} \tag{A.12}$$

$$\begin{aligned} p_d &= 3\cos\theta_{dL}\cos\theta_{dR}\sin\theta_{e_L}\sin\theta_{e_R}\sin\omega_{eL}\ , \\ q_d &= 3\cos\theta_{dL}\cos\theta_{dR}\sin\theta_{e_L}\sin\theta_{e_R}\cos\omega_{eL}\ . \end{aligned} \tag{A.13}$$

A.3 Left-handed Perturbation Vectors in a 3HDM

The vectors $\left|\delta\tilde{y}^{(a)}_{x_L}\right\rangle$ used to calculate the masses of the second and first generation of fermions in eqs. (5.19) and (5.20), are presented below for each different fermion type. The expressions for this section are calculated for a 3HDM. Hence are valid for $i = 2, 3$. The vectors are calculated using the β functions in Appendix A.1, and the rank-1 Yukawa matrices defined in eqs. (5.2) and (5.3).

Quark Sector

The vectors for the quark sector are calculated at the M_H scale. They are given by

$$\left|\delta\tilde{y}^{(i)}_{u_L}\right\rangle\Big|_{M_H} = \frac{1}{16\pi^2}\log\frac{\Lambda}{M_H}\left[A^{(i)}_u\left|y^{(i)}_{u_L}\right\rangle + B^{(i)}_u\left|y^{(i)}_{d_L}\right\rangle\right]. \tag{A.14}$$

$$\left|\delta\tilde{y}^{(i)}_{d_L}\right\rangle\Big|_{M_H} = \frac{1}{16\pi^2}\log\frac{\Lambda}{M_H}\left[A^{(i)}_d\left|y^{(i)}_{d_L}\right\rangle + B^{(i)}_d\left|y^{(i)}_{u_L}\right\rangle\right], \tag{A.15}$$

where

$$\begin{aligned} A^{(i)}_u &= 3\left\langle y^{(1)}_{u_L}\middle|y^{(i)}_{u_L}\right\rangle\left\langle y^{(1)}_{u_R}\middle|y^{(i)}_{u_R}\right\rangle + 3\left\langle y^{(1)}_{d_L}\middle|y^{(i)}_{d_L}\right\rangle\left\langle y^{(1)}_{d_R}\middle|y^{(i)}_{d_R}\right\rangle, \\ B^{(i)}_u &= -2\left\langle y^{(1)}_{d_L}\middle|y^{(i)}_{u_L}\right\rangle\left\langle y^{(1)}_{d_R}\middle|y^{(i)}_{d_R}\right\rangle, \\ A^{(i)}_d &= 3\left\langle y^{(1)}_{d_L}\middle|y^{(i)}_{d_L}\right\rangle\left\langle y^{(1)}_{d_R}\middle|y^{(i)}_{d_R}\right\rangle + 3\left\langle y^{(1)}_{u_L}\middle|y^{(i)}_{u_L}\right\rangle\left\langle y^{(1)}_{u_R}\middle|y^{(i)}_{u_R}\right\rangle, \end{aligned}$$

$$B_d^{(i)} = -2\left\langle y_{u_L}^{(1)} \middle| y_{d_L}^{(i)} \right\rangle \left\langle y_{u_R}^{(1)} \middle| y_{u_R}^{(i)} \right\rangle$$

Lepton Sector

As explicitly seen in Appendix A.1, the RGEs for the lepton sector in the context of an NHDM extended with right handed neutrinos depend on whether the energy scale is above or below the Majorana mass M_{M}. Here we present the $\left|\delta\tilde{y}_{x_L}^{(a)}\right\rangle$ vectors for the lepton sector above and below the scale of decoupling of the right-handed neutrinos

Above M_{M}

Above the M_{M} scale, only $\left|\delta\tilde{y}_{e_L}^{(i)}\right\rangle$ can be determined. The latter reads

$$\left|\delta\tilde{y}_{e_L}^{(i)}\right\rangle\Big|_{M_{\mathrm{M}}} = \frac{1}{16\pi^2}\log\frac{\Lambda}{M_{\mathrm{M}}}\left[A_e^{(i)}\left|y_{e_L}^{(i)}\right\rangle + B_e^{(i)}\left|y_{\nu_L}^{(i)}\right\rangle\right], \tag{A.16}$$

where

$$\begin{aligned} A_e^{(i)} &= 3\left\langle y_{u_L}^{(1)} \middle| y_{u_L}^{(i)} \right\rangle \left\langle y_{u_R}^{(1)} \middle| y_{u_R}^{(i)} \right\rangle + 3\left\langle y_{d_L}^{(1)} \middle| y_{d_L}^{(i)} \right\rangle \left\langle y_{d_R}^{(1)} \middle| y_{d_R}^{(i)} \right\rangle \\ &\quad + \left\langle y_{e_L}^{(1)} \middle| y_{e_L}^{(i)} \right\rangle \left\langle y_{e_R}^{(1)} \middle| y_{e_R}^{(i)} \right\rangle + \left\langle y_{\nu_L}^{(1)} \middle| y_{\nu_L}^{(i)} \right\rangle \\ B_e^{(i)} &= -2\left\langle y_{\nu_L}^{(1)} \middle| y_{e_L}^{(i)} \right\rangle. \end{aligned} \tag{A.17}$$

Below M_{M}

When calculating the RGEs below the M_{M} scale, $\left|\delta\tilde{y}_{e_L}^{(i)}\right\rangle$ receives loop suppressed corrections and $\left|\delta\tilde{y}_{\nu}^{(3)}\right\rangle$ arises. At the M_H scale these vectors read

$$\left|\delta\tilde{y}_{e_L}^{(i)}\right\rangle\Big|_{M_H} = \left|\delta\tilde{y}_{e_L}^{(i)}\right\rangle\Big|_{M_{\mathrm{M}}} + \frac{1}{16\pi^2}\log\frac{M_{\mathrm{M}}}{M_\phi}\left[A_e^{(i)}\left|y_{e_L}^{(i)}\right\rangle\right], \tag{A.18}$$

$$\left|\delta\tilde{y}_{\nu}^{(2)}\right\rangle\Big|_{M_H} = \frac{1}{M_{\mathrm{M}}}\frac{1}{16\pi^2}\log\frac{M_{\mathrm{M}}}{M_H}\left(2\lambda_{1212}\left|y_{\nu}^{(2)}\right\rangle + 2\lambda_{1213}\left|y_{\nu}^{(3)}\right\rangle\right),$$

$$\left|\delta\tilde{y}_{\nu}^{(3)}\right\rangle\Big|_{M_H} = \frac{1}{M_{\mathrm{M}}}\frac{1}{16\pi^2}\log\frac{M_{\mathrm{M}}}{M_H}\left(2\lambda_{1313}\left|y_{\nu}^{(3)}\right\rangle + 2\lambda_{1213}\left|y_{\nu}^{(2)}\right\rangle\right), \tag{A.19}$$

where

$$\begin{aligned} A_e^{(i)} &= 3\left\langle y_{u_L}^{(1)} \middle| y_{u_L}^{(i)} \right\rangle \left\langle y_{u_R}^{(1)} \middle| y_{u_R}^{(i)} \right\rangle + 3\left\langle y_{d_L}^{(1)} \middle| y_{d_L}^{(i)} \right\rangle \left\langle y_{d_R}^{(1)} \middle| y_{d_R}^{(i)} \right\rangle \\ &\quad + \left\langle y_{e_L}^{(1)} \middle| y_{e_L}^{(i)} \right\rangle \left\langle y_{e_R}^{(1)} \middle| y_{e_R}^{(i)} \right\rangle. \end{aligned} \tag{A.20}$$

Acknowledgments

Quiero agradecer a mi supervisor Alejandro Ibarra, la oportunidad de haber podido hacer mi tesis en su grupo. No solo por todo lo que he podido aprender trabajando junto a él, si no también por sus consejos y apoyo durante estos tres años. Y por todas *las últimas*.

Gracias a Concha, por que has sido un fuerte apoyo durante mi tesis. I am grateful to Jennifer Girrbach-Noe for the opportunity to collaborate with her and to Andzej Buras for the fruitful discussions and his advice. I am indebted to Andreas Trautner, Camilo García Cely, Marco Drewes, Sebastian Wild, Pedro Ruiz Femenía, Martin Vollmann, Jennifer Girrbach-Noe and Avelino Vicente for proofreading parts of my manuscript. Also to Anna Lamperstorfer for translating my abstract.

I feel very happy for having had such collegues in the physics department, in particular the T30 members. I would like to thank all of you, Basti, Paco, Emiliano, Stefan, Andre, Bhupal, Xiaoyuan, Andrea, Andi, Christian, Maxi, Jesús, Sebastian, Miguel and Max for creating such a nice working environment. I want to specially thank the best office mates I could have asked for, Anna Lamperstorfer and Camilo García Cely. Ich möchte mich bei Karin Ramm bedanken, für ihr Lächeln jeden Morgen.

Ich bin auch all den Leuten von Max Planck Institut für Physik dankbar, denn sie haben meine Zeit als Doktorandin viel einfacher gemacht. Insbesondere, Frank Steffen, für die ganz interessanten IMPRS Aktivitäten, die du organisiert hast. Prof. Hollik danke für alle die Anträge, die du untergeschrieben hast. Alle Sekretärinen, Rosita Jurgeleit, Monika Goldammer und Karin Gebhardt, ihr habt alle die Bürokratie so einfach gemacht!

I of course want to thank all the people that have shared these three years with me. First, to my dirty flatmates, Sebastian Paßehr and Alessandro Manfredini together with my neighbours, Sebastian Nowak, Marlene, Shangyu, Stephan, because you made me feel like home. También a Mariel, Jezabel y Clara. Os aseguro que estos años no habrian sido lo mismo sin vosotras. A Nico, que te voy a decir, es como haber tenido a un hermano en Alemania. Gràcies al Mario, perque després de tot encara ser a prop. A Ignacio, por hacerme reír siempre con tus comentarios. Alexander für deine Hilfe und deine Fröhlichkeit. Laura Fabbietti, grazie per il tuo aiuto e la tua amicizia di questi ultimi anni. Andi, ich freue mich, dass wir uns kennengelernt haben. Por supuesto, Mark Müller, Ricard, Juan y Esther, Marina, Susana, Monica y Richi, y toda la gente que han compartido mi experiencia en Munich, gracias.

Finalment, vull agrair a la meva gent de Barcelona haver sigut a prop meu malgrat ser lluny. A la Laura i la Anna (Bot), no podria tenir millors amigues. La Lidia, per ser sempre tant de debò.

A Eloy, gracias por todas las fotos, me han ayudado a echarte menos de menos. Javi, m'encanta seguir sentint les teves històries, tot i ser tant lluny. Al Didac, per totes les xuxes d'aquests anys (i les que queden). Al Giovanni, pels bons moments. I un munt d'amics que no menciono aquí. Als avis més moderns del món, per totes les hores de Skype, e-mails, i sobretot per tots els paquets de pernil que m'heu comprat perque mai me'n faltés. Als meus pares pel suport incondicional que sempre m'heu donat. I la meva germana petita, la Maria, per creure en mi més que ningú. Gràcies.

Bibliography

[1] A. Ibarra and A. Solaguren-Beascoa, *Radiative Generation of Quark Masses and Mixing Angles in the Two Higgs Doublet Model*, *Phys. Lett.* **B736** (2014) 16–19, [arXiv:1403.2382].

[2] A. Ibarra and A. Solaguren-Beascoa, *Lepton parameters in the see-saw model extended by one extra Higgs doublet*, *JHEP* **11** (2014) 089, [arXiv:1409.5011].

[3] A. Ibarra and A. Solaguren-Beascoa, *Standard Model Fermion Masses and Mixing Angles generated in 3HDM*, in *Proceedings of the XIV International Conference on Topics in Astroparticle and Underground Physics (TAUP2015), 7-11 September 2015, Torino, Italy*, 2015.

[4] J. Girrbach-Noe, A. Ibarra, and A. Solaguren-Beascoa, *Flavour Observables in a Radiative 2HDM*, *In preparation* (2016).

[5] A. Ibarra and A. Solaguren-Beascoa, *Generating Standard Model Fermion Parameters in a 3HDM*, *In preparation* (2016).

[6] **Particle Data Group** Collaboration, K. A. Olive et al., *Review of Particle Physics*, *Chin. Phys.* **C38** (2014) 090001.

[7] N. Arkani-Hamed, H.-C. Cheng, and L. J. Hall, *A Supersymmetric theory of flavor with radiative fermion masses*, *Phys. Rev.* **D54** (1996) 2242–2260, [hep-ph/9601262].

[8] F. Borzumati, G. R. Farrar, N. Polonsky, and S. D. Thomas, *Soft Yukawa couplings in supersymmetric theories*, *Nucl. Phys.* **B555** (1999) 53–115, [hep-ph/9902443].

[9] R. N. Mohapatra, *Gauge Model for Chiral Symmetry Breaking and Muon electron Mass Ratio*, *Phys. Rev.* **D9** (1974) 3461.

[10] B. S. Balakrishna, *Fermion Mass Hierarchy From Radiative Corrections*, *Phys. Rev. Lett.* **60** (1988) 1602.

[11] B. S. Balakrishna, A. L. Kagan, and R. N. Mohapatra, *Quark Mixings and Mass Hierarchy From Radiative Corrections*, *Phys. Lett.* **B205** (1988) 345.

[12] J. Charles et al., *Current status of the Standard Model CKM fit and constraints on $\Delta F = 2$ New Physics*, *Phys. Rev.* **D91** (2015), no. 7 073007, [arXiv:1501.05013].

[13] **CKMfitter Group** Collaboration, J. Charles, A. Hocker, H. Lacker, S. Laplace, F. R. Le Diberder, J. Malcles, J. Ocariz, M. Pivk, and L. Roos, *CP violation and the CKM matrix: Assessing the impact of the asymmetric B factories*, *Eur. Phys. J.* **C41** (2005) 1–131, [hep-ph/0406184].

[14] C. Jarlskog, *Commutator of the Quark Mass Matrices in the Standard Electroweak Model and a Measure of Maximal CP Violation*, *Phys. Rev. Lett.* **55** (1985) 1039.

[15] Z. Maki, M. Nakagawa, and S. Sakata, *Remarks on the unified model of elementary particles*, *Progress of Theoretical Physics* **28** (1962), no. 5 870–880, [http://ptp.oxfordjournals.org/content/28/5/870.full.pdf+html].

[16] C. Giunti, *Theory of neutrino oscillations*, in *15th Conference on High Energy Physics (IFAE 2003) Lecce, Italy, April 23-26, 2003*, 2003. hep-ph/0311241.

[17] M. C. Gonzalez-Garcia and M. Maltoni, *Phenomenology with Massive Neutrinos*, *Phys. Rept.* **460** (2008) 1–129, [arXiv:0704.1800].

[18] L. Wolfenstein, *Neutrino oscillations in matter*, *Phys. Rev. D* **17** (May, 1978) 2369–2374.

[19] S. P. Mikheev and A. Yu. Smirnov, *Resonance Amplification of Oscillations in Matter and Spectroscopy of Solar Neutrinos*, *Sov. J. Nucl. Phys.* **42** (1985) 913–917. [Yad. Fiz.42,1441(1985)].

[20] **GALLEX** Collaboration, W. Hampel et al., *GALLEX solar neutrino observations: Results for GALLEX IV*, *Phys. Lett.* **B447** (1999) 127–133.

[21] **Borexino** Collaboration, *Direct measurement of the ^{7}Be solar neutrino flux with 192 days of borexino data*, *Phys. Rev. Lett.* **101** (Aug, 2008) 091302.

[22] **SNO** Collaboration, B. Aharmim et al., *Combined Analysis of all Three Phases of Solar Neutrino Data from the Sudbury Neutrino Observatory*, *Phys. Rev.* **C88** (2013) 025501, [arXiv:1109.0763].

[23] **Super-Kamiokande** Collaboration, R. Wendell et al., *Atmospheric neutrino oscillation analysis with sub-leading effects in Super-Kamiokande I, II, and III*, *Phys. Rev.* **D81** (2010) 092004, [arXiv:1002.3471].

[24] J. N. Bahcall, A. M. Serenelli, and S. Basu, *New solar opacities, abundances, helioseismology, and neutrino fluxes*, *Astrophys. J.* **621** (2005) L85–L88, [astro-ph/0412440].

[25] **SNO** Collaboration, *Combined analysis of all three phases of solar neutrino data from the sudbury neutrino observatory*, *Phys. Rev. C* **88** (Aug, 2013) 025501.

[26] M. Maltoni, T. Schwetz, and J. W. F. Valle, *Combining the first kamland results with solar neutrino data*, *Phys. Rev. D* **67** (May, 2003) 093003.

[27] J. N. Bahcall, M. C. Gonzalez-Garcia, and C. Pena-Garay, *Solar neutrinos before and after KamLAND*, *JHEP* **02** (2003) 009, [hep-ph/0212147].

[28] **Soudan 2** Collaboration, M. C. Sanchez et al., *Measurement of the L/E distributions of atmospheric neutrinos in Soudan 2 and their interpretation as neutrino oscillations*, *Phys. Rev.* **D68** (2003) 113004, [hep-ex/0307069].

[29] **MACRO** Collaboration, M. Giorgini, *Atmospheric neutrino oscillations with the MACRO detector*, in *Beyond the desert: Accelerator, non-accelerator and space approaches into the next millennium. Proceedings, 3rd International Conference on particle physics beyond the standard model, Oulu, Finland, June 2-7, 2002*, pp. 353–363, 2002. hep-ex/0210008.

[30] **MINOS** Collaboration, P. Adamson et al., *Measurement of Neutrino and Antineutrino Oscillations Using Beam and Atmospheric Data in MINOS*, *Phys. Rev. Lett.* **110** (2013), no. 25 251801, [arXiv:1304.6335].

[31] **CHOOZ** Collaboration, M. Apollonio et al., *Search for neutrino oscillations on a long baseline at the CHOOZ nuclear power station*, *Eur. Phys. J.* **C27** (2003) 331–374, [hep-ex/0301017].

[32] **Double Chooz** Collaboration, F. Ardellier et al., *Double Chooz: A Search for the neutrino mixing angle theta(13)*, hep-ex/0606025.

[33] **RENO** Collaboration, J. K. Ahn et al., *Observation of Reactor Electron Antineutrino Disappearance in the RENO Experiment*, *Phys. Rev. Lett.* **108** (2012) 191802, [arXiv:1204.0626].

[34] **Daya Bay** Collaboration, *Observation of electron-antineutrino disappearance at daya bay*, *Phys. Rev. Lett.* **108** (Apr, 2012) 171803.

[35] **Daya Bay** Collaboration, *New measurement of antineutrino oscillation with the full detector configuration at daya bay*, *Phys. Rev. Lett.* **115** (Sep, 2015) 111802.

[36] M. C. Gonzalez-Garcia, M. Maltoni, and T. Schwetz, *Updated fit to three neutrino mixing: status of leptonic CP violation*, *JHEP* **11** (2014) 052, [arXiv:1409.5439].

[37] J. Bergstrom, M. C. Gonzalez-Garcia, M. Maltoni, and T. Schwetz, *Bayesian global analysis of neutrino oscillation data*, *JHEP* **09** (2015) 200, [arXiv:1507.04366].

[38] L. Wolfenstein, *Neutrino Oscillations in Matter*, *Phys. Rev.* **D17** (1978) 2369–2374.

[39] R. N. Cahn, D. A. Dwyer, S. J. Freedman, W. C. Haxton, R. W. Kadel, Yu. G. Kolomensky, K. B. Luk, P. McDonald, G. D. Orebi Gann, and A. W. P. Poon, *White Paper: Measuring the Neutrino Mass Hierarchy*, in *Community Summer Study 2013:*

Snowmass on the Mississippi (CSS2013) Minneapolis, MN, USA, July 29-August 6, 2013, 2013. arXiv:1307.5487.

[40] **Troitsk** Collaboration, V. N. Aseev et al., *An upper limit on electron antineutrino mass from Troitsk experiment*, *Phys. Rev.* **D84** (2011) 112003, [arXiv:1108.5034].

[41] **Planck** Collaboration, P. A. R. Ade et al., *Planck 2015 results. XIII. Cosmological parameters*, arXiv:1502.01589.

[42] **GERDA** Collaboration, G. Benato, *Search of Neutrinoless Double Beta Decay with the GERDA Experiment*, in *12th Conference on the Intersections of Particle and Nuclear Physics (CIPANP 2015) Vail, Colorado, USA, May 19-24, 2015*, 2015. arXiv:1509.07792.

[43] J. A. Casas, A. Ibarra, and F. Jimenez-Alburquerque, *Hints on the high-energy seesaw mechanism from the low-energy neutrino spectrum*, *JHEP* **04** (2007) 064, [hep-ph/0612289].

[44] G. C. Branco, P. M. Ferreira, L. Lavoura, M. N. Rebelo, M. Sher, and J. P. Silva, *Theory and phenomenology of two-Higgs-doublet models*, *Phys. Rept.* **516** (2012) 1–102, [arXiv:1106.0034].

[45] M. Krawczyk and D. Sokolowska, *The Charged Higgs boson mass in the 2HDM: Decoupling and CP violation*, *eConf* **C0705302** (2007) HIG09, [arXiv:0711.4900]. [,141(2007)].

[46] P. M. Ferreira and D. R. T. Jones, *Bounds on scalar masses in two Higgs doublet models*, *JHEP* **08** (2009) 069, [arXiv:0903.2856].

[47] I. P. Ivanov, *Minkowski space structure of the Higgs potential in 2HDM*, *Phys. Rev.* **D75** (2007) 035001, [hep-ph/0609018]. [Erratum: Phys. Rev.D76,039902(2007)].

[48] J. F. Gunion and H. E. Haber, *The CP conserving two Higgs doublet model: The Approach to the decoupling limit*, *Phys. Rev.* **D67** (2003) 075019, [hep-ph/0207010].

[49] H. Georgi and D. V. Nanopoulos, *Suppression of Flavor Changing Effects From Neutral Spinless Meson Exchange in Gauge Theories*, *Phys. Lett.* **B82** (1979) 95.

[50] S. Kanemura, T. Kasai, and Y. Okada, *Mass bounds of the lightest CP even Higgs boson in the two Higgs doublet model*, *Phys. Lett.* **B471** (1999) 182–190, [hep-ph/9903289].

[51] J. F. Gunion, H. E. Haber, G. L. Kane, and S. Dawson, *The Higgs Hunter's Guide*, *Front. Phys.* **80** (2000) 1–448.

[52] **BaBar** Collaboration, J. P. Lees et al., *Evidence for an excess of $\bar{B} \to D^{(*)}\tau^-\bar{\nu}_\tau$ decays*, *Phys. Rev. Lett.* **109** (2012) 101802, [arXiv:1205.5442].

[53] S. M. Barr and A. Zee, *Electric Dipole Moment of the Electron and of the Neutron*, *Phys. Rev. Lett.* **65** (1990) 21–24. [Erratum: Phys. Rev. Lett.65,2920(1990)].

[54] H. Georgi, *A Model of Soft CP Violation*, *Hadronic J.* **1** (1978) 155.

[55] L. J. Hall and M. B. Wise, *FLAVOR CHANGING HIGGS - BOSON COUPLINGS*, *Nucl. Phys.* **B187** (1981) 397.

[56] H. E. Haber, G. L. Kane, and T. Sterling, *The Fermion Mass Scale and Possible Effects of Higgs Bosons on Experimental Observables*, *Nucl. Phys.* **B161** (1979) 493.

[57] V. Barger, H. E. Logan, and G. Shaughnessy, *Identifying extended Higgs models at the LHC*, *Phys. Rev.* **D79** (2009) 115018, [arXiv:0902.0170].

[58] R. M. Barnett, G. Senjanovic, L. Wolfenstein, and D. Wyler, *Implications of a Light Higgs Scalar*, *Phys. Lett.* **B136** (1984) 191.

[59] Y. Grossman, *Phenomenology of models with more than two Higgs doublets*, *Nucl. Phys.* **B426** (1994) 355–384, [hep-ph/9401311].

[60] A. Pich and P. Tuzon, *Yukawa Alignment in the Two-Higgs-Doublet Model*, *Phys. Rev.* **D80** (2009) 091702, [arXiv:0908.1554].

[61] C. B. Braeuninger, A. Ibarra, and C. Simonetto, *Radiatively induced flavour violation in the general two-Higgs doublet model with Yukawa alignment*, *Phys. Lett.* **B692** (2010) 189–195, [arXiv:1005.5706].

[62] T. P. Cheng and M. Sher, *Mass-matrix ansatz and flavor nonconservation in models with multiple higgs doublets*, *Phys. Rev. D* **35** (Jun, 1987) 3484–3491.

[63] H. Fritzsch, *Weak Interaction Mixing in the Six - Quark Theory*, *Phys. Lett.* **B73** (1978) 317–322.

[64] H. Fritzsch and Z.-z. Xing, *Four zero texture of Hermitian quark mass matrices and current experimental tests*, *Phys. Lett.* **B555** (2003) 63–70, [hep-ph/0212195].

[65] **ATLAS** Collaboration, G. Aad et al., *Search for a CP-odd Higgs boson decaying to Zh in pp collisions at $\sqrt{s} = 8$ TeV with the ATLAS detector*, *Phys. Lett.* **B744** (2015) 163–183, [arXiv:1502.04478].

[66] **ATLAS** Collaboration, G. Aad et al., *Constraints on new phenomena via Higgs boson couplings and invisible decays with the ATLAS detector*, *JHEP* **11** (2015) 206, [arXiv:1509.00672].

[67] A. Djouadi, L. Maiani, G. Moreau, A. Polosa, J. Quevillon, and V. Riquer, *The post-Higgs MSSM scenario: Habemus MSSM?*, *Eur. Phys. J.* **C73** (2013) 2650, [arXiv:1307.5205].

[68] **ATLAS** Collaboration, G. Aad et al., *Search for flavour-changing neutral current top quark decays $t \to Hq$ in pp collisions at $\sqrt{s} = 8$ TeV with the ATLAS detector*, *JHEP* **12** (2015) 061, [arXiv:1509.06047].

[69] **ATLAS** Collaboration, G. Aad et al., *Search for charged Higgs bosons in the $H^{\pm} \to tb$ decay channel in pp collisions at $\sqrt{s} = 8$ TeV using the ATLAS detector*, arXiv:1512.03704.

[70] M. Carena, S. Heinemeyer, O. Stål, C. E. M. Wagner, and G. Weiglein, *MSSM Higgs Boson Searches at the LHC: Benchmark Scenarios after the Discovery of a Higgs-like Particle*, *Eur. Phys. J.* **C73** (2013), no. 9 2552, [arXiv:1302.7033].

[71] **ATLAS** Collaboration, *Search for Neutral Minimal Supersymmetric Standard Model Higgs Bosons $H/A \to \tau\tau$ produced in pp collisions at $\sqrt{s} = 13$ TeV with the ATLAS Detector*, .

[72] **ATLAS** Collaboration, *Search for resonances decaying to photon pairs in 3.2 fb^{-1} of pp collisions at $\sqrt{s}$ = 13 TeV with the ATLAS detector*, .

[73] **CMS** Collaboration, V. Khachatryan et al., *Searches for a heavy scalar boson* H *decaying to a pair of 125 GeV Higgs bosons* hh *or for a heavy pseudoscalar boson* A *decaying to* Zh*, in the final states with* $\mathrm{h} \to \tau\tau$, arXiv:1510.01181.

[74] **CMS** Collaboration, V. Khachatryan et al., *Search for a low-mass pseudoscalar Higgs boson produced in association with a b-bbar pair in pp collisions at sqrt(s) = 8 TeV*, arXiv:1511.03610.

[75] **CMS** Collaboration, V. Khachatryan et al., *Search for a light charged Higgs boson decaying to* $\mathrm{c\bar{s}}$ *in pp collisions at $\sqrt{s} = 8$ TeV*, arXiv:1510.04252.

[76] **CMS** Collaboration, C. Collaboration, *Search for new physics in high mass diphoton events in proton-proton collisions at 13TeV*, .

[77] M. Badziak, *Interpreting the 750 GeV diphoton excess in minimal extensions of Two-Higgs-Doublet models*, arXiv:1512.07497.

[78] N. Bizot, S. Davidson, M. Frigerio, and J. L. Kneur, *Two Higgs doublets to explain the excesses $pp \to \gamma\gamma(750$ GeV$)$ and $h \to \tau^{\pm}\mu^{\mp}$*, arXiv:1512.08508.

[79] W. Altmannshofer, J. Galloway, S. Gori, A. L. Kagan, A. Martin, and J. Zupan, *On the 750 GeV di-photon excess*, arXiv:1512.07616.

[80] A. Angelescu, A. Djouadi, and G. Moreau, *Scenarii for interpretations of the LHC diphoton excess: two Higgs doublets and vector-like quarks and leptons*, arXiv:1512.04921.

[81] R. S. Gupta, S. Jäger, Y. Kats, G. Perez, and E. Stamou, *Interpreting a 750 GeV Diphoton Resonance*, arXiv:1512.05332.

[82] A. Santamaria, *Masses, mixings, Yukawa couplings and their symmetries*, *Phys. Lett.* **B305** (1993) 90–97, [hep-ph/9302301].

[83] J. R. Ellis and S. Lola, *Can neutrinos be degenerate in mass?*, *Phys. Lett.* **B458** (1999) 310–321, [hep-ph/9904279].

[84] J. A. Casas, J. R. Espinosa, A. Ibarra, and I. Navarro, *Naturalness of nearly degenerate neutrinos*, *Nucl. Phys.* **B556** (1999) 3–22, [hep-ph/9904395].

[85] J. A. Casas, J. R. Espinosa, A. Ibarra, and I. Navarro, *General RG equations for physical neutrino parameters and their phenomenological implications*, *Nucl. Phys.* **B573** (2000) 652–684, [hep-ph/9910420].

[86] A. Ibarra and C. Simonetto, *Understanding neutrino properties from decoupling right-handed neutrinos and extra Higgs doublets*, *JHEP* **11** (2011) 022, [arXiv:1107.2386].

[87] E. Ma, *Splitting of three nearly mass degenerate neutrinos*, *Phys. Lett.* **B456** (1999) 48–53, [hep-ph/9812344].

[88] *Workshop on CP Studies and Non-Standard Higgs Physics*, 2006.

[89] I. P. Ivanov, V. Keus, and E. Vdovin, *Abelian symmetries in multi-Higgs-doublet models*, *J. Phys.* **A45** (2012) 215201, [arXiv:1112.1660].

[90] A. J. Buras, *Weak Hamiltonian, CP violation and rare decays*, in *Probing the standard model of particle interactions. Proceedings, Summer School in Theoretical Physics, NATO Advanced Study Institute, 68th session, Les Houches, France, July 28-September 5, 1997. Pt. 1, 2*, pp. 281–539, 1998. hep-ph/9806471.

[91] T. Inami and C. S. Lim, *Effects of Superheavy Quarks and Leptons in Low-Energy Weak Processes k(L) —> mu anti-mu, K+ —> pi+ Neutrino anti-neutrino and K0 <—> anti-K0*, *Prog. Theor. Phys.* **65** (1981) 297. [Erratum: Prog. Theor. Phys.65,1772(1981)].

[92] M. Blanke, A. J. Buras, A. Poschenrieder, C. Tarantino, S. Uhlig, and A. Weiler, *Particle-Antiparticle Mixing, epsilon(K), Delta Gamma(q), A**q(SL), A(CP) (B(d) —> psi K(S)), A(CP) (B(s) —> psi phi) and B —> X(s,d gamma) in the Littlest Higgs Model with T-Parity*, *JHEP* **12** (2006) 003, [hep-ph/0605214].

[93] A. J. Buras, *Flavor dynamics: CP violation and rare decays*, *Subnucl. Ser.* **38** (2002) 200–337, [hep-ph/0101336].

[94] A. Lenz and U. Nierste, *Theoretical update of $B_s - \bar{B}_s$ mixing*, *JHEP* **06** (2007) 072, [hep-ph/0612167].

[95] **LHCb** Collaboration, R. Aaij et al., *A precise measurement of the B^0 meson oscillation frequency*, arXiv:1604.03475.

[96] **Heavy Flavor Averaging Group (HFAG)** Collaboration, Y. Amhis et al., *Averages of b-hadron, c-hadron, and τ-lepton properties as of summer 2014*, arXiv:1412.7515.

[97] **LHCb** Collaboration, R. Aaij et al., *Precision measurement of CP violation in $B_s^0 \to J/\psi K^+ K^-$ decays*, *Phys. Rev. Lett.* **114** (2015), no. 4 041801, [arXiv:1411.3104].

[98] A. Badin, F. Gabbiani, and A. A. Petrov, *Lifetime difference in B_s mixing: Standard model and beyond*, *Phys. Lett.* **B653** (2007) 230–240, [arXiv:0707.0294].

[99] **Heavy Flavor Averaging Group** Collaboration, Y. Amhis et al., *Averages of B-Hadron, C-Hadron, and tau-lepton properties as of early 2012*, arXiv:1207.1158.

[100] J. Charles et al., *Predictions of selected flavour observables within the Standard Model*, *Phys. Rev.* **D84** (2011) 033005, [arXiv:1106.4041].

[101] T. Nakada, *Review on CP violation*, *AIP Conf. Proc.* **302** (1994) 425–463, [hep-ph/9312290].

[102] A. J. Buras and D. Guadagnoli, *Correlations among new CP violating effects in $\Delta F = 2$ observables*, *Phys. Rev.* **D78** (2008) 033005, [arXiv:0805.3887].

[103] A. J. Buras, D. Guadagnoli, and G. Isidori, *On ϵ_K Beyond Lowest Order in the Operator Product Expansion*, *Phys. Lett.* **B688** (2010) 309–313, [arXiv:1002.3612].

[104] S. Herrlich and U. Nierste, *Enhancement of the K(L) - K(S) mass difference by short distance QCD corrections beyond leading logarithms*, *Nucl. Phys.* **B419** (1994) 292–322, [hep-ph/9310311].

[105] S. Herrlich and U. Nierste, *Indirect CP violation in the neutral kaon system beyond leading logarithms*, *Phys. Rev.* **D52** (1995) 6505–6518, [hep-ph/9507262].

[106] S. Herrlich and U. Nierste, *The Complete /delta S/ = 2 - Hamiltonian in the next-to-leading order*, *Nucl. Phys.* **B476** (1996) 27–88, [hep-ph/9604330].

[107] A. J. Buras, M. Jamin, and P. H. Weisz, *Leading and Next-to-leading QCD Corrections to ϵ Parameter and $B^0 - \bar{B}^0$ Mixing in the Presence of a Heavy Top Quark*, *Nucl. Phys.* **B347** (1990) 491–536.

[108] J. Urban, F. Krauss, U. Jentschura, and G. Soff, *Next-to-leading order QCD corrections for the B0 anti-B0 mixing with an extended Higgs sector*, *Nucl. Phys.* **B523** (1998) 40–58, [hep-ph/9710245].

[109] J. Brod and M. Gorbahn, *ϵ_K at Next-to-Next-to-Leading Order: The Charm-Top-Quark Contribution*, *Phys. Rev.* **D82** (2010) 094026, [arXiv:1007.0684].

[110] J. Brod and M. Gorbahn, *Next-to-Next-to-Leading-Order Charm-Quark Contribution to the CP Violation Parameter ϵ_K and ΔM_K*, *Phys. Rev. Lett.* **108** (2012) 121801, [arXiv:1108.2036].

[111] A. J. Buras, F. De Fazio, J. Girrbach, R. Knegjens, and M. Nagai, *The Anatomy of Neutral Scalars with FCNCs in the Flavour Precision Era*, *JHEP* **06** (2013) 111, [arXiv:1303.3723].

[112] A. J. Buras and J. Girrbach, *Complete NLO QCD Corrections for Tree Level Delta F = 2 FCNC Processes*, *JHEP* **03** (2012) 052, [arXiv:1201.1302].

[113] A. J. Buras, S. Jager, and J. Urban, *Master formulae for Delta F=2 NLO QCD factors in the standard model and beyond*, *Nucl. Phys.* **B605** (2001) 600–624, [hep-ph/0102316].

[114] C. M. Bouchard, E. D. Freeland, C. Bernard, A. X. El-Khadra, E. Gamiz, A. S. Kronfeld, J. Laiho, and R. S. Van de Water, *Neutral B mixing from $2+1$ flavor lattice-QCD: the Standard Model and beyond*, *PoS* **LATTICE2011** (2011) 274, [arXiv:1112.5642].

[115] **RBC, UKQCD** Collaboration, P. A. Boyle, N. Garron, and R. J. Hudspith, *Neutral kaon mixing beyond the standard model with $n_f = 2+1$ chiral fermions*, *Phys. Rev.* **D86** (2012) 054028, [arXiv:1206.5737].

[116] **ETM** Collaboration, V. Bertone et al., *Kaon Mixing Beyond the SM from N_f=2 tmQCD and model independent constraints from the UTA*, *JHEP* **03** (2013) 089, [arXiv:1207.1287]. [Erratum: JHEP07,143(2013)].

[117] A. J. Buras, F. De Fazio, and J. Girrbach, *331 models facing new $b \to s\mu^+\mu^-$ data*, *JHEP* **02** (2014) 112, [arXiv:1311.6729].

[118] K. G. Chetyrkin, J. H. Kuhn, and M. Steinhauser, *RunDec: A Mathematica package for running and decoupling of the strong coupling and quark masses*, *Comput. Phys. Commun.* **133** (2000) 43–65, [hep-ph/0004189].

[119] **LHCb, CMS** Collaboration, V. Khachatryan et al., *Observation of the rare $B_s^0 \to \mu^+\mu^-$ decay from the combined analysis of CMS and LHCb data*, *Nature* **522** (2015) 68–72, [arXiv:1411.4413].

[120] W. Grimus and L. Lavoura, *Renormalization of the neutrino mass operators in the multi-Higgs-doublet standard model*, *Eur. Phys. J.* **C39** (2005) 219–227, [hep-ph/0409231].

[121] T. P. Cheng, E. Eichten, and L.-F. Li, *Higgs Phenomena in Asymptotically Free Gauge Theories*, *Phys. Rev.* **D9** (1974) 2259.

[122] G. Cvetic, S. S. Hwang, and C. S. Kim, *One loop renormalization group equations of the general framework with two Higgs doublets*, *Int. J. Mod. Phys.* **A14** (1999) 769–798, [hep-ph/9706323].